# OPTIMIZATION OF BIORETENTION HYDROLOGICAL PERFORMANCE AND NITRATE REDUCTION IN URBAN STORMWATER RUNOFF

A Thesis

by

SONIA C. ZAMARRIPA

Submitted to the Office of Graduate and Professional Studies of
Texas A&M University
in partial fulfillment of the requirements for the degree of

MASTER OF SCIENCE

| | |
|---|---|
| Chair of Committee, | Clyde Munster |
| Co-Chair of Committee, | Fouad Jaber |
| Committee Member, | Kung-Hui Chu |
| Head of Department, | Stephen Searcy |

August 2017

Major Subject: Biological and Agricultural Engineering

## ABSTRACT

A bioretention cell is a low-impact development practice that reduces urban stormwater runoff and improves water quality. The bioretention cell located at the Texas A&M AgriLife Research and Extension Center in Dallas, Texas was used for this study. The bioretention cell collects water from an adjacent parking lot and provides detention and filtration through vegetation, engineered media, a gravel layer, and an internal water storage zone. Due to equipment malfunction, out of 33 events from 2013 to 2015, only 22 events were used for the hydrological analysis, 19 for the nitrate analysis, and 10 for both hydrological and nitrate analysis. These evaluations showed that the bioretention cell reduced runoff by an average of 76%. The nitrate analysis yielded a statistically significant nitrate mean reduction of 26% with a p-value of 0.001. For the 10 events that had both qualitative and quantitative data, the nitrate reduction was first considered using a concentration reduction equation; the result was 39% nitrate concentration reduction. When considering the impact of volume reduction, the mean mass reduction equation resulted in 81% reduction. The variation between the nitrate concentration reduction (39%) and mean mass reduction (81%) showed that a majority of the reduction in nitrate was attributed to the reduction in runoff volume, indicating that by optimizing volume reduction, nitrate reduction would also improve.

Using a 1-D Hydrus model, the study of hydrological reduction performance for a bioretention cell in Dallas, Texas, resulted in a few optimization potentials. Only three

events had complete datasets with sufficient runoff volume reduction to compare the actual measured outflow against the simulated outflow. Two storm events (September 2, 2013 and September 28, 2013) were used for calibration purposes, and one event (September 21, 2013) was used to validate the model. A sensitivity analysis using Hydrus resulted in the following discoveries about the soil properties. Higher water volume attenuations can be achieved with smaller residual water content, larger saturated water content, larger inverse of the bubbling pressure (empirical value), and larger pore distributions (empirical value). The Hydrus sensitivity analysis also showed that increasing exfiltration into the native soil would result in higher reductions of runoff volume due to dryer media coinciding with smaller outflows. During the calibration, the initial water content values of the soil were estimated by trial and error to obtain the correct outflow volume. The two calibrated events were studied to discover that the initial water content conditions could be obtained since both storms required 55 cm of pressure to produce outflow and the pressure remained at 55 cm immediately after the storm. The results of the validated storm showed that Hydrus can simulate the water flowing through a bioretention cell very well, yielding an NSE value of 0.82 and an $R^2$ value of 0.92 when compared to the measured outflow data and also that the initial water content conditions can be determined without field data. A limitation of using Hydrus-1D is the inability to have two lower boundary conditions to simulate flow into the native soil. This limitation restricts the use of the model to single event simulations instead of longer continuous event simulations.

## DEDICATION

I dedicate this to my family and close friends who have always been supportive and have made this endeavor possible. I am extremely grateful.

## ACKNOWLEDGEMENTS

Thank you to my committee chairs: Dr. Clyde Munster and Dr. Fouad Jaber for the countless hours of advice. Thank you also to my committee member: Dr. Kuing-Hu Chu for also taking the time to make this possible. Thank you to Dr. Nandita Gaur for the relentless help in understanding the Hydrus model. I would also like to thank the Department of Biological and Agricultural Engineering for providing me with a foundation for this project and also for the funding that I received through teaching assistantships.

## TABLE OF CONTENTS

Page

## LIST OF FIGURES

Page

## LIST OF TABLES

Page

# CHAPTER I

# INTRODUCTION

## Background and Motivation

An increase in large stormwater runoff volumes, polluted streams, erosion and sedimentation can be attributed to the increasing percentages of urban areas. With the 82% projected population increase in Texas, or specifically from 25.4 million to 46.3 million, from the year 2010 to 2060 (TWDB 2012), rapid urbanization is a concern for stormwater management. The principal purpose of the current urban drainage infrastructure is to quickly carry away stormwater to prevent flooding and erosion. The conventional system incorporates the transportation network of primarily impermeable surfaces that provide a direct pathway for surface runoff to get into our public water supplies. On route, the stormwater accumulates pollutants including nutrients, bacteria, hydrocarbons, suspended solids, and heavy metals (Barrett et al. 2013; Liu et al. 2014) from these surfaces, and the unnaturally high concentrations cause problems for the environment and consequentially its inhabitants. As precipitation runs off or evaporates from the concrete sidewalks, asphalt roads, and metal roofs, the natural process is disrupted and the water gets diverted from infiltrating the soil, recharging groundwater, and maintaining other ecological functions (UNCE 2004; Liu et al. 2014).

The inevitable effects of climate change also further highlight the need to reevaluate the management of conventional stormwater systems. The shorter and higher intensity storms

forecasted due to climate change will result in higher runoff volumes (Walthall et al. 2012) that require better stormwater infrastructure. Currently, a potential solution to address these issues is utilizing low-impact development (LID) strategies.

Low-impact development (LID) is a proposed solution to diminish the negative impact of wide spread impervious surfaces introduced by urban development. LID offers alternative designs that reduce the anthropogenic effects of urbanization by utilizing the stormwater before it can result in flooding or pollutant transport. Dry and wet detention ponds have been used extensively as more natural methods of attenuating flow. However, low-impact development also includes other technologies that consist of bioretention cells, bioswales, wetlands, permeable pavements, green roofs, and rainwater harvesting. Among the LID technologies, the bioretention system is an effective control practice that mimics predevelopment hydrologic conditions and decreases pollutants that otherwise would affect downstream water systems (Meng et al. 2014). Bioretention systems, similar to permeable pavements, can also improve water quality. Yet, bioretention systems use less surface area per square foot of watershed and also contribute aesthetic features (Jaber 2014b).

Bioretention cells are typically shallow depressions that collect upstream runoff constructed with an engineered vegetated filter media, an overflow pipe, and an optional underdrain (Liu et al. 2014). Although the benefits of implementing correctly designed bioretention cells have been noted, the performance can vary vastly depending on factors

such as design purpose and design restrictions. It would be more beneficial to study the designs of these bioretention systems by controlling specific factors such as climates, soil types, slopes, vegetation, surface areas, and drainage areas to be able to appropriately and adequately replace old methods of conveying stormwater. Specifically, the reduction of nitrate could be optimized through localized bioretention studies by focusing on the denitrification process that occurs within the cell.

**Rational Significance**

Data gaps regarding the effects of changing certain parameters within the bioretention design warrant more research for improved local recommendations. Without region specific data guidelines, state and local government guidelines are often adopted from other state agencies (Davis et al. 2009), resulting in generalized designs that do not address local conditions and issues. Models have been used to evaluate the different designs for particular projects; however, most of the research in this area has occurred in the northeast region of the United States where different native soils are utilized and the climate has a varying impact on the system performance.

**Hypothesis and Objectives**

This project will use Hydrus-1D modeling software to simulate water transport through a bioretention cell to provide a pathway for improving local runoff attenuation and nitrate reduction design guidelines for Texas. Bioretention cell performance can be simulated using Hydrus-1D software and the model will be useful in identifying the source of

variability of outflow and effluent nitrate concentrations. The use of a model specifically for unsaturated soils will provide a platform for understanding how the characteristics of the profile media affect the efficiency of the bioretention cell.

The objectives of this study are to:

- Provide a summary on the nitrate reduction through the bioretention cell by analyzing field measured data,
- Develop a calibrated model using Hydrus 1-D for a bioretention cell suitable for Texas climate by evaluating measured inflow and outflow water data. Validation of this model will consist of comparing the measured data to the simulated results provided by Hydrus,
- Evaluate the model with respect to the simulation for runoff reduction and identify any limitations caused by the modeling software,
- Identify the cause of variability in bioretention performance results, and
- Make recommendations for future Hydrus modeling studies of bioretention cells.

# CHAPTER II

# LITERATURE REVIEW

## Bioretention Design

Initial design factors such as vegetation, media type, surface area, media depth, internal water storage zone, overflow basin and outside factors such as climate can all contribute to the variation in performance, and guidelines should vary accordingly. The size of the drainage area to be directed towards the bioretention cell will determine the dimensions of the bioretention cell. The rainfall in the drainage area will contribute to the amount of water that accumulates within the bioretention surface area. Other factors such as engineered soil properties and existing soil properties will also be important. The volume of the bioretention cell is determined by determining the volume required to maintain predevelopment peak runoff as a function of the SCS Curve Number and a design storm (PGDER 2007).

Engineered media are typically designed for high infiltration characteristics; therefore, the saturated hydraulic conductivity of the media is an important factor. The characteristics of the surrounding native soil are also important as those parameters define the exfiltration of the bioretention cell. Exfiltration is defined as water exiting the bioretention cell through the base or sides. After exfiltration, when the water reaches the groundwater table, it is referred to as groundwater recharge. An upturned elbow can also be included in the design to form an internal water storage zone. The upturned elbow physically allows

the bioretention cell profile to become saturated up to the depth of the upturned elbow outlet.

An overflow basin is an outlet structure that is raised above the bottom of the bioretention cell. It creates an initial storage compartment on the surface of the bioretention cell. This can be optimal for high intensity storms that cannot quickly infiltrate into the system and cause flooding. The ponding depth design factor determines the overflow basin height. By increasing the depth of the overflow basin drain, larger storms can benefit from the attenuation potential of the bioretention cell. This results in less pollutant conveying stormwater runoff. When designing the bioretention cell consideration must be given to the vegetation chosen, since larger ponding depths could cause negative effects. Very small ponding depths would also limit the reduction potential.

Field and lab experiments have been conducted by researchers and the results have been utilized to create design guidelines. The bioretention cell was introduced by Larry Coffman through the work produced by Prince George's County, Maryland Department of Environmental Resources (PGDER) (Funkhouser 2007). These publications include the 1997 "Low Impact Development Design Manual," the 1999 "Low-Impact Development Design Strategies: An Integrated Design Approach," and the Low-Impact Development Hydrologic Analysis (PGDER 1999). A bioretention specific manual was published in 2007 (PGDER 2007). The PGDER manuals are very useful in understanding the hydrologic principles necessary to design the bioretention cells. The PGDER

publications discuss the objective of mimicking predevelopment hydrologic conditions to size the bioretention cell (PGDER 1999). Many design guidelines have simply been adopted from these existing guidelines without modifications or emphasis for local conditions. Although the PGDER manuals are thorough for sizing the volume storage needs of a bioretention cell, the recommendations for media types, vegetation, and internal water storage zones can be broad. Specific research in design elements of the bioretention cell have highlighted the potential in creating site specific designs. For instance, the internal water storage (IWS) zone idea was introduced by Kim et al. (2003) with a successful 70-80% mass removal of nitrate plus nitrite in a pilot study. The introduction of the internal water storage zone was important especially to areas where nitrogen pollution is a concern as it added the benefit of improved denitrification to the reduction of stormwater volumes. By understanding the combined effects of the different design parameters (i.e. media type, depth, IWS, vegetation) aimed at performing in one region, improved guidelines can be obtained for the purpose of increasing the success of implementation. Successful implementation of bioretention cells is generally defined as improved volume reduction and increased water quality. The following sections will outline recommendations for design, variations in recommendations, and new performance results relating to the design parameters of vegetation, ponding depth, media profile, exfiltration, and climate. The overall volume and nitrate reduction performance study results will also be explored, as well as some results and recommendations from modeling experiments.

Vegetation

One of the most apparent benefits of bioretention cells is their aesthetic feature. Engineers and city planners easily promote the implementation of bioretention cells when this visual quality is addressed. Less obvious is how the vegetation choice can affect the performance as vegetation properties such as plant size, root depth, and root penetration width vary. The vegetation must be chosen on a site specific basis so that it is able to thrive in the local conditions which include climate and media properties. The root dimensions can have an effect on the uptake of water and solutes as well as the pore space within the structure. A column experiment compared two types of common Texas grasses: Buffalograss 609 (Buchloe dactyloides; turf grass) and Big Muhly (Mulenbergia lindheimeri; bunch grass) (Barrett et al. 2013). The experiment results showed a potential 59-79% reduction of total nitrogen and a 77-97% reduction of phosphorous. The Big Muhly had an increased reduction of total nitrogen when compared to the Buffalograss 609, but no difference was shown between the plants in the reduction of phosphorous (Barrett et al. 2013). A reason for some of the improvement with nitrogen reduction for Big Muhly versus Buffalograss was attributed to its overall size and to the roots that take up the entire media profile (46 cm) (Barrett et al. 2013). Care must be taken such that the roots do not increase the infiltration so much that it negatively effects the reduction of solids (Li et al. 2010). As roots grow and expand in the soil profile the soil pore space may increase causing a consequential increase in infiltration and the release of pollutants. In a Texas study by Li et al. (2010), shrubs, native grass seedmix, TxDOT (Texas Department of Transportation) seedmix, bermudagrass, and a no vegetation control were used to evaluate the effects of

vegetation on water quality. The results showed that the vegetation did not increase the reduction of metals (Zn, Pb) solids (TSS), or phosphorous (P), but did increase the reduction of nitrogen (N) (Li et al. 2010). The amount of water needed to maintain the vegetation will vary depending on the species used, it is preferred that the plant selection can thrive in the target environment with limited amounts of required irrigation to promote reduction efficiency (Jaber 2014b). A theoretical ecological report suggests that utilizing different species in combination would be optimal in order to increase performance (Levin and Mehring 2015). This study also suggests that the bioretention cell be implemented in a variety of stages to prevent clogging or to increase nutrient removal (Levin and Mehring 2015). This way the age of the bioretention cell is varied and long-term sustainability is promoted. Although vegetation takes part in the removal of pollutants, it does not have a key role in the hydraulic performance of the bioretention cell (Jennings et al. 2015).

Ponding Depth

Clogging and mosquito breeding are potential problems that can be diminished with an appropriate design depth (Davis et al. 2009). The ponding depth will determine the time it takes for the water to completely infiltrate the bioretention cell after incoming flow has stopped (He and Davis 2011). The design goal is to infiltrate the runoff within 48 hr (PGDER 2007). The ponding depth for bioretention cells is typically 150 mm (Davis 2008). The ponding depth for residential (smaller) bioretention cells can range depending on the slope of the cell: 80 to 130 mm at 4% slope; 150 to 180 mm at 5 to 7% slope; and 200 mm at 8 to 12% slope (Christianson et al. 2012). When comparing media with

different ratios of soil (Cecil sandy clay loam) to sand, Christianson et al. (2012) found that increasing the soil portion from 25% to 75% increased the ponding depth from 0.0 to 138 mm (unmulched) and from 0.0 to 2.5 mm (mulched). This indicates that the ponding depth will depend on the infiltration rate characteristic of the media (Christianson et al. 2012). He and Davis (2011) also found that soils with finer media (smaller saturated hydraulic conductivities) produced smaller outflow volumes attributed to increased ponding and time for exfiltration.

## Media Profile

### *Size*

A study evaluating design recommendations shows the sizing guidelines for surface areas of residential bioretention cells for 42 U.S. states and how they can range from 4% to 80% of the drainage area (Jennings et al. 2015). In the development of a software tool, different surface area sizing guidelines (Virginia, Idaho, Prince George Department of Environmental Resources (PGDER), Darcy's law and the rational method) were compared for the same drainage area and the results ranged from 40.5 to 140 $m^2$ (Roy-Poirier et al. 2010). That is a very large difference between the recommendations that could potentially lead to overdesign. Jennings et al. 2015 is cautious to recommend the state guidelines without further research to each source and also reports that revisions should be made to increase hydrologic performance. Larger ratios of media volume to drainage area show increased runoff reductions (He and Davis 2011) due to more space for water storage; however simply designing a cell as large as possible may not be the most effective use of

the space available if efficiency can be reached through careful design. Moreover, a larger bioretention cell will increase the influence of storm size versus storm intensity on outflow, as storage and infiltration are primary factors in the bioretention cell function (Olszewski and Davis 2013). A surface area that is 10 to 30% of the drainage area is the consensus in the sizing guidelines (Jennings et al. 2015), and as stated before careful consideration of local conditions must be taken. He and Davis (2011) recommend a minimum length to width ratio of 2. To achieve the goal of predevelopment hydrology, Olszewski and Davis (2013) recommend comparing flow duration curves (flow rates of inflow, outflow, and natural stream versus flow durations) along with the hydrographs. A global sensitivity analysis that considered the hydrologic performance in regards to predevelopment values showed that the surface area is the most sensitive element followed by saturated infiltration rate of native soil and underdrain size (for cells with underdrains) (Sun et al. 2011).

Over-sizing a bioretention cell is not the only issue; bioretention cells that are too small also present concerns. Bioretention cells constructed inadequately can reduce performance results. In one study, bioretention cells constructed at 28% of its designed size had a 59% overflow occurrence, while bioretention cells constructed at 35% had a 55% overflow (Brown et al. 2011a). Therefore, there is a higher potential for overflow in undersized bioretention cells (Brown et al. 2011a). When bioretention cells are undersized the design saturated hydraulic conductivity value will drop more rapidly in the first four weeks than for cells that are correctly sized (Le Coustumer et al. 2007). A more drastic

initial drop in the saturated hydraulic conductivity could lead to decreased reduction performance.

Furthermore, studies have shown that deeper media profiles promote more exfiltration (drainage to native soils) and less outflow volumes (Brown and Hunt 2011a). The deeper media profiles represent longer retention times and larger storage volumes, which give bioretention cells the opportunity to foster enhanced environments for water quality improvements and better volume reduction performances. The study showed that deeper media depth reduced outflow volume by slightly more than 50% between cells with a 0.3 m variation in design depth (Brown and Hunt 2011a).

*Saturated Hydraulic Conductivity*

Saturated hydraulic conductivity is a soil property that represents the infiltration potential of the stormwater into the system. The saturated hydraulic conductivity is a very important factor since infiltration is regarded as a vital component for cell performance and for modeling bioretention cells (Jennings et al. 2015; Christianson et al. 2012). Better hydrologic effectiveness is associated with higher saturated hydraulic conductivities (Meng et al. 2014). Soil media are engineered to provide soil parameters that are designed to quickly attenuate the stormwater runoff. Some engineered media have been designed to have saturated hydraulic conductivity values up to two to three orders of magnitude larger than the values of the surrounding native soil using combinations of sand, loam, and compost (Thompson et al. 2008). For example, an engineered soil mixture can have a

saturated hydraulic conductivity value of 122 cm $hr^{-1}$ compared to a native soil with saturated hydraulic conductivity value of 0.33 cm $hr^{-1}$. Jennings et al. (2015) reports that for residential bioretention cells (9.3 to 27.9 $m^2$) a saturated hydraulic conductivity value of 0.318 cm $hr^{-1}$ can achieve a 75% runoff reduction and the recommended minimum value of 0.635 cm $hr^{-1}$ can achieve greater than 85% runoff reduction. A study that varied the surrounding soils between silt loam, clay loam, and sandy clay loam found that the soil with the larger saturated hydraulic conductivity (sandy clay loam) had better runoff volume reductions due to exfiltration (He and Davis 2011). Le Coustumer et al. (2007) showed that the saturated hydraulic conductivity decreased rapidly during the first four weeks of bioretention use and then steadily plateaued to a particular value. The long term value reached will depend on the characteristics of the bioretention cell design, such as vegetation density, root density, surface area, and media type (Le Coustumer et al. 2007).

*IWS*

The internal water storage (IWS) zone was specifically designed to enhance denitrification within the bioretention cell via this anoxic zone. An increased reduction of nitrate is achieved by improving the denitrification process in a bioretention cell. This may be attained by increasing the residence or retention time in the bioretention cell by increasing the IWS zone. The IWS zone is created by placing an upturned elbow drain within the system. The height of the drain is equivalent to the depth of the bioretention cell that would remain saturated if the cell contained an impermeable layer. Conversely, if the IWS zone completely drains, groundwater recharge increases and outflow decreases

(Brown and Hunt 2011b). The depth of the IWS zone can be altered by changing the depth of the drain. Zinger et al. (2007) recommends a depth of at least 450 mm (17.7 in) for complete denitrification.

To illustrate the value of utilizing an IWS zone, bioretention cells without IWS (non-IWS) and bioretention cells with IWS (IWS) were compared in a field study. The non-IWS design had mostly but not entirely positive removal results, and the IWS design resulted in more consistent and positive nitrogen removal values (Li et al. 2014). This signified an improved performance for bioretention cells with IWS.

Exfiltration

Although impermeable membranes are an option for bioretention cells, exfiltration is important to completely optimize natural hydrologic conditions. Impermeable membranes are utilized when contamination of the groundwater table is a concern such as near gas stations or industrial sites (MPCA, 2016). Under normal conditions an impermeable membrane is not recommended to increase hydrologic performance (Davis 2008). Even when impermeable membranes are not utilized, the native soils can contain properties resembling impermeable material. The saturated hydraulic conductivity of the surrounding soils is an important factor that affects exfiltration (as discussed in the saturated hydraulic conductivity section). The dimensions and shape of the bioretention cell can also be designed to promote exfiltration. For instance, deeper bioretention cells with wider bases have potential for higher exfiltration (Brown and Hunt 2011a; Davis et

al. 2009). The majority of the exfiltration (88-95%) is attributed to flow through the bottom of the cell versus the sides (He and Davis 2011). This is important to note for models that require exfiltration to be simulated.

Climate

Bioretention cells have shown to improve hydrologic functions overall, yet the performances between climates can vary. For instance, with overall increases in groundwater recharge, semi-arid and humid climates had more similar results than an arid climate where recharge levels were much lower (Dussaillant et al. 2005). Studies such as these can provide rationale for creating local guidelines based on existing guidelines for similar climates. A different study in Caloundra, Australia, with simulated rainfall events produced slightly variable results in runoff reduction ranging from 80% to 94% (Lucke and Nichols 2015). Some of the variability in the results was attributed to drier filter media that had higher reduction values (Lucke and Nichols 2015). A drier filter media can be indicative of either longer dry periods between storms, smaller consecutive storms, or shorter duration events. The climate is an external factor that cannot be controlled, but its effects still need to be understood for the purpose of improving the performance of the bioretention cell.

**Volume Reduction**

Bioretention cells were introduced in the early 1990s specifically as a stormwater management technology (Jennings et al. 2013). Bioretention cells are designed to reduce

volume runoff through infiltration, soil storage, and water uptake by vegetation (PGDER 2007). The design factors such as ponding depth, saturated hydraulic conductivity, and cell size contribute to the hydrologic reduction performance of a bioretention cell. Each design factor and the recommended ranges discussed previously should be considered during the design phase of any bioretention cell implementation project. Bioretention systems have proven to be effective hydrologically and so versatile regarding location that residential systems are promoted widely (Jennings et al. 2013).

However, runoff volume reductions can range from 50% to 100% as shown in a table summary by Liu et al. (2014). The variation in runoff volume reduction varies with changes in media depth, depth of internal water storage (IWS) layer, and with vegetation changes (Liu et al. 2014). The field experiments summarized by Liu et al. (2014), as the majority of current studies, are from the southeastern United States specifically: North Carolina, Maryland, and Virginia. A potential factor for the variability in performance results are that design guidelines have yet to be locally adapted, resulting in the implementation of bioretention cells not specifically designed for particular locations.

**Nitrate Reduction**

Urban stormwater polluted with contaminants produced by activities such as "motor vehicles, animal wastes, and lawn maintenance" is a significant cause of degradation of many waterways (Jiang et al. 2015). Negative impacts on ecosystem structure, habitat quality, and algal blooms can be attributed to excessive amounts of nitrogen inputs (Li

and Davis 2014). Through understanding the fate and transport of nitrogen, eutrophication and drinking water contamination, which are global problems, can be minimized (Ergas et al. 2010).

In a field study utilizing two bioretention cells, although nitrate reduction was low and some nitrate production was observed, the author attributed the removal of nitrate and other pollutants to primarily the depth of the media (Davis 2007). This study also noted that changes in hydrologic parameters such as flow rate, intensity, and duration also had a noticeable effect on decreasing nutrient content (Davis 2007). Significant reductions of nitrate (measured as nitrate plus nitrite) were noted for bioretention cells treating roof runoff in Connecticut and for undersized cells in North Carolina (Dietz and Clausen 2006; Brown and Hunt 2011a), however no significant reductions were found in other bioretention cells in North Carolina or in bioretention cells treating highway runoff in Texas (Hunt et al 2006; Li et al. 2014). Continued research is required to provide more specific design recommendations to effectively reduce nitrogen via bioretention systems in areas where nitrate pollution is a concern.

The reduction of nitrogen (N) is more complicated than the reduction of runoff because of the transformation from one nitrogen species to another. These transformations are dependent on the microbial community within a bioretention cell. The modes of nitrate transportation can be divided into two categories: physical and biochemical. Although the physical transport of N consists of advection, dispersion, diffusion, assimilation, and

adsorption (Radcliffe and Simunek 2010; Hillel 2004; Nielson et al. 1986), the process of nitrogen transport can be described by simply using the advection-dispersion equation (Mthandi et al. 2014). An adsorption term can be included if necessary or left out for simplification (Hillel 2004).

Physically, the nitrogen species can leave the bioretention system in the effluent, it can leach into the surrounding media, or it can be taken up by vegetation (Li and Davis 2014; Barrett et al. 2014). The biochemical transformation of nitrogen consists of ammonification, nitrification, denitrification and volatilization (Li and Davis 2014; Colins 2010). Denitrification is usually targeted to convert nitrate ($NO_3^-$) to nitrogen gas ($N_2$) as this transformation is favorable for the environment. This process is enhanced in the bioretention cell with an internal water storage (IWS) zone, as discussed beforehand.

**Models**

Bioretention cells have been previously modeled using RECHARGE, RECARGA, DRAINMOD, SWMM, Hydrus, and other models to evaluate different designs and the resulting hydrologic performances (Meng et al. 2014; Liu et al. 2014). RECHARGE is described as the most comprehensive model as it is based on the Richard's equation and it can simulate ponding and an underdrain (Roy-Poirier et al. 2010). RECARGA, a Matlab application (Roy-Poirier et al. 2010), can accurately replicate bioretention hydrology, but it is not capable of evaluating the water treatment process, and it cannot compute very short period simulations (Liu et al. 2014; Meng et al. 2014). The RECARGA model is

based on the Green-Ampt equation (less complicated than Richard's equation) for infiltration (He and Davis 2011). The SWMM model can provide continuous simulation; yet the solute transport results are limited to mass load reductions (Liu et al. 2014). DRAINMOD has been used successfully to simulate an Internal Water Storage (IWS) layer and replicate soil water characteristics (Liu et al. 2014); however, this model is not suitable for short-term simulations (Meng et al. 2014).

An extension of DRAINMOD, HyPer Tool, was used to evaluate the reduction performance of suspended solids (SS) and chemical oxygen demand (COD) of bioretention cells with four different soil types (Quan et al. 2014). Although, this long-term continuous tool based on a macro-embedded excel spreadsheet is useful, it has a limited selection of soil properties (Quan et al. 2014) that can be restrictive when it comes to engineered media that are combinations of soil types. For instance, the best performing design had a measured saturated hydraulic conductivity value of 6 to 9 cm $hr^{-1}$, the theoretical values chosen were 6.4 cm $hr^{-1}$ (Sand) and 3.05 cm $hr^{-1}$ (Loamy Sand), and the model output was 3.0 cm $hr^{-1}$ (a maximum subgrade saturated hydraulic conductivity based on the model procedure) (Quan et al. 2014). It is unclear how accurate the theoretical values describe the measured values.

A 1D bioretention cell model based on the Integrated Design, Evaluation, and Assessment of Loadings (IDEAL) model, studied the required specificity of input parameters (Christianson et al. 2012). The recommendation result from this study was that a level 3

input specificity (soil type ratios and adjusted bulk density) would be adequate for future model analysis as it predicted drainage volume and maximum drainage flow rate at 0.7% to 18% deviation and at 30% to 39% deviation from measured, respectively (Christianson et al. 2012).

A 2D bioretention cell model based on Richard's equation was created using COMSOL Mutltiphysics (He and Davis 2011). He and Davis (2011) define a storage point as the volume of the bioretention cell at which outflow starts. The storage point and exfiltration decrease while outflow increases for bioretention cells with surrounding media that have lower permeability characteristics (He and Davis 2011). Therefore, exfiltration can be significant with cells that are placed in locations with surrounding soils of high saturated hydraulic conductivity values.

Hydrus is a software program that computes Richard's equation to model variably saturated water flow and advection-dispersion equations to simulate heat and solute transport (Simunek et al. 2012). This model that simulates the movement of water and solutes through the vadose zone may be reliable in providing design recommendations for hydrologic and pollutant issues or for simply getting a better understanding of the processes that take place.

Very few studies that utilize the Hydrus model for hydrologic assessment of bioretention cells were found. An experiment in a semiarid climate yielded inconclusive results due to

difficulties in stabilizing the Hydrus-3D model (Steffen 2012). The bioretention evaluated in this study had a clayey sand topsoil layer (31-43 cm) and a Utelite storage layer (61 cm) (Steffen 2012). Various issues such as gravel parameters that quickly dried the cell and large head differences between varying layers resulted in an unstable numerical solution (Steffen 2012). In contrast, a different study using Hydrus-1D showed that the bioretention cell could be successfully calibrated (Meng et al. 2014). This study utilized two bioretention cells in Beijing with varying soil media, geometry, vegetation, and time information to provide design recommendations to improve hydrologic performance (Meng et al. 2014). These studies show the inconsistencies in results within a model due to design variations and parameter selections and highlight the need for more work to be done to address limitations and provide a model that can accurately depict water and solute transport within a bioretention cell specific for local interests.

Wetlands are similar to bioretention cells with the exception that they remain completely saturated during the entire treatment process. When evaluating a wetland with controlled outflow used for wastewater treatment, a virtual layer with a theoretical saturated hydraulic conductivity parameter was used to simulate the throttle outflow (controlled outlet ball valve) (Fournel et al. 2013). The controlled outflow was used to achieve specific retention times (Fournel et al. 2013). The virtual layer was used to overcome the boundary condition limitation that occurs when saturation is reached and the pressure head is not accurately simulated (Fournel et al. 2013). However, the Hydrus study found that the model was not repeatable without continuous calibration of the virtual saturated hydraulic

conductivity due to changing rates of outflow and the associated outlet pressure head that have a square root relationship versus a linear relationship (Fournel et al. 2013). Controlled outflow has also been attempted in bioretention mesocosms. Mesocosoms are simpler, smaller scale laboratory studies (Liu et al. 2014). It was discovered that a longer retention time could be achieved with controlled outflow, and it could increase effectiveness of a bioretention system geared towards differing runoff event sizes (Lucas and Greenway 2011).

Hydrus-1D may provide a model that can be used to predict performance of the bioretention cell that can be used to better understand the hydrologic system in preparation for future solute transport simulations. As the advection-dispersion equations are embedded in the Hydrus software, modeling bioretention cells with Hydrus provides an opportunity to understand the process of nitrate reduction. The potential for Hydrus to adequately simulate the performance of the bioretention cell exists if the hydrological model is successful.

No studies using the solute transport function in this model were discovered, but solute models have been created for other pollutants. Matlab was used to model transport of suspended solids (Roy-Poirier et al. 2010; Li and Davis 2008b). Li and Davis (2008b) concluded that a media depth of 20 cm, media depth replacement of 5 to 20 cm every 5 years, and field inspection 1 to 2 times a year was recommended for reduction of effluent total suspended solids (TSS). Li and Davis (2008a) also successfully used a 1D filtration

equation for particulate metals and advection/dispersion/adsorption transport equations for dissolved metals to reach the conclusions that a shallow design depth of 20 to 40 centimeters is recommended for metal capture and that a low copper content media is appropriate for reducing copper polluted effluent.

# CHAPTER III

# MATERIALS AND METHODS

## Bioretention Site Description

A bioretention cell was constructed at the Texas A&M AgriLife Research and Extension Center in Dallas, Texas, for a previous Environmental Protection Agency (EPA) / Texas Commission of Environmental Quality (TCEQ) funded study (Jaber 2014a). This system was used to collect water hydrology and quality data for performance evaluation. The surface area of the bioretention cell is 186 $m^2$ (2000 $ft^2$) (30.5 m x 6.1 m), and the corresponding runoff area is from a parking lot that is 3344 $m^2$ (36,000 $ft^2$). The surface area to drainage area is about 5.6%. A curb cut, inlet flume, and rip rap forebay direct and slow the runoff into the bioretention cell. The bioretention cell contains plants, such as sunflowers and hibiscus that can withstand the extreme variations in growing conditions. The photos in Figure 1 and Figure 2 depict the bioretention cell in Dallas, Texas.

**Figure 1.** Photo of forebay and bioretention cell at the Texas A&M AgriLife Research and Extension Center in Dallas, Texas. Image by author.

The bioretention cell is irrigated one to two times a year during the months of July and August. An engineered, 0.91 m (3 ft) deep media composed of 50% yard waste compost, 25% sand, and 25% native soil (Houston Clay) was used. The infiltration rate was designed to be 127 cm $hr^{-1}$ (50 in $hr^{-1}$). The bioretention cell itself is 1.17 m (3.8 ft) deep, and it was designed for a ponding depth of 38.1 mm (1.5 in). An internal water storage zone was created using a 100 mm (4 in) perforated pipe with an upturned elbow to slowly release the treated runoff causing the bottom of the cell to remain saturated forming an anaerobic layer. Two gravel layers (processed coarse limestone aggregate grade of 1" to No. 4 and ½" to No. 4, #57 stone and #78 stone, respectively) hold the perforated pipe in place. An overflow inlet lies 0.53 m (1.75 ft) above the soil, and a 300 mm (12 in) connecting pipe discharges the outflow from both overflow and perforated pipe to a nearby detention pond. Figure 3 shows the underdrain and outlet structure detail.

**Figure 2.** Photo of bioretention cell, drainage parking lot, and overflow basin at the Texas A&M AgriLife Research and Extension Center in Dallas, Texas. Image by author.

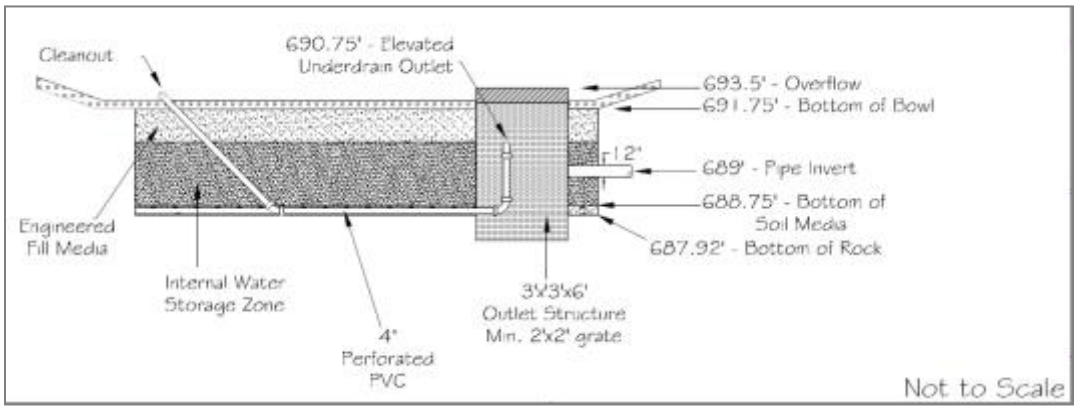


**Figure 3.** Cross section of the bioretention cell at the Texas A&M AgriLife Research and Extension Center in Dallas, Texas. (adapted from Jaber, 2014a; not to scale).

## Field Data Analysis

### Data Collection

An ISCO bubbler flow meter was used to measure the inflow at the 1.0 H flume (flow range of 2 to 720 gallons per minute) and the outflow from the perforated pipe and the

overflow pipe flow (Jaber 2014a; Plasti-fab 2015). The flow meter was tested throughout the experiment to verify that the correct water depth was recorded. Water samples were collected with ISCO 6712 and ISCO 3700 automatic samplers (Jaber 2014a). The water samples were sent to TTI Environmental Laboratories in Arlington, Texas, for quality evaluation through measurements of nitrogen (as N) (Jaber 2014a). Storm data was collected and analyzed for 33 events from June 2013 to February 2015. Due to some equipment malfunction, a few events had missing data such as missing inflows, outflows, or quality measurements. Inflow data was estimated for 8 events using standard equations discussed further below. Events that were missing outflow values were omitted from the runoff reduction analysis. Only 19 events contained nitrate outflow data, and only 10 events had both volume and nitrate data. A summary of this data is included in the Appendix.

Storm Event Analysis

The meteorological data for three years (2013, 2014, and 2015) was collected and analyzed from a weather station (Campbell Scientific) on site. This data included hourly rainfall, temperatures, wind speed, and average daily evapotranspiration rates. The duration of each storm event was noted to determine storm intensity. The antecedent moisture conditions were determined for each flow event using the rainfall groups (SCS 1972) as shown in Table 1. The time between storm events was also taken into consideration to determine the corresponding antecedent moisture condition for the curve number calculation.

**Table 1.** The Antecedent Moisture Conditions Classification used to identify soil conditions for each event (SCS 1972).

| | Total 5-day Antecedent Rainfall | |
|---|---|---|
| AMC | Dormant Season mm(in.) | Growing Season mm(in.) |
| I (dry) | < 12 (0.5) | <35 (1.4) |
| II (normal) | 12-28 (0.5-1.1) | 35-53 (1.4-2.1) |
| III (wet) | >28 (1.1) | >53 (2.1) |

Hydrologic Performance

Inflow volumes were estimated for the storm events for which an outflow volume was measured but had an inflow volume missing. The inflow volumes, ($V_{in}$), were calculated using Equation 1.

$$V_{in} = A * Q \tag{1}$$

Where A= drainage area. The runoff depth, Q, was determined using the SCS curve number method equation

$$Q = \frac{(P-0.2S)^2}{(P+0.8S)} \; for \; P > 0.2S \tag{2}$$

$$Q = 0 \; for \; P \leq 0.2S$$

where Q= runoff depth, P= storm precipitation, and S= soil and surface storage (SCS 1972). Soil and surface storage (S) can be estimated by

$$S = \frac{1000}{CN} - 10 \tag{3}$$

where the curve number, CN (II) was found to be 95 since the average CN(I) was 89 with a standard deviation of 9 for the events with measured inflow volumes, see Table A-3 in the Appendix. Using the antecedent moisture condition associated with each

rainfall/runoff event, the curve number was adjusted to dry and wet conditions using the following equations (SCS 1972).

$$CN(I) = \frac{4.2 * CN(II)}{10 - 0.058 * CN(II)} \quad (4)$$

$$CN(III) = \frac{23 * CN(II)}{10 + 0.13 * CN(II)} \quad (5)$$

The percentage reduction in volume ($V_R$) of runoff from the parking lot and precipitation over the surface area attained with the bioretention cell was calculated using the following equation.

$$V_R = \left(1 - \frac{V_{out}}{V_{in}}\right) * 100 \quad (6)$$

where $V_{out}$ = volume of water leaving the bioretention cell and $V_{in}$ = volume of water that enters the bioretention cell. The mean, median, and range for the volume reductions were noted to summarize the data.

Nitrate Removal Performance

The missing nitrate inflow concentration values were taken to be the calculated average for all inflow concentrations equal to 1.11 mg $L^{-1}$. The percentage reductions of nitrate event mean concentration ($EMC_R$) were calculated using the following equation

$$EMC_R = \left(1 - \frac{EMC_{out}}{EMC_{in}}\right) * 100 \quad (7)$$

where $EMC_{out}$ = event mean concentration out and $EMC_{in}$ = event mean concentration in. Each of these percentage reduction calculations were performed for each storm event and an overall average was noted for nitrate concentration. The paired t-test with a 0.05

level of significance was used to determine if there was a reduction of nitrate in the effluent compared to the influent.

A mass reduction calculation was used to evaluate the effects of the flow attenuation on the nitrate reduction. The following calculation was used to determine the total pollutant mass as in (Davis 2007)

$$Mass = M = \int_0^{t_0} C(t)Q(t)dt \quad (8)$$

where C(t)= pollutant concentration and Q(t)= runoff flowrate. Similar to the event mean concentration reduction, the mass reduction should better describe the results with the incorporation of the reduction in flow (Davis 2007). To get a better visualization of the relationship between inflow and outflow concentration values, probability plots were created using the following equation

$$p = \frac{i-a}{(n+1-2a)} \quad (9)$$

where $i$= ranking number, $n$= total number of observations, and α= 3/8 (normal distribution) (Davis 2007). A log scale y axis was used to plot the data (Davis 2007).

**Soil Parameters**

The Hydrus model requires inputs of soil parameters for the soil media in order to simulate water flow. Saturated hydraulic conductivity and water contents at varying pressure were determined experimentally.

Data Collection

Ten soil cores were collected from the bioretention cell in Dallas. The soil cores were collected from various random locations within the bioretention cell as depicted in the diagram below. The circles within the cell in Figure 4 represent the location where the soil cores were collected. The soil cores averaged 9 cm in height from the top media in the bioretention cell excluding mulch.

Saturated Hydraulic Conductivity

Saturated hydraulic conductivity ($K_s$) is a very important soil parameter as it determines how fast water flows through a saturated media. It is most commonly used in Darcy's law to determine flow rate. To determine the saturated hydraulic conductivity a constant head experiment was conducted. The device maintained a constant head on the top of each soil core, the depth of the ponded water was measured, and the amount of water that flowed through the soil core in an average of 10 minutes was also measured. Equation 10 was used to calculate the saturated hydraulic conductivity

$$K_s = \frac{Q}{A(\frac{\Delta H}{\Delta L})} \tag{10}$$

where Q= flow rate ($cm^3\ s^{-1}$), A= surface area of column ($cm^2$), H= hydraulic head on the soil column (cm), and L= length of soil column (cm).

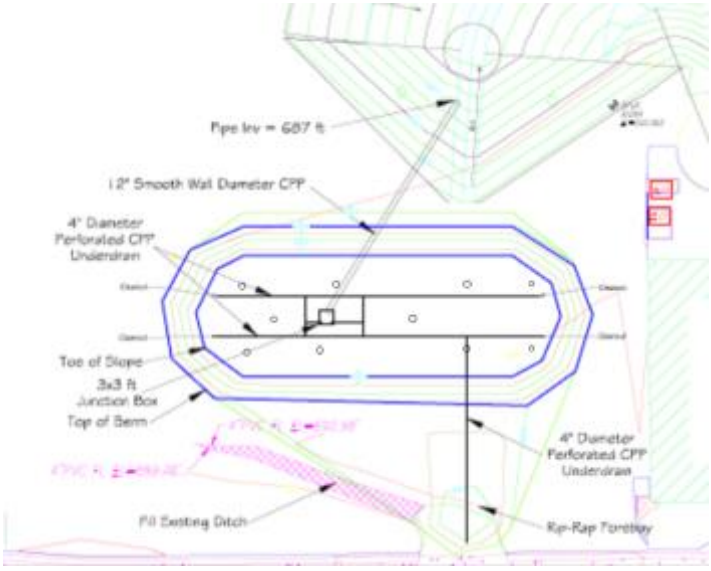


**Figure 4.** The location of the soil cores collected in the bioretention cell at the Texas A&M AgriLife Research and Extension Center in Dallas, Texas (adapted from Jaber, 2014a; not to scale).

The saturated hydraulic conductivities were calculated three times for each soil core using Equation 10 resulting in thirty $K_s$ values. An average $K_s$ and standard deviation was calculated for each soil core and for the overall bioretention cell.

Pressure Chamber Experiment

The van Genuchten (1980) model for the hydraulic properties was chosen for use in simulating the uniform water flow system in Hydrus. In order to correctly represent the bioretention system, water contents were calculated using a pressure chamber experiment. Both gravimetric and volumetric water contents were obtained from the pressure chamber experiments. Three soil samples for each pressure setting were placed within pvc rings with 50 mm diameters and heights ranging between 18 to 23 mm. The measured volumes

(ranging between 31 and 45 $cm^3$) of the soil samples were taken from the soil cores previously collected. After saturation, the media in each ring were placed on top of a 100 kPa (1 bar) ceramic porous pressure plate in the chamber. The pressure chamber experiment yielded water contents for different pressure settings including 0 kPa, 10 kPa, 33 kPa, and 98 kPa. The samples were left in the chamber until no water was released from the chamber. The samples were then dried at 105°C for 24 hours. The weights of the samples were recorded before and after drying. Equations 11 through 14 were utilized to solve for the water contents. The bulk density and porosity were calculated using Equations 15 through 17. Equation 11 was used to calculate the gravimetric water content (u) as follows:

$$u = \frac{M_w}{M_s} \tag{11}$$

where $M_w$= mass of water (g) and $M_s$= mass of soil (g). The mass of water was calculated using Equation 12

$$M_w = M_{cms} - M_{cds} \tag{12}$$

where $M_{cms}$= Mass of container and moist sample (g) and $M_{cds}$= Mass of container and dry sample (g). The mass of soil was calculated using Equation 13

$$M_s = M_{cds} - M_c \tag{13}$$

where $M_c$ = Mass of container (g). The volumetric water content (θ) was calculated using Equation 14

$$\theta = \frac{M_w}{V_t * \rho_w} \tag{14}$$

where $V_t$= Total volume of soil ($cm^3$) and $\rho_w$= Density of water (1 g $cm^{-3}$). The average specific gravity ($SG_b$) was calculated for each pressure setting (4 pressure settings, 3 samples each) using Equation 15.

$$\theta = u * SG_b \tag{15}$$

The average specific gravities (one for each pressure setting) were then used to determine an average bulk density.

$$SG_b = \frac{\rho_b}{\rho_w} \tag{16}$$

where $\rho_b$ = bulk density (g $cm^{-3}$). The average bulk density was determined to be 1.2 g $cm^{-3}$. Porosity ($\varepsilon$) was calculated using Equation 17

$$\varepsilon = 1 - \frac{\rho_b}{\rho_p} \tag{17}$$

where $\rho_p$= particle density (g $cm^{-3}$). The particle density was assumed to be a typical value of 2.65 g $cm^{-3}$ (Hillel, 2004).

**Model Setup**

Geometric Profile

The depth of the soil profile was set to 117 cm as shown in Figure 5. Figure 5 also shows other dimensions of the bioretention cell and the outlet inside the overflow basin. The profile was modeled with the two different soil materials: 1) the engineered media (92 cm) and 2) gravel (25 cm). This material distribution was expressed using the graphical profile tool within Hydrus as shown in Figure 6. Because limited data was obtained on the soil parameters, no hysteresis was selected in the Hydrus model for simplification. Hysteresis

is used when there are significant differences between the wetting and drying soil water characteristic curve.

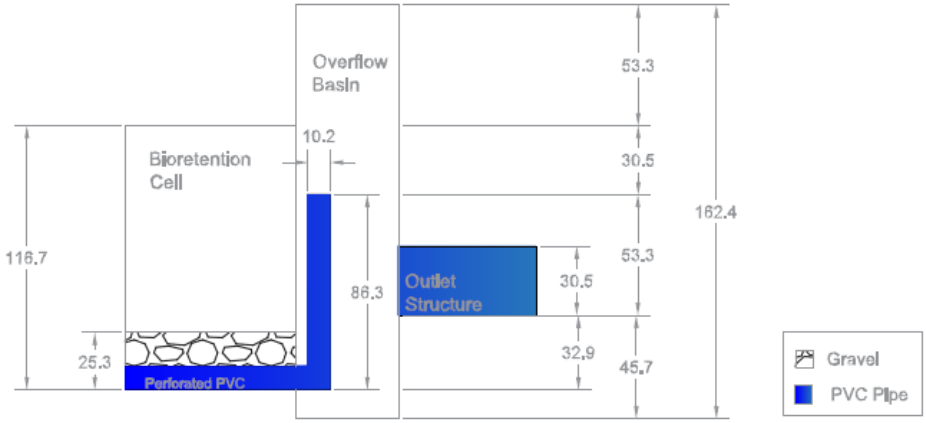


Note: Dimensions are in centimeters.

**Figure 5.** Drawing of bioretention cell and overflow basin at the Texas A&M AgriLife Research and Extension Center in Dallas, Texas.

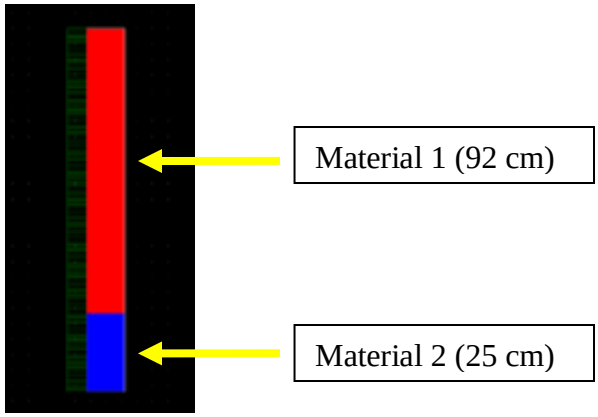


**Figure 6.** The geometric profile used to delineate the different media material in Hydrus.

Boundary Conditions

From the Hydrus boundary condition options, the upper boundary condition selected was "Atmospheric Boundary Condition with Surface Runoff". This boundary condition allowed for the inputs to include the storm runoff from the parking lot and the precipitation that falls directly within the bioretention cell in terms of velocity at 5-minute intervals. Because only one lower boundary condition can be selected in Hydrus-1D, the native soil was assumed to be an impervious layer during each storm event and the perforated drain was taken to be the only possible outflow. The lower boundary condition that best represented the conditions and assumptions was "Seepage Face". This lower boundary condition sets the minimum pressure and no outflow is produced until the selected pressure is reached. The bottom pressure head selected was 44 cm to represent the water pressure at the level of the outlet as shown in Figure 7.

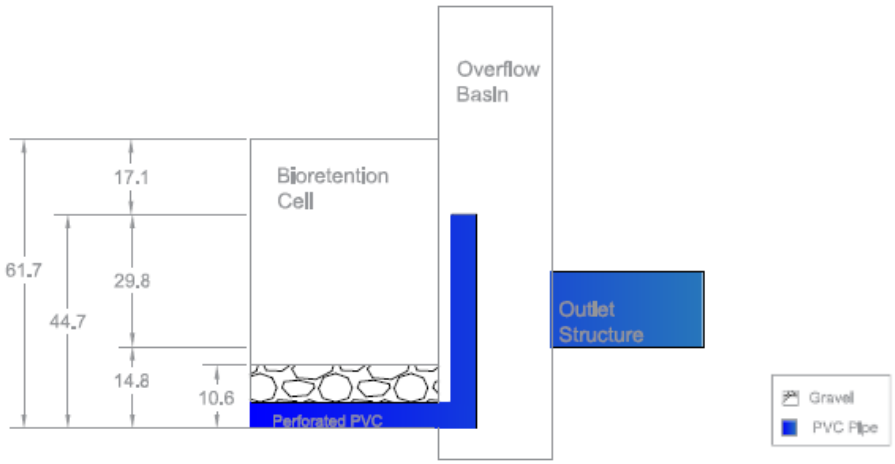


**Figure 7.** Calculated water pressure (cm) dimensions for the bioretention cell at the Texas A&M AgriLife Research and Extension Center in Dallas, Texas.

## Sensitivity Analysis

The sensitivity analysis was conducted on a set of soil parameters by changing the residual water content, the saturated water content, inverse of the bubbling pressure, the pore size distribution index, saturated hydraulic conductivity, and the initial water content by a target of -50% and +50% and noting the results. The sensitivity analysis was conducted before the pressure chamber experiments were completed. Therefore, the residual water content, saturated water content, inverse of the bubbling pressure, and pore distribution index for the engineered media were randomly estimated values based on reference soil parameters (Meng et al. 2014; Fournel et al. 2013; Carsel et al. 1988; He and Davis 2011; Filipovic 2014; and Steffen 2012).

The initial estimates for the gavel layer were based on a gravel layer used in a study by Filipovic (2014). Only the pore distribution index value was increased to 2.5 by trial and error to have the simulation converge to a solution. Other gravel parameter references had values of pore distribution index values of 3.3 and 3.8 (Fournel et al. 2013 and Steffen 2012). The input parameters used for the gravel layer are shown in Table 2.

**Table 2.** Soil properties for the engineered and gravel layer used in the sensitivity analysis.

| Media | Residual Water Content, $\theta r$ | Saturated Water Content, $\theta s$ | Inverse Bubbling Pressure, $\alpha$ | Pore Distribution Index, n | Saturated Hydraulic Conductivity, Ks | Tortuosity parameter, l |
|---|---|---|---|---|---|---|
| Engineered | 0.06 | 0.5 | 0.002 | 1.36 | 107 | 0.5 |
| Gravel[a] | 0.005 | 0.42 | 0.1 | 2.5 | 3000 | 0.5 |

[a]Adapted from Filipovic (2014).

Using these parameters in Table 2 to represent the bioretention cell media layers along with the storm data for the event on September 28th, the changes to the outflow depth between Hydrus simulations were recorded. The results of the sensitivity analysis were then used to direct the calibration of the model.

**Calibration**

Two storms in September 2013 were used to calibrate the model in order to reach a conclusion on whether or not Hydrus was an adequate model for simulating flow through the bioretention cell at the Texas A&M AgriLife Research and Extension Center in Dallas, Texas. These two storms were selected because they were two storms out of three that did not have greater than 90% runoff volume reduction and that had inflow data that was not calculated. The hydrological data is summarized in Table A-1 in the Appendix.

Storm Information

The two storms took place on September 2, 2013 and September 28, 2013. The summaries of the storms are provided in Table 3 and Table 4 below. The two storms are similar in size with total water depth going into the bioretention cell equivalent to 7.1 cm and 11.8 cm, respectively. This total incoming water depth is a result of both the runoff from the adjacent parking lot and the precipitation that falls onto the bioretention cell itself. The outflows of 1.4 cm and 5 cm were the target values for the Hydrus simulations. For the storm input data in Hydrus, the measured flowrates at 5 minute intervals where converted to depths by dividing by the time interval and the bioretention surface area. The

precipitation depths for each storm were added to the runoff flowrate depths. The input storm depths were then converted to velocities in cm $hr^{-1}$ for each time. All times with zero velocities (excluding at the beginning and end of the event) as well as any consecutive repeating velocities were omitted from the input. The input storm summaries are included in Table A-8 in the Appendix.

**Table 3.** Summary of the storm on September 2, 2013.

| Storm: 9.2.13 | |
|---|---|
| Duration (hrs) | 21 |
| Total Runoff Depth In (cm) | 6.3 |
| Total Precipitation In (cm) | 0.8 |
| Total Depth In (cm) | 7.1 |
| Total Depth Out (cm) | 1.4 |

**Table 4.** Summary of the storm on September 28, 2013.

| Storm: 9.28.13 | |
|---|---|
| Duration (hrs) | 13 |
| Total Runoff Depth (cm) | 10.9 |
| Total Precipitation In (cm) | 0.9 |
| Total Depth In (cm) | 11.8 |
| Total Depth Out (cm) | 5.0 |

Soil Parameters

The Hydrus model requires the saturated hydraulic conductivity ($k_s$), residual water content ($\theta_r$), saturated water content ($\theta_s$), the inverse of the bubbling pressure ($\alpha$), and the pore distribution index (n) for both the engineered media and the gravel media. For a completely saturated media, the saturated water content is equivalent to one; the soil

sample is not subjected to pressure in order to measure this parameter. The residual water content is measured at very high pressures to describe a dry media. The inverse of the bubbling pressure and the pore distribution index are empirical parameters that help shape the soil water characteristic curve in the van Genuchten equation and are determined by the relationship between water content and pressure.

The results from the pressure chamber experiment and Hydrus simulations of the calibrated storms were utilized to obtain the unknown soil parameters for the engineered media. The measured water content at 0 kPa, 0.56 $cm^3$ $cm^{-3}$, was used as a saturated water content estimate. The initial value of the inverse of the bubbling pressure was a small random value, 0.002. The initial iteration value assumed for the pore size distribution index was 1.001, the minimum Hydrus value. The residual water content initial value was set to 0.23 $cm^3$ $cm^{-3}$, because it was understood that this value had to be less than the water content at 98 kPa, which was equal to 0.24 $cm^3$ $cm^{-3}$. The residual water content, inverse bubbling pressure, and pore distribution index were calibrated such that the following requirements were met: (1) all values were greater than zero (2) the residual sum of squares was as close to zero as possible, and (3) the measured output matched the simulated output for each calibrated event. The solver function in Excel was used to meet these requirements. The solver function is an iterative optimization tool in Excel that allows users to set a target value by changing other cells. The target value was 0 for the residual sum of squares (RSS) and the cells changed were the residual water content, pore distribution index, and the inverse of the bubbling pressure.

An estimated soil water characteristic curve was created for the bioretention media using the van Genuchten (1980) Equations 18 and 19. The equation for volumetric water content in terms of pressure head is as follows

$$\theta(h) = \theta_r + \left[\frac{\theta_s - \theta_r}{1+(\alpha * h)^n}\right]^m \quad h < 0 \tag{18}$$

$$\theta(h) = \theta_s \qquad h \geq 0$$

where $\theta_r$ = residual water content, $\theta_s$= saturated water content, $\alpha$ = inverse of bubbling pressure (1 $cm^{-1}$), m= empirical parameter, h= pressure head (cm). The empirical parameter (m) was calculated using Equation 19

$$m = 1 - \frac{1}{n} \tag{19}$$

where n= pore size distribution index.

A plot of calculated volumetric water contents with pressures ranging from 0 to 10000 kPa was used to visually compare against the measured values from the pressure chamber. The Hydrus model was also used in conjunction to achieve the target output for each storm by changing the unknown parameters based on the results from the sensitivity analysis. The sensitivity analysis showed that increasing the residual water content, decreasing the inverse of the bubbling pressure, and increasing the pore size distribution index would decrease the output.

The soil parameters for the engineered media were set to the results from the soil water characteristic curve and the saturated hydraulic conductivity tests. The soil parameters for

the gravel layer remained the same from the sensitivity analysis. The soil parameters used for the Hydrus simulation inputs are shown in Table 5.

**Table 5.** Hydrus simulation soil parameter input for the engineered media and gravel media profile.

| Media | Depth (cm) | Residual Water Content, θr | Saturated Water Content, θs | Inverse Bubbling Pressure, α | Pore Distribution Index, n | Saturated Hydraulic Conductivity, Ks | Tortuosity parameter, l |
|---|---|---|---|---|---|---|---|
| Engineered | 25-117 | 0.19 | 0.56 | 0.039 | 1.54 | 107 | 0.5 |
| Gravel[a] | 0-25 | 0.005 | 0.42 | 0.1 | 2.5 | 3000 | 0.5 |

[a]Adapted from Filipovic (2014).

## Initial Conditions

No data on the initial water content conditions within the bioretention profile was measured or collected; therefore, the initial conditions in pressure heads were obtained through calibration. The initial conditions can be set using the graphical tool in Hydrus similar to setting the material distribution as shown in Figure 8. The graphical tool allows users to set the initial conditions by selecting the node range based on depth and setting top and bottom values.

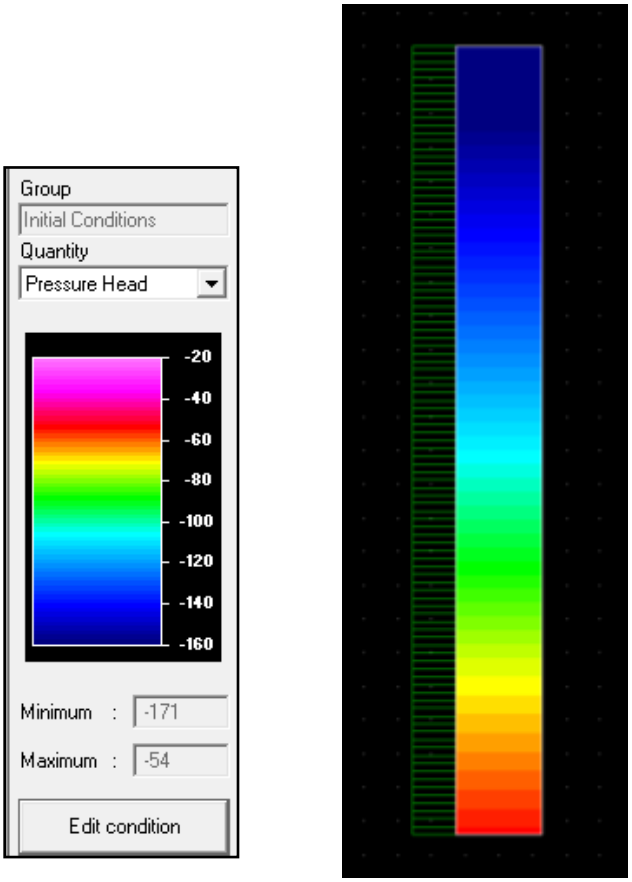


**Figure 8.** Photo of graphical tool used in Hydrus to set initial pressure conditions.

Hydrus provides a soil profile summary table with the specific pressure heads for each node and the corresponding depth. This table was exported into Excel to calculate the total water content within the bioretention cell for various pressure settings. It was assumed that the water content in the bioretention cell had to be greater than 44 centimeters to generate outflow as that is the water content at the level of the upturned elbow (as shown in Figure 7) and also the limit of the seepage face boundary condition. The time that outflow was generated as seen on the measured data was used to get an estimate of how full the cell was. Also, by understanding the effects of changing the initial water content

from the sensitivity analysis, the initial conditions were calibrated by finding the pressure settings that resulted in total simulated outflows that matched the measured outflows for each storm.

Iteration Criteria

The iteration parameters, time step control, internal interpolation tables, time discretization were important in generating accurate results. The Hydrus model allows users to set limits to control the iterative process. The Hydrus index manual provides recommendations for these criteria (Simunek et al. 2012). The recommended values or ranges were used for the time step control and interpolation limits. The maximum number of iterations and pressure head tolerance were increased from the recommended 10 to 100 and 1 to 10, respectively (Simunek et al. 2012). These values had to be increased due to simulations that would not generate results with the recommended values more than likely caused by iteration errors. The parameters were also selected to ensure a water balance near zero was reached indicating that the simulation had run properly as no water was lost or gained in the process.

**Validation**

From the calibration results, a method for estimating the initial conditions was determined and tested during the validation phase. Using the simulation results, the water content within the bioretention cell during the storm events was analyzed and a threshold parameter was discovered at which the bioretention cell produced outflow. The results

showed that the water content for both events reached an equivalent value of 55 cm that was over the 44 cm as originally assumed.

Since the initial conditions were estimated and the threshold value was unknown before the simulation, an error was quantified using Equation 20. The percent error was calculated to verify the difference in storage between the measured and simulated results. The water stored value was estimated by taking the difference of the output and input for both the measured data and the calibrated event simulations using Equation 21.

$$\%\text{Error} = \frac{|\text{Measured Storage} - \text{Hydrus Storage}|}{\text{Measured Storage}} \tag{20}$$

$$\text{Storage} = \text{Input} - \text{Output} \tag{21}$$

$$\text{Initial Water Content} = \text{Final Threshold} - \text{Hydrus Storage} \tag{22}$$

For the validated storm, using Equation 22 the threshold value was used to calculate the initial conditions by subtracting how much water was stored within the bioretention cell during the storm event, from Equation 20. The validated storm was evaluated at three different error percentages to note any variation with increasing error percentages. The estimated initial water content conditions were then converted to pressure terms using the van Genuchten equation in order to set the pressure delineation in the graphical tool and simulate the validation storm.

Storm Information

The storm on September 21, 2013 was used to validate the model. This storm was the only storm remaining after calibration from the 33 events that had significant outflow (less than 90% reduction) and five minute runoff and precipitation data. The details summarizing this storm are included in Table 6. The input storm summary is included in Table A-8 in the Appendix.

**Table 6.** Summary of the storm on September 21, 2013.

| Storm: 9.21.13 | |
|---|---|
| Duration (hrs) | 30 |
| Total Runoff Depth (cm) | 51.4 |
| Total Precipitation In (cm) | 4.9 |
| Total Depth In (cm) | 56.3 |
| Total Depth Out (cm) | 29.1 |

## Statistical Analysis

Nash-Sutcliffe Efficiency (NSE) and the coefficient of determination ($R^2$) values were calculated to determine the accuracy of the Hydrus model using three storms. The $R^2$ value was calculated using the Excel function for regression summaries. The Nash-Sutcliffe Efficiency was calculated using the following equation (Moriasi et al. 2007).

$$NSE = 1 - \left[\frac{\sum_{i=1}^{n}(Y_i^{obs} - Y_i^{sim})}{\sum_{i=1}^{n}(Y_i^{obs} - Y_i^{mean})^2}\right] \quad (23)$$

One is the optimal value for both of these statistical measures (Moriasi et al. 2007).

# CHAPTER IV

# RESULTS AND DISCUSSION

## Field Data Analysis

### Storm Event Analysis

The total rainfall in 2013 and 2014 was 30.07 and 20.3 in., respectively. The rainfall for the first part of 2015 (January 1 to July 6) amounted to 34.48 in. The average annual precipitation is 40.97 in. for Dallas, TX (U.S. Climate Data 2015). The hydrologic and quality performance evaluation utilized a total of 33 events. The first 11 events were from June to November 2013; the next 17 events were from January to December 2014, and the remaining 5 were from January to February 2015. The precipitation depths and duration of each storm event can be found in Figure 9.

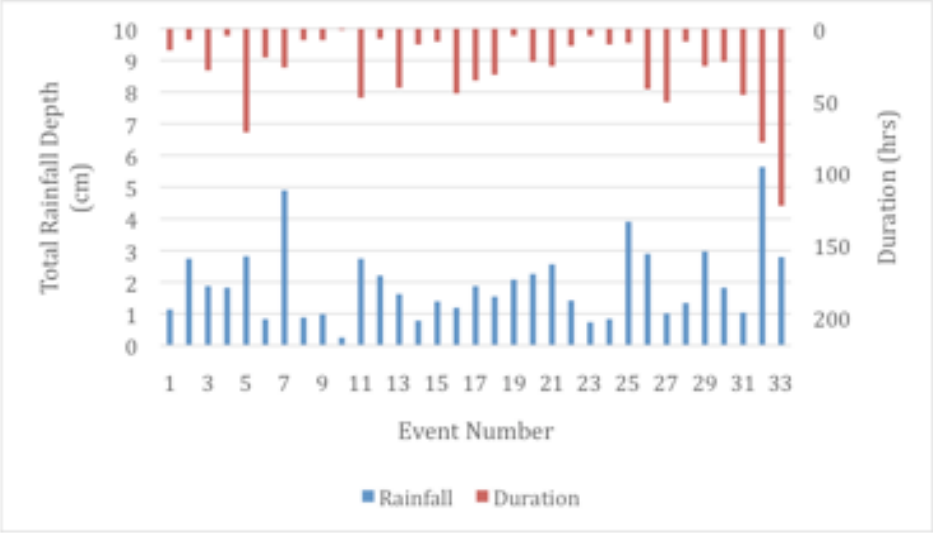


**Figure 9.** Rainfall and duration for 33 rain events monitored at the bioretention site in Dallas, TX, at the AgriLife Research and Extension Center from 2013 to 2015.

The antecedent moisture condition analysis yielded dry conditions for most events except for 2 events (event numbers 16 and 24) that had normal antecedent moisture conditions. The storms evaluated for the Hydrus model are storm event numbers 6, 7 and 8 for September 2, 21, and 28, respectively.

Hydrologic Performance

For the hydrologic analysis, necessary outflow volumes were recorded for only 22 of the 33 storm events. This data is provided in Table A-1 in the Appendix. The inflow volume for 8 of those 22 events between April to August 2014 (event numbers 13 to 22) were calculated using the SCS Curve Number method (Equations 1 through 4). Using a curve number (CN(I)) for dry antecedent moisture conditions equal to 89, two events (15 and 22) yielded inflows smaller than outflows. This is more than likely caused by the variation (standard deviation = 9) in the estimated curve number. Comparing the measured inflow to calculated inflow using a CN(I) equal to 89 resulted with an $R^2$ value of 0.6. The curve number for the measured inflow ranges between 75 and 99 as shown in Table A-3 in the Appendix.

The 20 events that contained hydrological data (excluding events 15 and 22) resulted in a volume reduction of 76%. The summary for the inflow and outflow volumes are presented in Table 7.

**Table 7.** The inflow, outflow and water volume reduction bioretention summary for 20 rainfall/runoff events at the bioretention site at the AgriLife Research and Extension Center in Dallas, TX.

| | Mean | Median | Range |
|---|---|---|---|
| Inflow (L x$10^3$) | 16.9 | 12.2 | [1.5, 96] |
| Outflow (L x $10^3$) | 5.4 | 0.14 | [0, 54] |
| Reduction (%) | 76 | 97.8 | [24, 100] |

There were two events (10 and 24) for which the runoff volume was completely attenuated and 0 outflow was recorded. Both of these events were in the top 20% of events with smaller rainfall depths as shown in Table A-4 in the Appendix. However, having less total rainfall per event was not a clear indication of better attenuation as events in the lower 10% with larger rainfall depths were also able to have high attenuation percentages. There is a large range in attenuation potential within this bioretention cell from 24% to 100%; therefore, it makes sense that there are large discrepancies in volume reduction averages when comparing different bioretention cells. It is likely that a combination of rainfall total, duration, AMC, and design guidelines contribute to the variation of runoff volume reduction.

Nitrate Removal Performance

Due to equipment malfunction, only 19 events were analyzed for nitrate removal performance. Events without measured outflow nitrate concentrations were not used. For four of the events for which outflow data was provided or assumed (100% volume reduction) but where the inflow measurements were missing an average inflow

concentration (1.11 mg $L^{-1}$) was used. Input concentrations ranged from 0.03 to 4.02 mg $L^{-1}$ and had a mean of 1.11 mg $L^{-1}$ and a standard deviation of 0.89 mg $L^{-1}$. The output concentrations ranged from 0 to 2.72 mg $L^{-1}$ and had a mean of 0.67 mg $L^{-1}$ and a standard deviation of 0.61 mg $L^{-1}$. By comparing the input and output nitrate concentration levels from the bioretention cell in Dallas, the paired t tests showed that there was a statistically significant nitrate mean reduction of 26% with a p-value of 0.002. The summary data for this analysis can be found in Table A-5 in the Appendix.

The mean reduction of nitrate concentration included two additional events (10 and 24) for which the volume was completely attenuated and 100% reduction was assumed and the average inflow concentration (1.11 mg $L^{-1}$) was used. There were five events (numbered 11, 13, 17, 26, and 28) where effluent nitrate increased from 9% to 72% of the input concentration as shown in Table A-5 in the Appendix. This is typically attributed to buildup of grass clippings and other contributing organic materials that drain into the bioretention cell or simply infrequent vegetation maintenance that causes overgrowth within the bioretention cell (Chen et al. 2013; Hunt et al 2006; Li and Davis 2009). The insignificant reductions could be attributed to occasional increases in nitrate due to inadequate levels of cell maintenance required to prevent accumulation of nutrient pollutants as discussed previously, but also simply due to the production of nitrate from ammonium during the nitrate cycle.

The mean mass reduction computed to evaluate the effect of volume reduction was 81% with a range of 16.4% to 100% as compared to a concentration reduction of 39% with a range of -72.7% to 100% for 10 events for which both volume and nitrate concentrations were known or implied (100% volume reduction). The mean mass and concentration reductions for these 10 events were statistically significant with a p-value of 0.02 and 0.01, respectively. The negative reductions in these 10 events were attributed to events numbered 13 and 17 as in the previous analysis. The summary data for this analysis can be found in Table A-7 in the Appendix. As percentage mean mass reduction is more representative of bioretention pollutant removal efficiency (Davis 2007), these results show that the bioretention cell in Dallas is effective at removing most of the nitrate. It also shows how attenuation of water quantity greatly affects the water quality results.

The nitrate (as N) limit set by EPA is 10 mg $L^{-1}$ for drinking water standards (EPA 2014). None of the samples exceeded this limit as can be seen in Figure 10; however, there is a concern for nitrate concentrations in the Upper Trinity River watershed where this bioretention cell is located (TCEQ 2012). Therefore, it is imperative to understand how effective a bioretention cell can function within this region. The probability plot in Figure 10 is a good tool to identify the probability of exceedance for future target limits, and also serves to compare output and input concentrations. In order to ensure that this graphical representation depicted the treatment for the bioretention cell the two events with 100% attenuation were not included (Davis 2007). The input and output nitrate concentrations were arranged from largest to smallest and then both data sets were assigned rankings (i=1

(largest) to 17 (smallest)). The probability (p) was calculated for each event. The input and output concentrations were plotted versus the corresponding probabilities on a graph with a log y axis. The x axis was set to plot in reverse order.

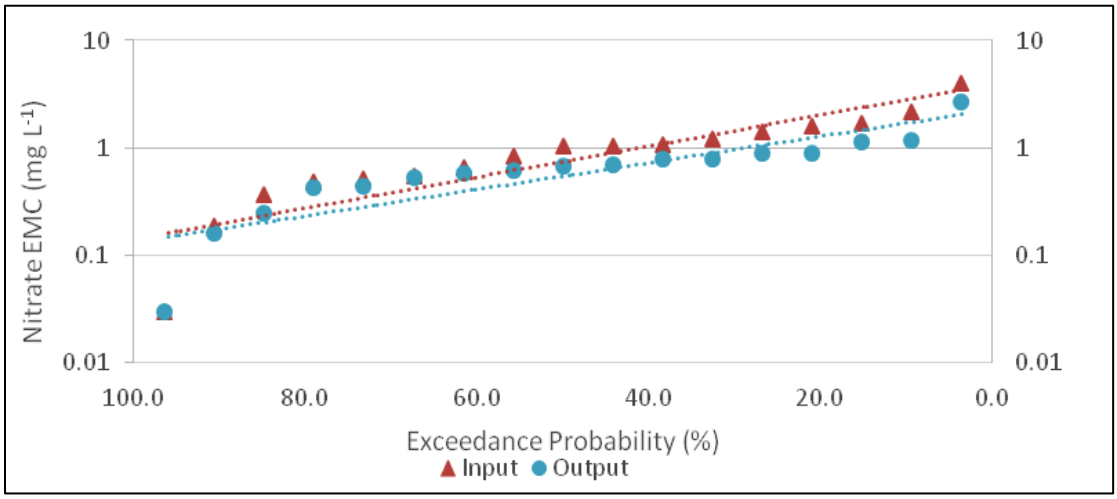


**Figure 10.** Probability plot of input and output nitrate as nitrogen EMC for the bioretention cell at the Texas A&M AgriLife Research and Extension Center in Dallas, Texas.

From the exceedance probability plot, it is shown that the output nitrate concentration can be reduced from the input through the utilization of the bioretention treatment. The bioretention cell can decrease the percent probability that a nitrate threshold value will be reached. When using water quality parameters describing the Potomac River Basin used to evaluate bioretention cells in Maryland (Li and Davis 2009; Davis and McCuen 2005), the results of nitrate reduction performance of a site with or without a bioretention cell become more applicable for evaluating the benefits of implementing a bioretention cell at a certain site. As shown in Table 8, in order to produce a water quality characterized as fair, the bioretention cell provides a 16% improvement and reduces the probability of

exceedance to 5%. As the criteria get stricter the bioretention cell is less beneficial to implement in terms of nitrate reduction. The 0.2 mg $L^{-1}$ is much more stringent than the 10 mg $L^{-1}$ designated for drinking water. Therefore, upon deciding whether or not to implement bioretention cells for nitrate reduction, it is important to note desired nitrate limits, average inflow concentrations, and potential bioretention nitrate reductions. Producing average potential bioretention nitrate reductions from similar areas (climate and soil) from field experiments such as this can help generate background information to make implementation decisions.

**Table 8.** Probability of nitrate as nitrogen exceedance for specific water quality parameters.

| | | Prob. Of Exceedance % | | |
|---|---|---|---|---|
| Water Quality | Nitrate EMC max[a] (mg $L^{-1}$) | W/out Bioretention | W/ Bioretention | % Improvement |
| Fair | 2 | 21 | 5 | 16 |
| Good | 0.6 | 57 | 47 | 10 |
| Excellent | 0.2 | 90 | 87 | 3 |

[a]Davis and McCuen (2005).

## Soil Parameters

Saturated Hydraulic Conductivity

The 30 measured saturated hydraulic conductivities ranged overall from 10.4 to 289.5 cm $hr^{-1}$. The 10 location average saturated hydraulic conductivities ranged from 14 to 234 cm $hr^{-1}$. The saturated hydraulic conductivity map is shown in Figure 11; these values are also

provided in Table A-6 in the Appendix. The forebay is located above where sample 3 was taken.

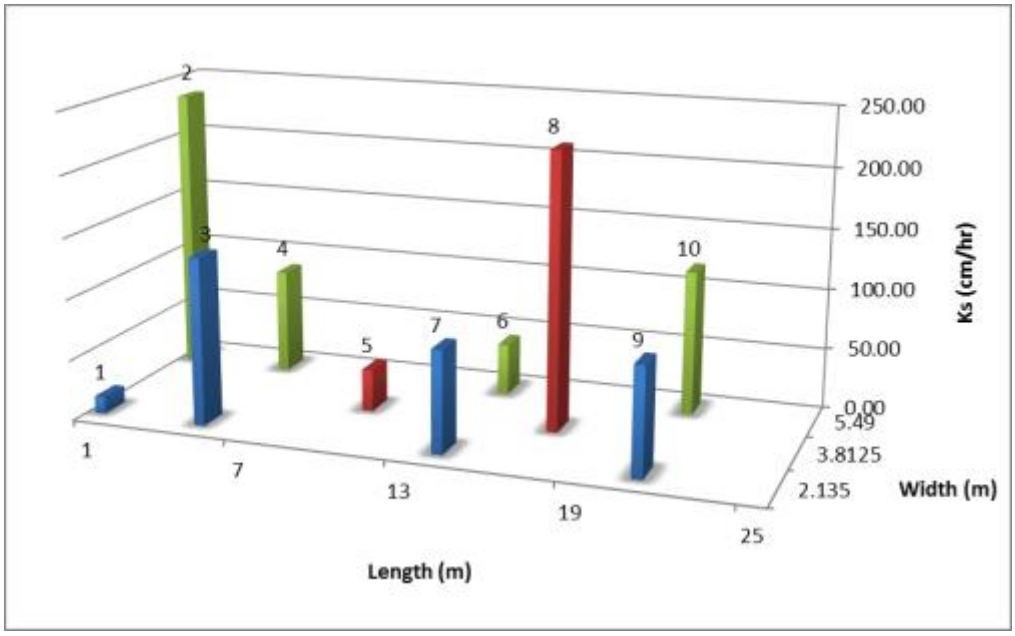


**Figure 11.** A saturated hydraulic conductivity map based on the soil core collected as located within the bioretention cell at the Texas A&M AgriLife Research and Extension Center in Dallas, Texas.

The overall range in values can be attributed to the location from which each sample was taken. There is no clear reason for the variation between each. It can be assumed that in location 8 the surface is not as compressed or clogged due to protection from the overflow basin as opposed to location 5. Although care was taken to obtain consistent samples, it is also possible that media interferences in the sample such as small roots or rocks resulted in higher saturated hydraulic conductivity values for samples that had larger standard deviations such as sample location 8. Figure 12 shows the standard deviation for each

core sample. The sample numbers correspond with the labeled numbers in the saturated hydraulic conductivity map.

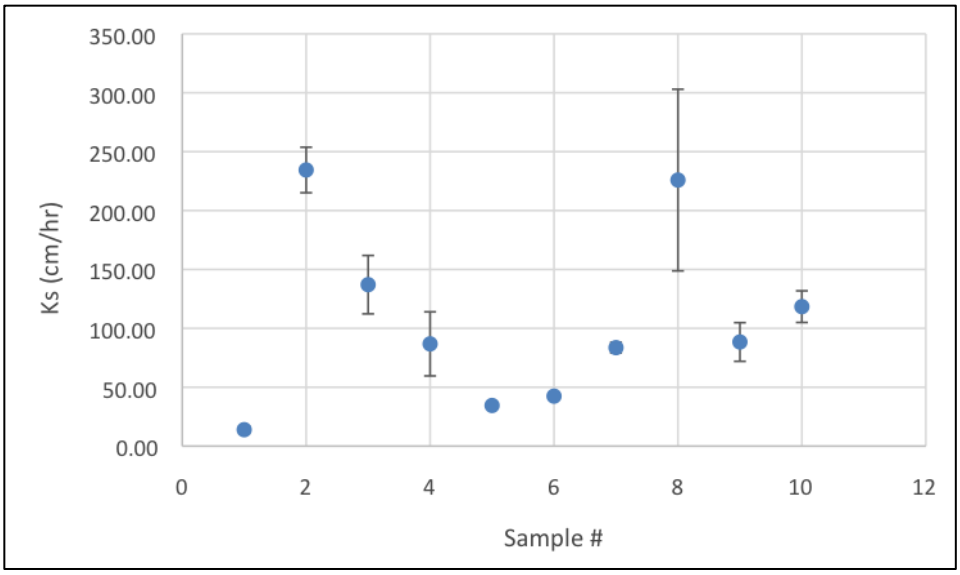


**Figure 12.** The standard deviation of the average saturated hydraulic conductivity for each of the ten core samples.

Although sample #8 had the highest standard deviation at 77 cm $hr^{-1}$**,** possibly attributed to experimental error, sample #2 with a similar saturated hydraulic conductivity had a much lower standard deviation at 19 cm $hr^{-1}$. The mean saturated hydraulic conductivity was 107 cm $hr^{-1}$ (42 in $hr^{-1}$) with a standard deviation of 76 cm $hr^{-1}$. This value is very similar to the design value of 127 cm $hr^{-1}$ (50 in $hr^{-1}$). The reduction in the overall saturated hydraulic conductivity can be attributed to clogging over time. It can also be explained by the four week drop phenomenon described by (Le Coustumer et al. 2007).

Pressure Chamber Experiment

Four water contents were obtained at different pressure settings up to 98 kPa. The results from the pressure chamber experiment are shown in Table 9. The standard deviation for each pressure setting (0 kPa, 10 kPa, 33 kPa, and 98 kPa) is as follows 0.08, 0.02, 0.07, and 0.04, respectively.

**Table 9.** Gravimetric water content (u), volumetric water content ($\theta$), bulk density ($\rho_b$), and porosity ($\varepsilon$) for the bioretention media using a pressure chamber.

| Pressure (kPa) | Gravimetric Water Content, u ($g\ g^{-1}$) | Volumetric Water Content, $\theta$ ($cm^3\ cm^{-3}$) | Average Bulk Density, $\rho_b$ ($g\ cm^{-3}$) | Average Porosity, $\varepsilon$ |
|---|---|---|---|---|
| 0 | 0.47 | 0.56 | 1.19 | 0.55 |
| 10 | 0.3 | 0.36 | | |
| 33 | 0.25 | 0.3 | | |
| 98 | 0.21 | 0.24 | | |

These water content values along with the results from the sensitivity analysis and calibration process were used to obtain a soil water characteristic curve.

**Sensitivity Analysis**

A sensitivity analysis was conducted using Hydrus. The sensitivity analysis consisted of changing initial estimates, from the values in Table 2, of the residual water content, saturated water content, inverse of the bubbling pressure, pore size distribution index, saturated hydraulic conductivity, and initial conditions (in terms of pressure head) by a

targeted 50% increase and decrease. The cumulative depth output with the initial inputs was 4.62 cm.

Residual Water Content

A decrease in the residual water content from 0.06 to 0.03 for the engineered layer resulted in a smaller cumulative output depth (4.08 cm versus 4.62 cm) as shown in Figure 13. An increase in the residual water content from 0.06 to 0.09 for the engineered layer resulted in a larger cumulative output depth of 4.99 cm. The sensitivity analysis resulted in no visible change for the manipulation of the residual water content for the gravel layer and was therefore excluded from the visual representation.

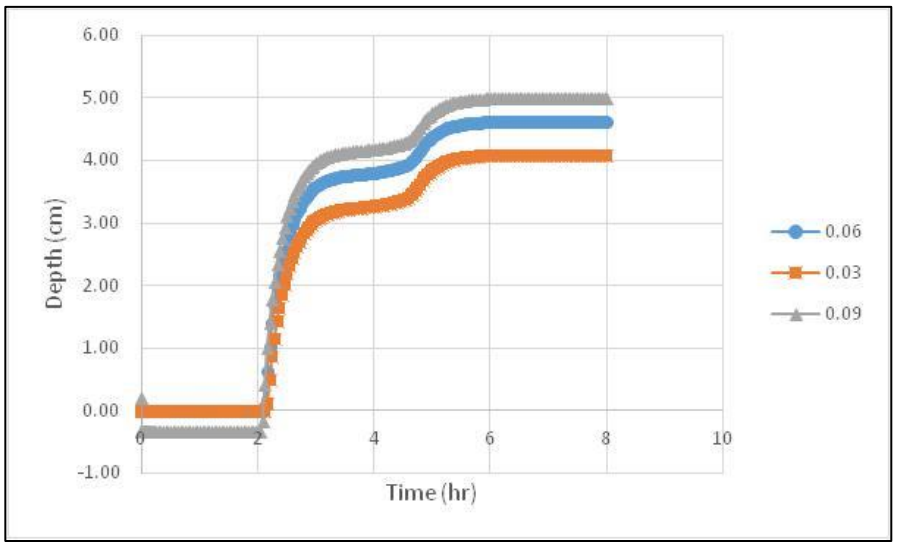


**Figure 13.** Sensitivity analysis of the residual water content for the engineered media layer.

Saturated Water Content

The initial saturated water content was set to 0.5 for the engineered media layer and 0.42 for the gravel layer resulting in an outflow of 4.62 cm. A smaller saturated water content (0.25) for the engineered media layer showed an output that was twice as large at 9.23 cm, and a larger saturated water content (0.75) showed a much smaller output of 0.08 cm as shown in Figure 14. An increase in the saturated water content for the gravel layer (0.63) showed a very small increase in output with an outflow of 4.76 cm, and the decrease in this value (0.21) showed no change.

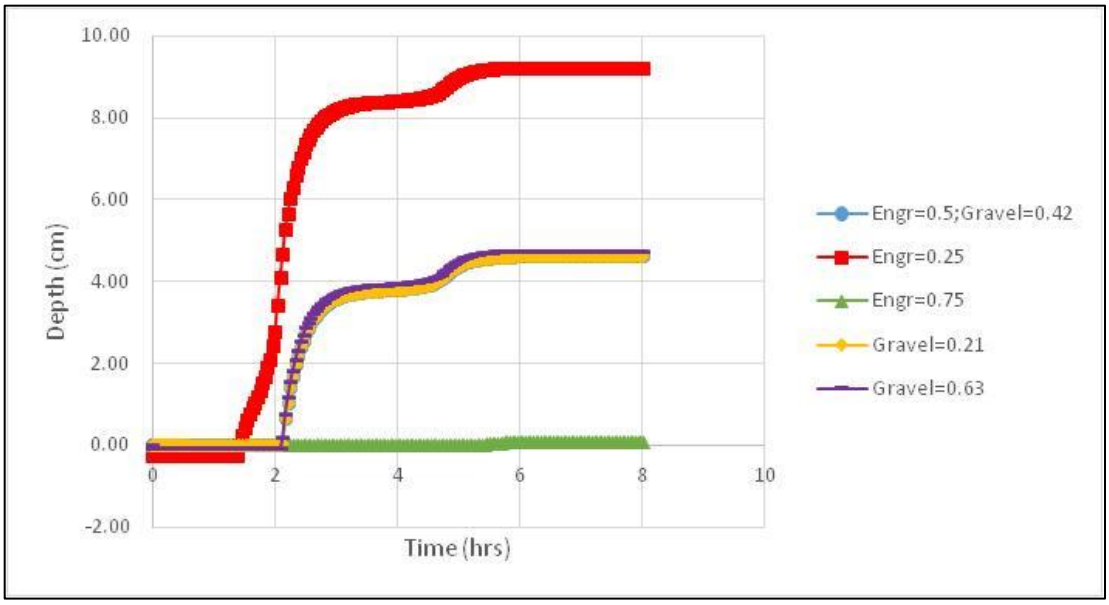


Note: Gravel= 0.21 overlaps Engr=0.5; Gravel=0.42

**Figure 14.** Sensitivity analysis for the saturated water content for the engineered and gravel media layers.

Bubbling Pressure Inverse

An increase in the inverse of the bubbling pressure for the engineered media from 0.002 to 0.003 decreases the output from 4.62 cm to 2.64 cm. A slight decrease (15%) to 0.0017 resulted in an increase in output to 5.52 cm. Only a 15% decrease was applied, because anything larger resulted in a water balance larger than zero indicating that an error had occurred with the simulation. The changes in the gravel bubbling pressure inverse showed no changes in output as shown in Figure 15 via the overlap of the gravel output curves with settings equal to 0.01, 0.05, and 0.075.

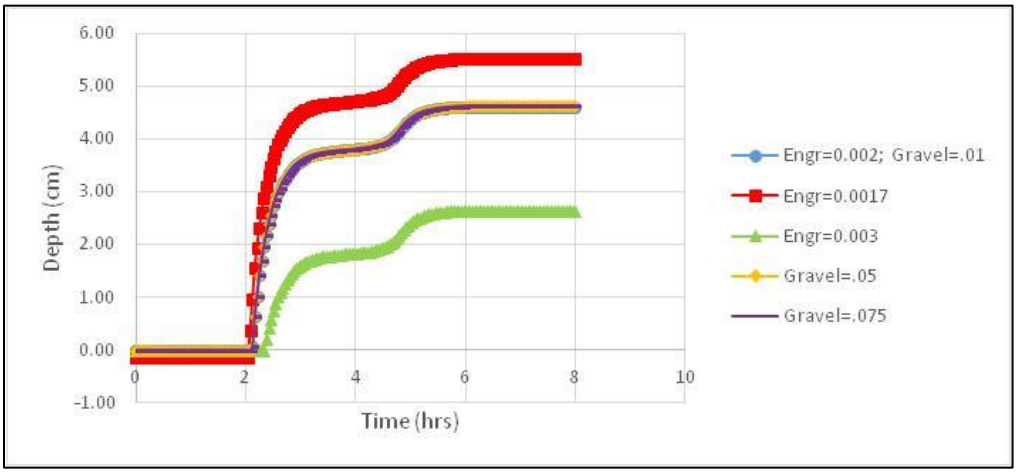


**Figure 15.** Sensitivity analysis of the inverse of the bubbling pressure for both engineered and gravel layers.

Pore Distribution Index

The pore distribution index values were initially set to 1.36 and 2.5 for the engineered media and gravel layers with an output of 4.62 cm. Decreasing the n value by 26% to the smallest possible n value of 1.001 (Hydrus limit) for the engineered media, resulted in a

very large output of 51.3 cm with a different rate of increase as the original as shown in Figure 16. Increasing this value by 21% (the highest possible that generated a water balance percentage near 0) to 1.64 yielded a smaller output and a negative portion indicating an error. It is unclear what would result in this error; it may be that increasing this parameter requires the iteration criteria to be changed in order for the Hydrus simulation to converge properly. There was no change in the output when changing the value of n for the gravel layer by positive and negative 50% (1.25 and 3.75); therefore, these were omitted from the graphical representation below in Figure 16.

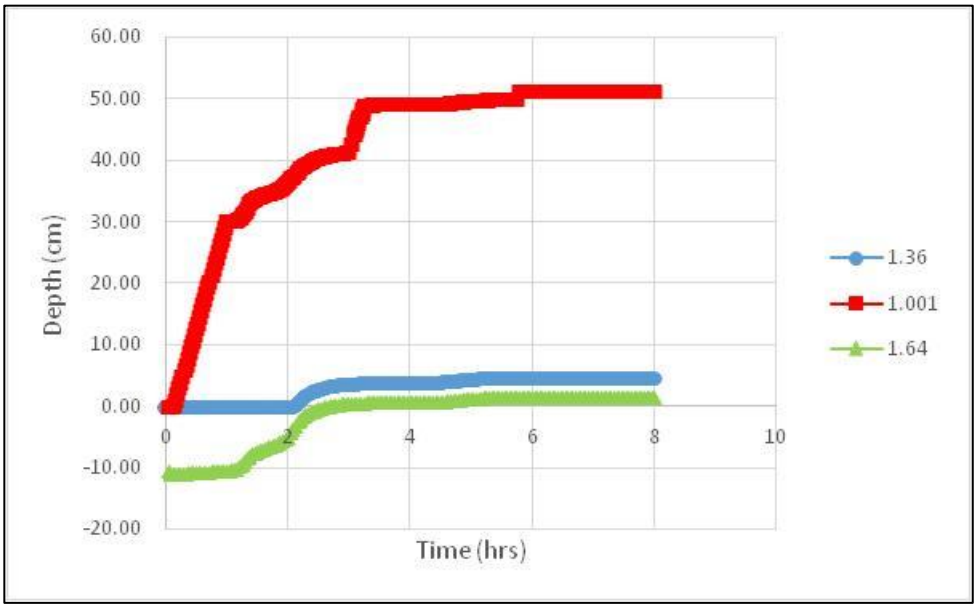


Note: n=1.001 is 26% smaller and n=1.64 is 21% larger.

**Figure 16.** Sensitivity analysis of the pore distribution index for the engineered media layer.

Saturated Hydraulic Conductivity

The initial saturated hydraulic conductivity was set to 107 cm $hr^{-1}$. The 50% reduction in the saturated hydraulic conductivity value to 53.5 cm $hr^{-1}$ did not differentiate the outflow from the original value. Due to water balance errors, a 17% and 100% increase were used to denote change in the output. The 17% increase (125 cm $hr^{-1}$) showed little change from 4.62 cm to 4.68 cm, but the 100% increase (214 cm $hr^{-1}$) showed a substantial increase in output to 7.45 cm. No significant changes were noticed when the saturated hydraulic conductivity value for the gravel media was changed, and therefore, it was not included in the graphical representation below in Figure 17.

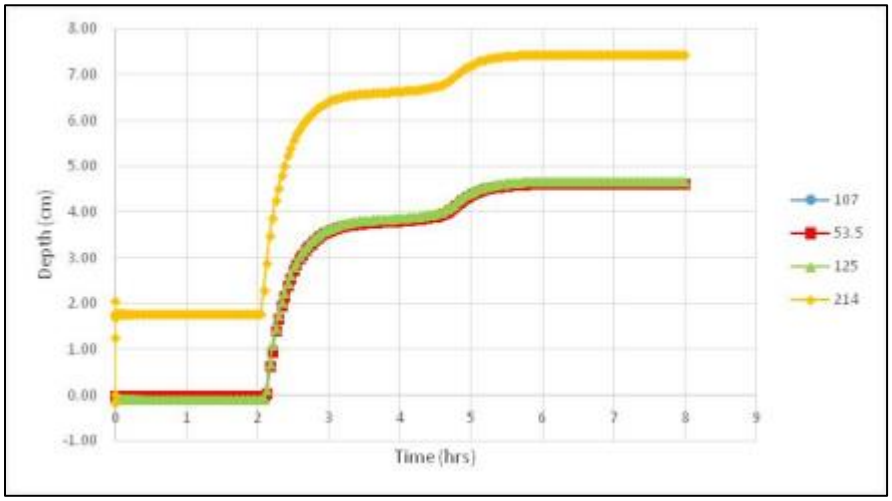


Note: The increases in the saturated hydraulic conductivity are by 17% and 100% larger than the initial value.

**Figure 17.** Sensitivity analysis for the saturated hydraulic conductivity in the engineered media.

Initial Conditions

The initial moisture conditions in the cell were varied to see the effects on the outflow. It can be seen from Figure 18 that wet conditions substantially increase outflow when compared to dry conditions.

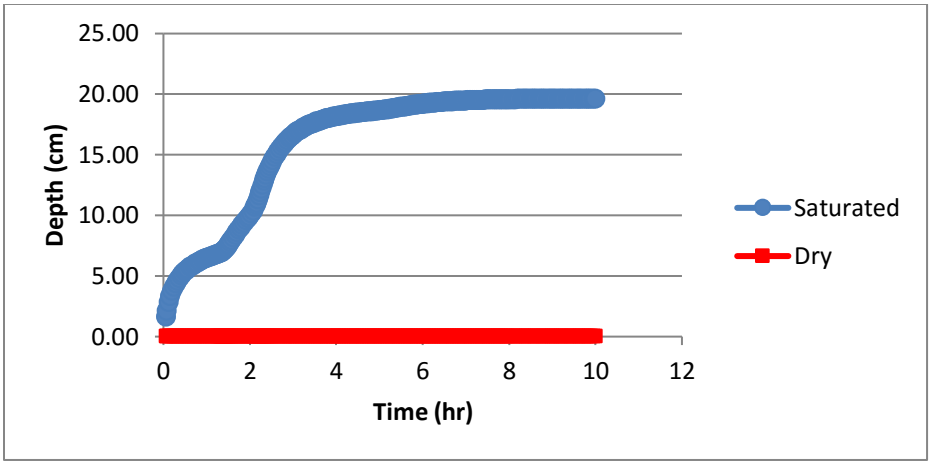


**Figure 18.** Sensitivity analysis for initial water conditions within the bioretention profile.

The initial conditions were defined such that for the saturated curve a zero cm pressure head is at the top of the bioretention cell and a 61 cm pressure head is at the bottom of the bioretention cell with a linear distribution in between. The dry initial conditions were determined by the field capacity of each material. The bottom of the profile was set to a random parameter of -54 and the top of the gravel layer was set to field capacity (-74 cm) with a linear distribution. The top of the cell was also set to field capacity (-171 cm) with a linear distribution from the gravel layer. Equidistant nodes (the Hydrus default) were used to assign the initial conditions via linear distribution using the Hydrus tool in the graphical analysis as shown in Figure 8. The graphical tool allows users to set the initial

conditions by selecting the node range based on depth and setting top and bottom values. The specific node parameters selected are shown in Table 10.

**Table 10.** Saturated and dry initial conditions for the sensitivity analysis.

| | Pressure Head (cm) | |
|---|---|---|
| Depth (cm) | Saturated | Dry |
| 117 | 0 | -171 |
| 25 | | -74 |
| 0 | 61 | -54 |

## Calibration

To achieve adequate levels of outflow the soil parameters, time discretization parameters, iteration criteria, and the initial conditions were calibrated within the Hydrus model. The initial values were based on the pressure chamber experiment, the estimated soil water characteristic curve, literature recommendations, and model simulations as discussed previously.

### Soil Parameters

The predicted curve created from the pressure chamber results and target outflow simulations is shown in Figure 19. The resulting RSS for the predicted curve was 0.0003. The yielded engineered media parameters for the soil water characteristic curve can be found in Table 11.

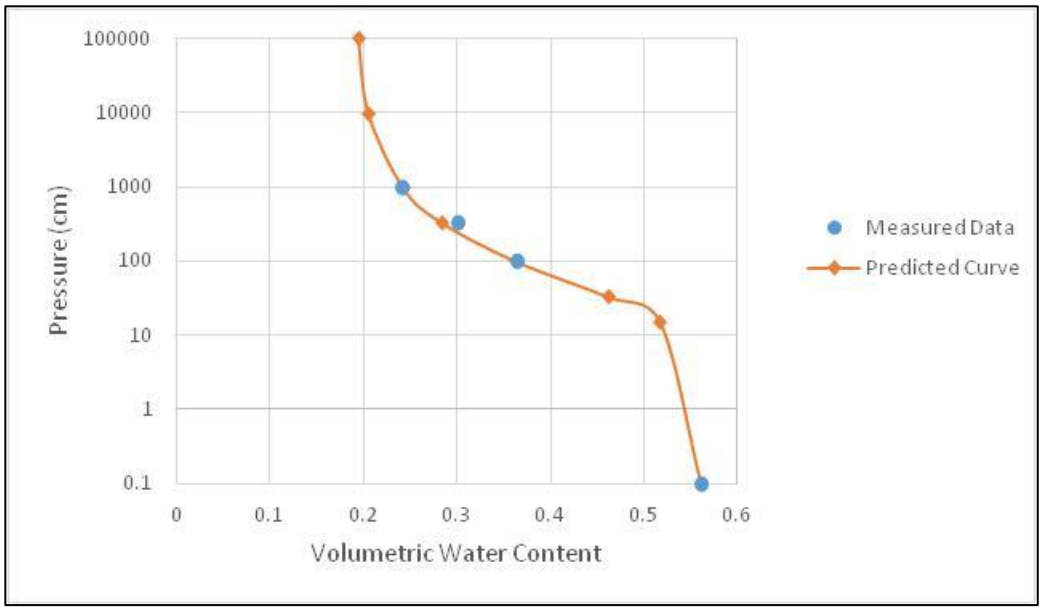


**Figure 19.** The predicted soil water characteristic curve for the bioretention cell and the actual measured points from the pressure chamber experiment.

**Table 11.** Resulting engineered media input summary for Hydrus model based on soil water characteristic curve estimation.

| Media | Depth (cm) | Residual Water Content, θr | Saturated Water Content, θs | Inverse Bubbling Pressure, α | Pore Distribution Index, n | Saturated Hydraulic Conductivity, Ks | Tortuosity parameter, l |
|---|---|---|---|---|---|---|---|
| Engineered | 25-117 | 0.19 | 0.56 | 0.039 | 1.54 | 107 | 0.5 |

The parameters shown in Table 11 for the engineered media were used as input for the Hydrus model. The highest residual water content value reported by Carsel et al. (1988) is that of sandy clay (0.1+/-0.013). The bioretention cell residual water content had a standard deviation of 0.08, putting it within range of this soil type. Moreover, the resulting saturated water content falls within the range for a silt soil (0.46+/-.11) (Carsel et al. 1988). Because the composition of the engineered media is 50% yard waste compost, 25% sand, and 25% native soil (Houston Clay), it seems that these properties are representative of

the media. The slightly higher value for the residual water content could be attributed to characteristics of the engineered media such as the high saturated conductivity. It is also possible that the soil parameters could range with location throughout the bioretention cell as the saturated hydraulic conductivity did. However, the location was not specifically accounted for within this experiment as an explicit system for using the soil cores systematically for the pressure experiments could not be defined with the number of samples needed for each test.

The input parameters used for the gravel layer remained the same as in the sensitivity analysis, shown in Table 12.

**Table 12.** Soil properties for the gravel layer.

| Media | Depth (cm) | Residual Water Content, $\theta_r$ | Saturated Water Content, $\theta_s$ | Inverse Bubbling Pressure, $\alpha$ | Pore Distribution Index, n | Saturated Hydraulic Conductivity, Ks | Tortuosity parameter, l |
|---|---|---|---|---|---|---|---|
| Gravel[a] | 0-25 | 0.005 | 0.42 | 0.1 | 2.5 | 3000 | 0.5 |

[a]Adapted from Filipovic (2014).

Initial Conditions

The initial conditions were varied until the outflow in Hydrus was equivalent to the measured outflow. The starting point for calibration was a total of 44 cm in water content. The resulting initial conditions for the two calibrated storms are as follow in Table 13. The initial pressure head for September 2$^{nd}$ and 28$^{th}$ is equivalent to a total of 48.3 and 47.8 cm in water content, respectively. The total water content was calculated using the

soil water characteristic curve equation to solve for individual water contents at specific locations on the media profile as outlined from the graphical tool using Hydrus.

**Table 13.** Initial conditions for the calibrated storms in terms of pressure head.

| | Pressure Head (cm) | |
|---|---|---|
| Depth (cm) | 9.2.13 (cm) | 9.28.13 (cm) |
| 117 | -22 | -194 |
| 33 | | 0 |
| 0 | -21 | 15 |

Iteration Criteria

The time discretization, iteration parameters, time step control, and interpolation limits used to simulate the model were determined through Hydrus recommendations and trial and error with the goals of being able to obtain some results and obtaining a zero water balance error. The Hydrus model would not converge with small maximum number of iterations or smaller pressure head tolerance limits; however, the parameters chosen for the model simulations as shown in Figure 20 and Figure 21 simulated results with zero water balance errors. Note that the final time in Figure 20 varied depending on the storm event.

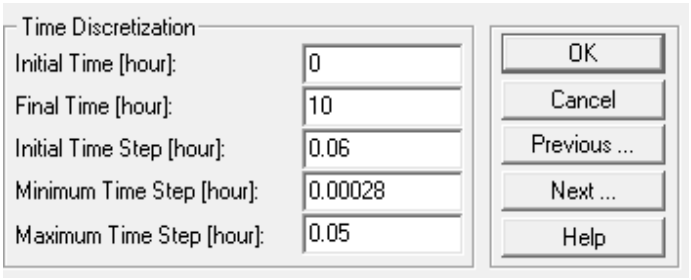


**Figure 20.** The time discretization used within the Hydrus model.

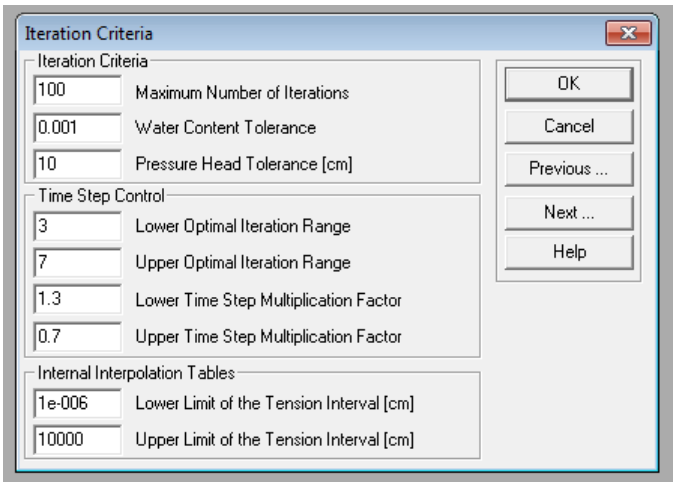


**Figure 21.** The iteration criteria used for calibration after runs that resulted in good results.

Storm Results

The results of the two calibration storms yielded good results after several trials. For the September 2nd storm the NSE value was 0.91 and the $R^2$ value was 0.92 when comparing the simulated outflow and measured outflow. The results are shown in Figure 22. The simulated outflow and saturated water level curve are from Hydrus output data. The saturated water level curve was taken from the bottom pressure output from Hydrus and converted to a bioretention level using the soil porosity. The measured outflow and the inflow are plotted from the measured data.

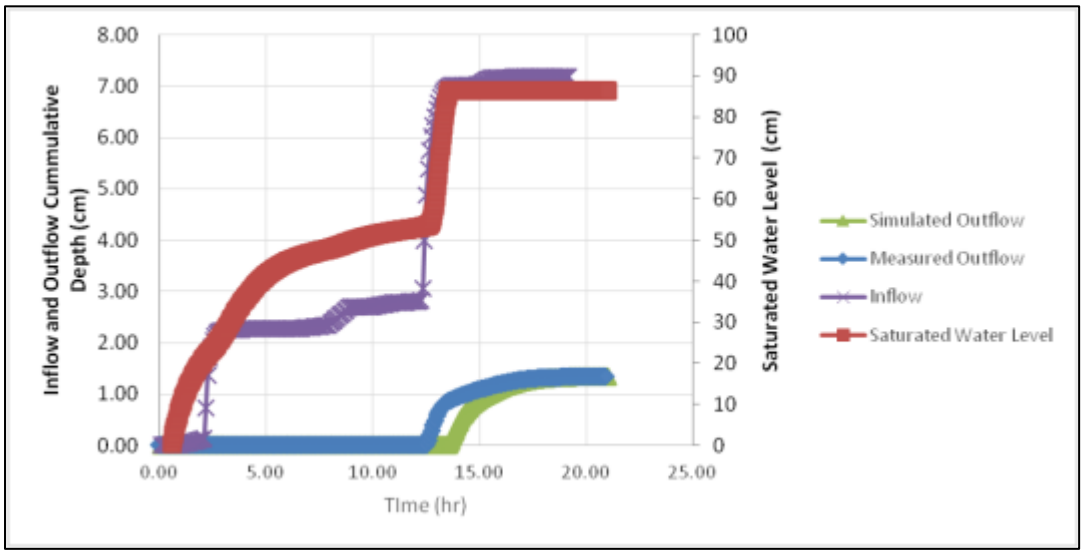


**Figure 22.** Results from the Hydrus simulated storm on September 2, 2013.

For the storm on September 2, 2013, the saturated water level reached 0 cm at the bottom of the profile within the first half hour and then it continued to rise to an 86.3 cm depth in the bioretention cell as precipitation and runoff accumulate within the profile as indicated by the inflow curve. The level of the outlet is at 86.3 cm. The water table within the bioretention cell remains at this level for the remainder of the storm. Outflow was observed when the outlet level was reached as indicated by the simulated and measured outflow curves.

The water storage curve from Hydrus in Figure 23 shows that the bioretention cell stores 6.4 cm of water with this event. The initial water stored is 48.6 cm and a total of 55 cm are stored before outflow begins (in terms of water measurements).

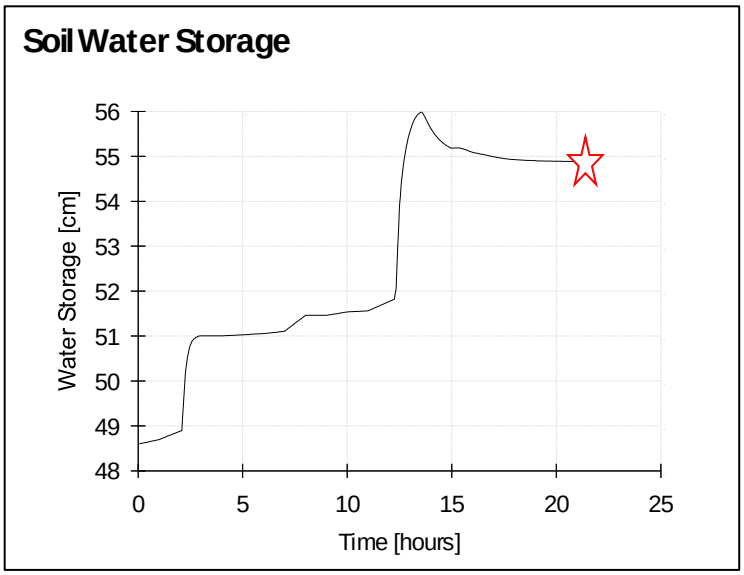


Note: The star denotes the final water pressure at 55 cm.

**Figure 23.** Soil water storage curve output from Hydrus simulation for storm on September 2, 2013.

For the storm on September 28, 2013, the saturated water level was 48.6 cm initially, as shown in Figure 24. This indicates that the bioretention cell had not been emptied from the previous storm, but some water was lost to exfiltration and evapotranspiration. If the bioretention cell would have an impermeable membrane to inhibit water lost through exfiltration the initial water level in the cell would remain at 55 cm since it was known that an outflow event occurred on September 21, 2013. The water level drops to 33.6 cm within the first two hours of the event without any outflow. It is unclear why this drop occurs, but it could be an error attributed to the estimated initial pressure conditions. There could be a variation from the initial water content displacement between the actual field conditions and the values indicated with the graphical tool via linear distribution. As inflow continues to accumulate the water reaches the outlet level at 86.3 cm.

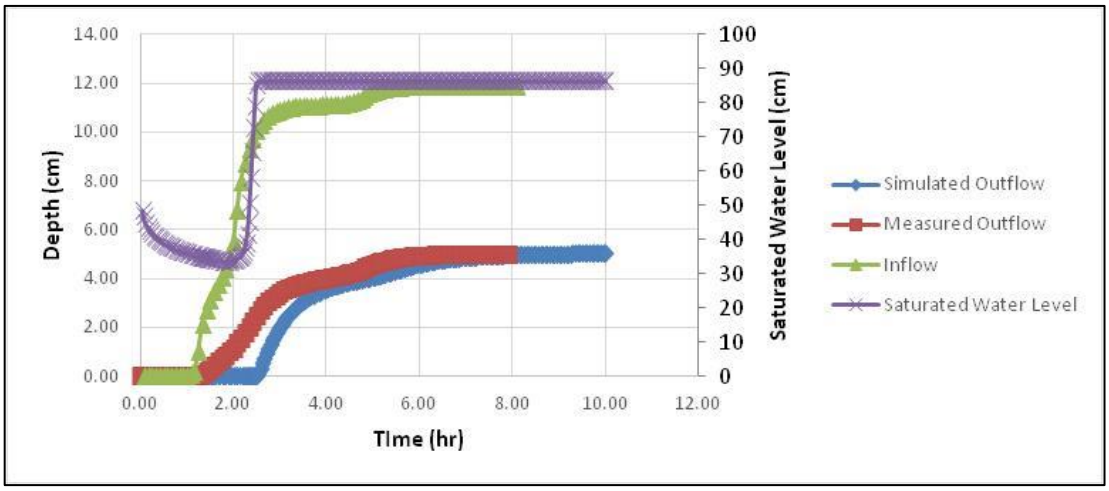


**Figure 24.** Results from the simulated storm on September 28, 2013.

The water storage curve from Hydrus in Figure 25 shows that the bioretention cell stores 7.6 cm of water with this event (in terms of water content). The initial water content is 47.4 cm and it begins to empty at 55 cm. The storm on September 2nd and 28th both resulted in an 11% error between the measured (5.8 cm; 6.8 cm) and the simulated water storage (6.4 cm; 7.6 cm) as shown in Table 14.

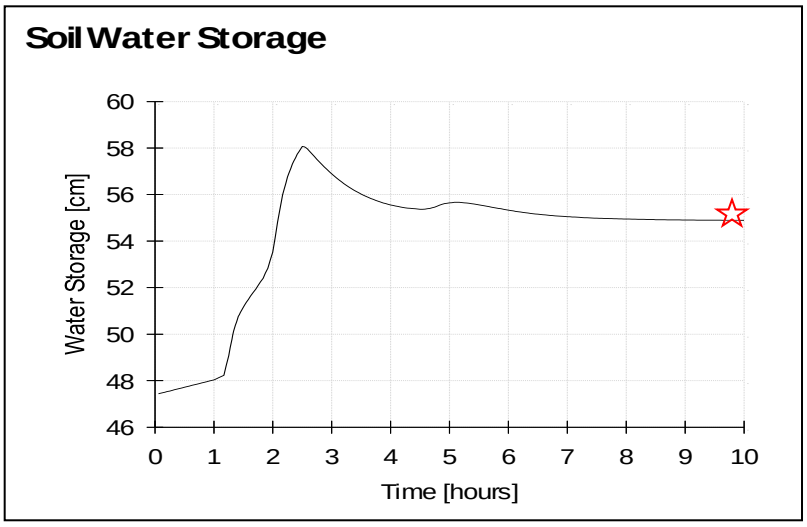


Note: The star denotes the final water pressure at 55 cm.

**Figure 25.** Soil water storage curve output from Hydrus simulation for storm on September 28, 2013.

**Table 14.** Error between measured storage and Hydrus storage.

| Storm | Measured In (cm) | Measured Out (cm) | Measured Stored (cm) | Hydrus Initial (cm) | Hydrus Final (cm) | Hydrus Stored (cm) | Error (%) |
|---|---|---|---|---|---|---|---|
| 9.2.13 | 7.14 | 1.35 | 5.79 | 48.6 | 55 | 6.4 | 10.5 |
| 9.28.13 | 11.8 | 5 | 6.8 | 47.4 | 55 | 7.6 | 10.5 |

## Validation

Storm Results

The calibration of the two storms on September 2nd and September 28th, yielded that the difference in the simulation storage (initial water content estimates subtracted from the threshold value of 55 cm) and the measured storage value yielded 11% errors. By knowing what the threshold or final value needed to be for this bioretention cell, it was possible to estimate the initial water content (Threshold Value-Measured Stored=Initial Water

Content). The rest of the initial inputs for the validation simulation, including the soil parameters and the iteration criteria, were kept the same from the calibration runs.

Initial Conditions

Setting the Hydrus storage to the measured storage at 27.2 cm, the required initial water content was determined to be 27.8 cm to achieve a 55 cm final threshold. This storm was further simulated with varying initial conditions to determine how different this estimated initial condition would be in comparison to one with an 11% error (as in the calibration run and a 5% error). The required initial estimates corresponding to those error percentages are shown in Table 15.

**Table 15.** Simulated storage goals based on a percent error for the storm on September 21st.

| Measured In (cm) | Measured Out (cm) | Measured Stored (cm) | Hydrus Initial (cm) | Hydrus Final (cm) | Hydrus Stored (cm) | Error (%) |
|---|---|---|---|---|---|---|
| 56.3 | 29.13 | 27.2 | 27.8 | 55 | 27.2 | 0 |
| | | | 26.43 | 55 | 28.57 | 5 |
| | | | 30.8 | 55 | 24.2 | 11 |

The initial water content was set using the graphical tool in Hydrus to set the linear distribution that best resulted in a total water content value as close to the required value (27.2 cm) as possible. The initial pressure head for the September 21st simulation is shown in Table 16.

**Table 16.** Initial conditions for validated storm on September 21, 2013 in terms of pressure head.

| | Pressure Head (cm) |
|---|---|
| Depth (cm) | 9.21.13 |
| 117 | -700 |
| 0 | 0 |

Figure 26 shows the results of the simulations for the storm on September 21, 2013 with different initial conditions based on error percentage. Although a 0% error would be optimal, estimates for initial conditions based on 5% and 11% errors were also recorded to evaluate the simulation performance.

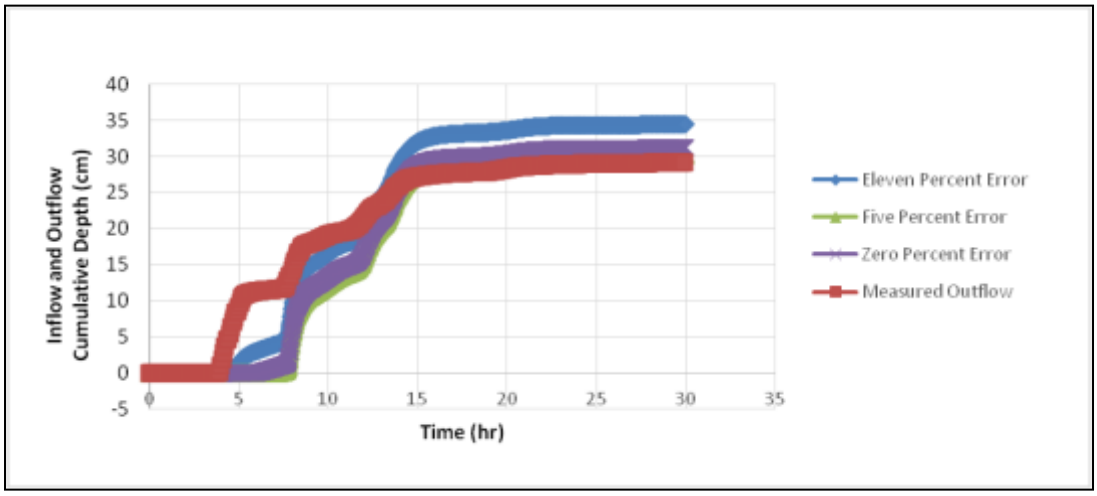


**Figure 26.** Results of simulations for the storm on September 21, 2013 with varying storage errors.

## Statistical Analysis

The results for the storm were good for all the attempted trials. The different statistics are recorded in the Table 17 below. The results of the statistics comparing the simulated outflow and measured outflow depths show that the calibration of the model yielded a

valid method for determining initial water content based on stored water and the threshold value of 55 cm of water stored until outflow. A table showing the simulated outflow and measured outflow depths can be found in Table A-9 in the Appendix.

**Table 17.** Statistics for the different simulations for the storm on September 21, 2013.

| Error (%) | NSE | $R^2$ |
|---|---|---|
| 0 | 0.82 | 0.92 |
| 5 | 0.81 | 0.95 |
| 11 | 0.79 | 0.91 |

**Further Analysis**

The 55 cm threshold is over the 44 cm water capacity, depicted in Figure 7, indicating that an initial total water content of 44 cm is not sufficient as the water is not uniformly displaced throughout the media profile. The total water content at the level of the upturned elbow outlet has to reach 44 cm, and for this bioretention cell in particular it takes a total of 55 cm of water to provide the adaquate 44 cm of pressure at that depth.

Further analysis was conducted to attempt to understand this displacement of water and the threshold value. Although Hydrus does not provide final water content throughout the profile, the initial water content conditions were evaluated. The initial conditions for the storms on September 2$^{nd}$ and September 28$^{th}$ with errors of 11% were used, respectively. The zero percent error was used for the September 21$^{st}$ storm. The initial pressure heads were converted to water contents using the soil water characteristic curve equations for the respective materials. The volumetric water contents were compared to the saturated

water contents to determine an initial percent saturation throughout the media profile. The results are shown in Figure 27.

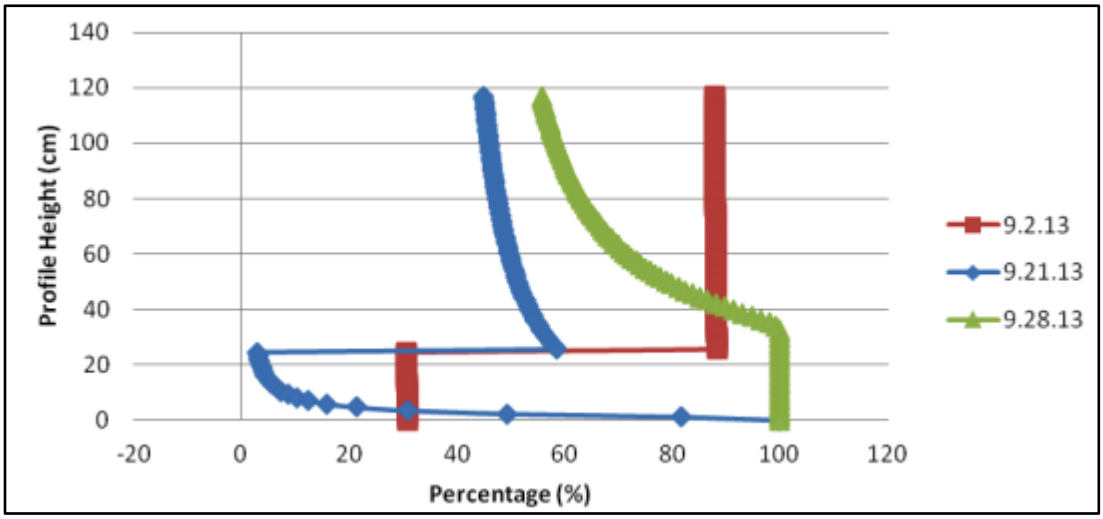


**Figure 27.** Initial percent saturation throughout the media profile for the three storms.

Although 27.5 cm of water is initially found in the bioretention cell for the storm on September 21st the 27.5 centimeters is not the level of water saturation rather the water is distributed throughout the profile such that only the very bottom of the cell is at 100% saturation and the top of the cell is at 45% saturation. The saturated water level curves in Figure 22 and Figure 24 show at what time during the storm and what depth in the profile the percent saturation reaches 100%. Since the saturated water curves in Figure 22 and Figure 24 are at the level of the outlet, it can be assumed that the 55 centimeters it takes for outflow to occur are distributed such that 11 centimeters (55 minus 44) at the top of the profile are dispersed and not at 100% saturation and the 44 cm at the bottom of the profile must be at 100% saturation.

Figure 28 compares the water content depths for the three storms with 55 centimeters being the final water content as determined from the Hydrus simulations. Although the Hydrus simulation assumption was an impermeable layer for the native soil, it is shown in Figure 28 that the water does exfiltrate into the native soil with potential evaporation losses in between storm events.

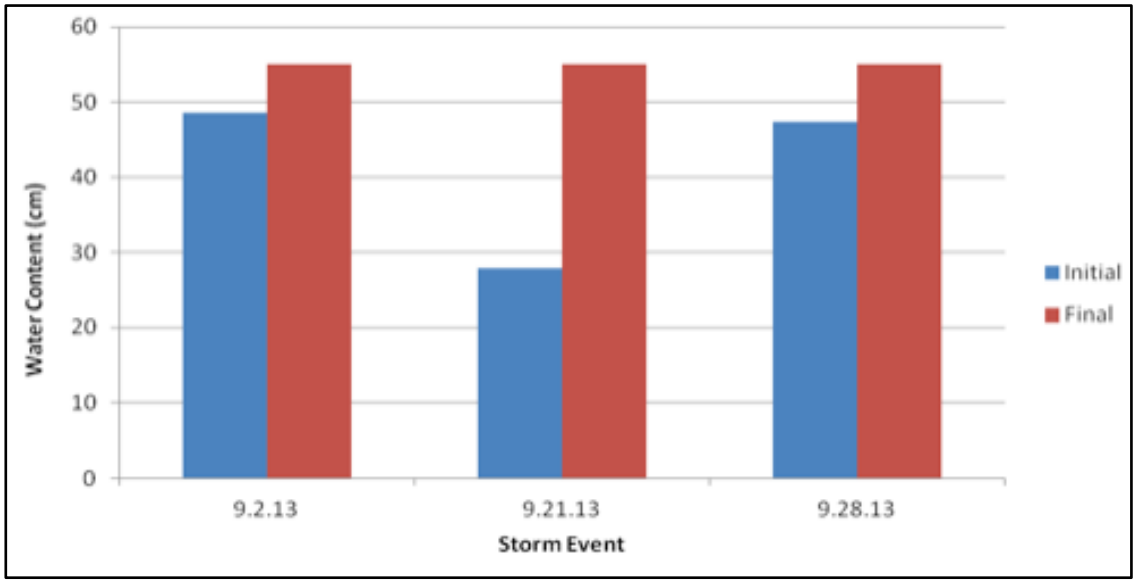


**Figure 28.** Water storage in the bioretention cell for the three storms.

More storm events would need to be analyzed in order to adequately describe the losses in between events. However, by knowing the estimated losses for a system one could potentially predict the percent reduction for upcoming storms.

Table 18 shows the percent volume reductions for each storm, the storm size, total inflow, duration, and initial conditions. As it was determined in the hydrologic data analysis the

storm size between these three events does not appear to have a direct correlation with the percent reduction. The storm on September 2nd is ranked in the top 20% of the 33 storms indicating a smaller storm size in comparison to the storm on September 21 which was the largest of the 33 events (bottom 10%), and the percent volume reductions do not appear to correlate with the storm sizes as storm event # 5 on July 17, 2013 makes up the bottom 10% and has a high percent volume reduction (greater than 90%) similar to the storms in the top 10%. This analysis can be found in Table A-4 in the Appendix.

**Table 18.** Summary of storms with percent reduction and potential factors.

| Storm | Reduction (%) | Storm Size (cm) | Total Inflow (cm) | Duration (hrs) | Initial Conditions (cm) |
|---|---|---|---|---|---|
| 9.2.13 | 81 | 0.8 | 7.1 | 21 | 48.6 |
| 9.21.13 | 58 | 4.9 | 56.3 | 30 | 27.5 |
| 9.28.13 | 48 | 0.9 | 11.8 | 13 | 47.4 |

When comparing the storms on September 2nd and September 28th, the storm on September 2nd had 1.66 times less inflow than the storm on September 28th and the reduction is 1.68 times larger. So even though the storm sizes seem similar, the total water going into the cell differs a bit more drastically and may explain the large difference in percent reduction.

The initial conditions as determined by Hydrus do not show a clear representation of the water distribution within the profile. Figure 27 shows that the 48.6 cm of water contained initially on September 2nd does not fill up the pore space in the same manner as the 47.4 cm contained initially on September 28th. A possible factor contributing to the variation

in water content distribution could be the time between previous storms. For example, the gravel layer during initial conditions on September 28th is still at 100% saturation, because very little exfiltration has taken place since September 21st (the previous storm event). Yet, the gravel layer for September 2nd has been losing water to exfiltration since the previous storm in July. Although the water may not be displaced in the same position, the total amounts are similar. It is unclear how much the initial disposition of the water contributes to the difference in percent reduction.

It could also be possible for some correlation to exist between percent reduction and storm duration. More analysis would need to be carried out to verify the intensity of the storm during the two events. However, by looking at the bottom velocity output from Hydrus as shown in Figure 29, it can be seen that the storm on the 28th with the smaller reduction has faster outflows. This can be attributed to the disposition of the water since the initial conditions in Figure 25 show that on the 28th the bottom portion of the cell was more saturated than on the 2nd. More analysis should be conducted to see if a correlation exists between faster outflows and percent reductions.

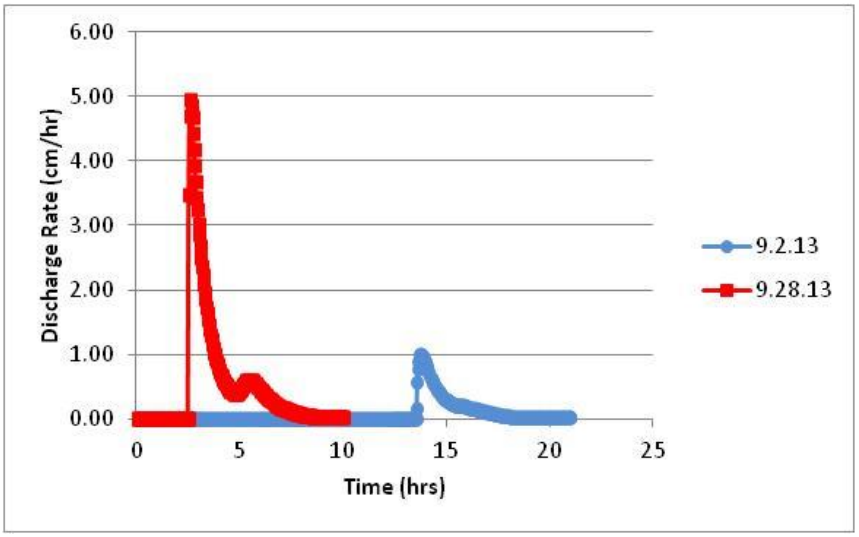


**Figure 29.** Comparison between the discharge rates for the two similar storms.

# CHAPTER V

# CONCLUSION

Data from a bioretention cell in Dallas, Texas, was used to assess the hydrological function and nitrate reduction potential for bioretention cells. The Hydrus-1D software was used to simulate the hydrological functions to provide an in depth look at the performance of the bioretention cell. The Hydrus model was used to provide information on possible avenues for optimizing the volume efficiencies. The following conclusions were made from this study.

The bioretention cell showed a 76% volume reduction for 20 rainfall/runoff events. The inflows ranged from $1.5x10^3$ L to $96x10^3$ L, and the outflows ranged from 0 L to $54x10^3$ L. Interestingly, the size of the storm does not directly relate to attenuation potential to reduce runoff. The bioretention cell reduced nitrate concentration by 26% for 19 events. Attenuation of runoff volume played a crucial role as the concentration reduction was only 39% but had an 81% mean mass reduction for 10 events. The inflow nitrate (as nitrogen) concentrations ranged from 0.48 mg $L^{-1}$ to 2.15 mg $L^{-1}$, and the outflow concentrations ranged from 0 mg $L^{-1}$ to 1.16 mg $L^{-1}$. For those 10 events, the volume reduction in combination with the concentration reduction yielded an inflow mass range of 2,219 mg to 39,538 mg and outflow range of 0 to 10,296 mg for nitrate (as nitrogen). If the runoff volume reduction can be improved, the mean mass reduction of nitrate will also improve. Therefore, by targeting improvements in runoff volume reduction nitrate reduction can

also be optimized. The bioretention cell can increase the probability of not exceeding 2 mg $L^{-1}$ of nitrate (as N) mean concentration by 16% as opposed to no treatment.

The soil properties affected the outflow as determined by the sensitivity analysis. To reduce runoff output the following soil properties would be useful: smaller residual water content, larger saturated water content, larger inverse of the bubbling pressure, and a larger pore distribution index. Exact ranges of optimal values were not determined, but this could be the objective of a future study. A 50% reduction in the saturated hydraulic conductivity value of 107 cm $hr^{-1}$ did not have any significant effect on the outflow, so it may be possible to target lower values during design for optimal performance. More studies should be conducted to evaluate whether different input conditions may decrease bioretention cell performance if the saturated hydraulic conductivity is decreased. The increase to 214 cm $hr^{-1}$ did show a significant increase in runoff output.

Dry initial conditions as compared to wet conditions have smaller outflows. Increasing exfiltration into the native soil would potentially improve volume and nitrate reductions. This could be accomplished by changing the shape of the bioretention cell to increase the surface area, increasing the depth of the cell, or choosing a native soil with higher permeability.

A 55 cm water pressure was found to be the threshold value required for outflow to begin for this bioretention cell. This water pressure was larger than the saturated capacity at the

level of the outlet (44 cm). In order to run simulations on future bioretenion cell studies, this threshold value needs to be found if moisture data is not collected within the bioretention cell profile.

Once the threshold outflow value was found, Hydrus was able to simulate a storm event with zero percent error in storage and with NSE and $R^2$ values of 0.82 and 0.92, respectively. It is assumed that this value is a constant for this bioretention cell. It would be favorable to evaluate the use of this value for additional events, but more events that produced significant output and that contain measured data are required.

The disposition of the water for the initial conditions of the profile will contribute to how fast the water flows out. However, it is unclear if the disposition of the water or outflow velocities contribute to the percent reduction.

The variability in performance within one bioretention cell is to be expected because of the variability in climate conditions and initial conditions. The variability in performance of one bioretention cell would potentially approximate the variability in performance of other cells in similar settings. Therefore, the objectives of future studies should be to optimize volume reduction versus achieving uniform efficiency; however, by understanding which factors, if any, have a significant effect on the variability one could target this factor to yield the most optimal performance.

Hydrus could be used in future studies to analyze storm sizes, inflows, durations, initial conditions, water disposition, and bottom velocity to continue optimizing bioretention cell performance. A possible limitation for the modeling software includes the inability to have two lower boundary conditions. This limitation may be addressed by using the Hydrus-2D software. Future studies can address the lack of success with utilizing Hydrus-2D for bioretention cell hydrology.

## REFERENCES


Barrett, M., Limouzin, M., and Lawler, D. (2013). "Effects of media and plant selection on biofiltration performance." *J. Environ. Eng.,* 139(4), 462-470.

Brown, R. and Hunt, W. (2011a). "Impacts of media depth on effluent water quality and hydrologic performance of undersized bioretention cells." *J. Irrig. Drain. Eng.,* 137(3), 132-143.

Brown, R. and Hunt, W. (2011b). "Underdrain configuration to enhance bioretention exfiltration to reduce pollutant loads." *J. Environ. Eng.,* 137(11), 1082-1091.

Carsel, R. and Parrish, R. (1988). "Developing joint probability distributions of soil water retention characteristics." *Water Resour. Res.,* 24(5), 755-769.

Chen, X., Peltier, E., Sturm, B., and Young, C.B. (2013). "Nitrogen removal and nitrifying and denitrifying bacteria quantification in a stormwater bioretention system." *Water Res.,* 47, 1691-1700.

Christianson, R., Brown, G., Barfield, B., and Hayes, J. (2012). "Development of a bioretention cell model and evaluation of input specificity on model accuracy." *Trans. of ASABE,* 55(4), 1213-1221.

Colins K., Lawrence, T., Stander, E., Jontos, R., Kaushal, S., Newcomer, T., Grimm, N., and Ekberg, M. (2010). "Opportunities and challenges for managing nitrogen in urban stormwater: A review and synthesis." *Ecol. Eng.*, 36, 1507-1519.

Davis, A. (2007). "Field performance of bioretention: Water quality." *Environ. Eng. Sci.*, 24, 1048-1064.

Davis, A. (2008). "Field performance of bioretention: Hydrology impacts." *J. Hydrol. Eng.*, 13(2), 90-95.

Davis, A., Hunt, W., Traver, R., and Clar, M. (2009). "Bioretention technology: Overview of current practice and future needs." *J. Environ. Eng*., 135(3), 109-117.

Davis, A. and McCuen, R. (2005). *Stormwater management for smart growth.* Springer. New York, NY.

Dietz, M., and Clausen, J. (2006). "Saturation to improve pollutant retention in a rain garden." *Environ. Microbiol.*, 12(12), 3137-3149.

Dussaillant, A., Cuevas, A., and Potter, K. (2005). “Raingardens for stormwater infiltration and focused groundwater recharge: Simulations for different world climates.” *Water Sci. Technol.: Water Supply*, 5(3-4), 173-179.

Ergas, S., Sengupta, S., Siegel, R., Pandit, A., Yao, Y., and Yuan, X. (2010). “Performance of nitrogen-removing bioretention systems for control of agricultural runoff.” *J. Environ. Eng*., 136, 1105-1112.

Environmental Protection Agency (EPA). (2014). “Table of regulated drinking water contaminants.” <https://www.epa.gov/ground-water-and-drinking-water/table-regulated-drinking-water-contaminants> (Oct. 20, 2014).

Filipovic, V., Mallman, F., Coquet, Y., and Simunek, J. (2014). “Numerical simulation of water flow in tile and mole drainage systems.” *Ag. Water Management,* 146, 105-114.

Fournel, J., Forquet, N., Molle, P., and Grasmick, A. (2013). “Modeling constructed wetlands with variably saturated vertical subsurface-flow for urban stormwater treatment.” *Ecol. Eng*., 55, 1-8.

Funkhouser, L. (2007). "StormCon news: Interview with Larry Coffman, the low-impact development innovator." *Stormwater*, 8(6), 16-20.

He, Z. and Davis, A. (2011). "Process modeling of storm-water flow in a bioretention cell." *J. Irrig. Drain. Eng.*, 137(3), 121-131.

Hillel, D. 2004. *Introduction to environmental soil physics*. Elsevier Science. San Diego, CA.

Hunt, W., Jarrett, A., Smith, J., and Sharkey, L. (2006). "Evaluating bioretention hydrology and nutrient removal at three field sites in North Carolina." *J. Irrig. Drain. Eng.*, 132(6), 600-608.

Jaber, F. (2014a). *Upper Trinity Watershed low impact development infrastructure for stormwater management – Final Report*. Submitted to TCEQ on April 2014. Texas A&M AgriLife Extension Service. Dallas, TX.

Jaber, F. (2014b). Personal communication. October 2014. Texas A&M AgriLife Extension Service. Dallas, TX.

Jennings, A., Adeel, A., Hopkins, A., Litofsky, A., and Wellstead, S. (2013). "Rain barrel - urban garden stormwater management performance." *J. Environ. Eng.*, 139, 757-765.

Jennnings, A., Berger, M. and Hale, J. (2015). “Hydraulic and hydrologic performance of residential rain gardens.” *J. Environ. Eng.*, 141(11), 1-15. 04015033.

Jiang, S. Lim, K., Huang, X., McCarthy, D., and Hamilton, A. (2015). “Human and environmental health risks and benefits associated with use of urban stormwater.” *WIREs Water*, 2, 683-699. doi:10.1002/wat2.1107.

Kim, H., Seagren, E., and Davis A. (2003). “Engineered bioretention for removal of nitrate from stormwater runoff.” *Water Environ. Res*., 75(4), 355-367.

Le Coustumer, S., Fletcher, T., Deletic, A., and Barraud, S. (2007). “Hydraulic performance of biofilters for stormwater management: first lessons from both laboratory and field studies. *Water Sci. Technol.,* 56(10), 93-100.

Levin, L. and Mehring A. (2015). “Optimization of bioretention systems through application of ecological theory.” *WIREs Water*, 2, 259-270. doi: 10.1002/wat2.1072.

Li., H. and Davis, A. (2008a). “Heavy metal capture and accumulation in bioretention media.” *Environ. Sci. Technol.,* 42, 5247-5253.

Li., H. and Davis, A. (2008b). "Urban particle capture in bioretention media. II: Theory and model development." *J. Environ. Eng.*, 134(6), 419-432.

Li., H. and Davis, A. (2009). "Water quality improvement through reductions of pollutant loads using bioretention." *J. Environ. Eng.*, 135, 567-576.

Li, L. and Davis, A. (2014). "Urban stormwater runoff nitrogen composition and fate in bioretention systems." *Environ. Sci. Technol*., 48, 3403-3410.

Li, M., Sung, C., Kim, M., and Chu, K. (2010). *Bioretention for stormwater quality improvement in Texas: Pilot experiments. – Report 0-5949-2*. National Technical Information Service (NTIS). Springfield, VA.

Li, M., Swapp, M., Kim, M., Chu, K., and Sung, C. (2014). "Comparing bioretention designs with and without an internal water storage layer for treating highway runoff." *Water Environ. Res*., 86(5), 387-397.

Liu, J., Sample, D., Bell, C., and Guan, Y. (2014). "Review and research needs of bioretention used for the treatment of urban stormwater." *Water*, 6, 1069-1099.

Lucas, W. and Greenway, M. (2011). "Hydraulic response and nitrogen retention in bioretention mesocosms with regulated outlets: Part 1- Hydraulic response." *Water Environ. Res*., 83(8), 692-702.

Lucke, T. and Nichols, P. (2015). "The pollution removal and stormwater reduction performance of street-side bioretention basins after ten years in operation." *Sci. Total Environ.,* 536, 784-792.

Madison Materials. (2013). Products: Crushed stone, sand and gravel. <http://madisonmaterial.com/products.php> (June 1, 2017).

Meng, Y., Wang, H., Chen, J., and Zhang, S. (2014). "Modelling hydrology of a single bioretention system with Hydrus-1D." *The Scientific World Journal*, 2014, 1-10.

Minnesota Pollution Control Agency (MPCA). (2016). Minnesota stormwater manual: Bioretention terminology. < https://stormwater.pca.state.mn.us/index.php?title=Bioretention_terminology> (October 12, 2016).

Moriasi, D., Arnold, J., Van Liew, M., Bingner, R., Harmel, R., and Veith, T. (2007). "Model evaluation guidelines for systematic quantification of accuracy in watershed simulations." *Trans. of ASABE*, 50(3), 885-900.

Mthandi, J., Kahimba, F., Tarimo, A., Salim, B., and Lowole, M. (2014). "Nitrogen distribution model: A farmer and farm-centred model to monitor N movement in the soil." *J. Water Resour. and Protection*, 6, 1546-1552. http://dx.doi.org/10.4236/jwarp.2014.616141.

Nielsen, D., van Genuchten, M., and Biggar, J. (1986). "Water flow and solute transport processes in the unsaturated zone." *Water Resour. Res.*, 22(9), 89S-108S.

Olszewski, D. and Davis, A. (2013). "Comparing the hydrologic performance of a bioretention cell with predevelopment values." *J. Irrig. Drain. Eng.*, 139(2), 124-130.

Plasti-fab. (2015). H-flume flow ranges and equations. <http://www.plasti-fab.com/wp-content/uploads/2015/07/H-Flume-Flow-Data.pdf> (June 1, 2017).

Prince George's County Department of Environmental Resources (PGDER). (1999). "Low-impact development hydrologic analysis." Division of Environmental Management, Watershed Protection Branch. Landover, MD.

Prince George's County Department of Environmental Resources (PGDER). (2007). "Design manual for use of bioretention in storm water management." Division of Environmental Management, Watershed Protection Branch. Landover, MD.

Quan, Q., Dong, L., Li, J., Shen, B., and Jin, C. (2014). "Application of bio-retention hydrologic performance tool for urban runoff pollutants removal." *Nat. Env. & Poll. Tech.*, 0972-6268(13:3), 595-600.

Radcliffe, D. and Simunek, J. (2010). *Soil physics with Hydrus: Modelling and applications.* CRC Press. Boca Raton, FL.

Roy-Poirier, A., Champagne, P., and Filion, Y. (2010). "Review of bioretention system research and design: Past, present, and future." *J. Environ. Eng.*, 136(9), 878-889.

Soil Conservation Service (SCS). (1972). *National engineering handbook, Section 4, Hydrology.* Soil Conserv. Serv., Washington, D.C.

Simunek, J., Sejna, M., Saito, H., Sakai, M., and van Genuchten, M. (2012). "The Hydrus-1D software package for simulating the one-dimensional movement of water, heat, and multiple solutes in variably-saturated media." Version 4.15. HYDRUS Software Series 3:338.

Steffen, J. (2012). "Bioretention hydrologic performance in a semiarid climate." M.S. Thesis. University of Utah.

Sun, Y., Wei, X., and Pomeroy, C. (2011) "Global analysis of sensitivity of bioretention cell design elements to hydrologic performance." *Water Sci. and Eng.*, 4(3), 246-257.

Thompson, A., Paul, A., and Balster, N. (2008). "Physical and hydraulic properties of engineered soil media for bioretention basins." *Trans. of ASABE*, 51(2), 499-514.

Texas Commission of Environmental Quality (TCEQ). (2012). *Water Bodies with Concerns for Use Attainment and Screening Levels*. 2012 Texas Integrated Report. Austin, TX.

Texas Water Development Board (TWDB). (2012). *Water for Texas: 2012 State Water Plan*. Austin, TX.

University of Nevada Cooperative Extension (UNCE) (2004). *The effects of urbanization on the water cycle.* Fact Sheet 04-43. <https://www.unce.unr.edu/publications/files/nr/2004/FS0443.pdf> (Oct. 15, 2015).

US Climate Data. (2015). "Climate Dallas-Texas." <http://www.usclimatedata.com/climate/dallas/texas/united-states/ustx1575> (Oct. 15, 2015).

Walthall, C., Hatfield, J., Backlund, P., Lengnick, L., Marshall, E., Walsh, M., Adkins, S., Aillery, M., Ainsworth, E., Ammann, C., Anderson, C., Bartomeus, I., Baumgard, L., Booker, F., Bradley, B., Blumenthal, D., Bunce, J., Burkey, K., Dabney, S., Delgado, J., Dukes, J., Funk, A., Garrett, K., Glenn, M., Grantz, D., Goodrich, D., Hu, S., Izaurralde, R., Jones, R., Kim, S-H., Leaky, A., Lewers, K., Mader, T., McClung, A., Morgan, J., Muth, D., Nearing, M., Oosterhuis, D., Ort, D., Parmesan, C., Pettigrew, W., Polley, W., Rader, R., Rice, C., Rivington, C., Rosskopf, E., Salas, W., Sollenberger, L., Srygley, R., Stöckle, C., Takle, E., Timlin, D., White, J., Winfree, R., Wright-Morton, L., and Ziska, L. (2012). "Climate change and agriculture in the United States: Effects and adaptation." USDA Technical Bulletin 1935. Washington, DC.

Zinger, Y. Fletcher, T., Deletic, A., Blecken, G., and Viklander, M. (2007). "Optimisation of the nitrogen retention capacity of stormwater biofiltration systems." *Proc., Novatech 2007, 6th Int. Conf. on Sustainable Techniques and Strategies in Urban Water Management*. Rhone-Alpes Research Group on Water Infrastructure. Lyon, France.

# APPENDIX

Table A-1. Hydrology Data including measured and calculated inflows and reduction percentages.

| Event Number | Date | Rainfall in | Rainfall cm | AMC | Duration hrs | Inflow L | Outflow L | Reduction % |
|---|---|---|---|---|---|---|---|---|
| **1** | 6/6/2013 | 0.45 | 1.143 | 1 | 15 | 1537 | 11 | 99.26 |
| **2** | 6/9/2013 | 1.08 | 2.7432 | 1 | 8 | 4671 | 204 | 95.62 |
| **3** | 6/18/2013 | 0.74 | 1.8796 | 1 | 29 | 2892 | 61 | 97.91 |
| **4** | 7/11/2013 | 0.72 | 1.8288 | 1 | 5 | 3221 | 72 | 97.77 |
| **5** | 7/17/2013 | 1.11 | 2.8194 | 1 | 72 | 4387 | 53 | 98.79 |
| **6** | 9/2/2013 | 0.33 | 0.8382 | 1 | 20 | 11761 | 2498 | 78.76 |
| **7** | 9/21/2013 | 1.93 | 4.9022 | 1 | 27 | 95990 | 54112 | 43.63 |
| **8** | 9/28/2013 | 0.35 | 0.889 | 1 | 8 | 20384 | 9312 | 54.32 |
| **9** | 10/5/2013 | 0.39 | 0.9906 | 1 | 8 | 21789 | 288 | 98.68 |
| **10** | 10/18/2013 | 0.1 | 0.254 | 1 | 1 | 1999 | 0 | 100.00 |
| **11** | 11/4/2013 | 1.08 | 2.7432 | 1 | | | | |
| **12** | 3/16/2014 | 0.87 | 2.2098 | 1 | 7 | 3710 | 79 | 97.86 |
| **13** | 4/7/2014 | 0.64 | 1.6256 | 1 | 41 | 82371 | 7075 | 91.41 |
| **14** | 4/13/2014 | 0.31 | 0.7874 | 1 | | | | |
| **15** | 5/25/2014 | 0.55 | 1.397 | 1 | 9 | 5059 | 11220 | -121.78 |
| **16** | 5/28/2014 | 0.47 | 1.1938 | 2 | | | | |
| **17** | 6/9/2014 | 0.74 | 1.8796 | 1 | 36 | 11927 | 9032 | 24.27 |
| **18** | 6/23/2014 | 0.61 | 1.5494 | 1 | 32 | 6990 | 1435 | 79.48 |
| **19** | 7/3/2014 | 0.82 | 2.0828 | 1 | 5 | 15401 | 11315 | 26.53 |
| **20** | 7/17/2014 | 0.89 | 2.2606 | 1 | 23 | 18672 | 10005 | 46.42 |
| **21** | 7/31/2014 | 1.01 | 2.5654 | 1 | 26 | 24716 | 18068 | 26.90 |
| **22** | 8/6/2014 | 0.56 | 1.4224 | 1 | 12 | 5364 | 10550 | -96.69 |
| **23** | 10/2/2014 | 0.29 | 0.7366 | 1 | 5 | 12159 | 8 | 99.94 |
| **24** | 10/11/2014 | 0.33 | 0.8382 | 2 | 11 | 6995 | 0 | 100.00 |
| **25** | 10/13/2014 | 1.54 | 3.9116 | 1 | | | | |
| **26** | 11/4/2014 | 1.14 | 2.8956 | 1 | | | | |
| **27** | 12/18/2014 | 0.4 | 1.016 | 1 | 51 | 15195 | 15 | 99.90 |
| **28** | 12/23/2014 | 0.53 | 1.3462 | 1 | | | | |
| **29** | 1/21/2015 | 1.17 | 2.9718 | 1 | | | | |
| **30** | 1/31/2015 | 0.72 | 1.8288 | 1 | | | | |
| **31** | 2/16/2015 | 0.41 | 1.0414 | 1 | | | | |
| **32** | 2/22/2015 | 2.22 | 5.6388 | 1 | | | | |
| **33** | 2/28/2015 | 1.1 | 2.794 | 1 | | | | |

| **LEGEND** |
|---|
| Calculated using SCS Curve Number method |
| Negative Reduction caused by smaller estimated inflow |

Table A-2. Hydrology Summary for the 20 events with data.

| | Mean | Median | Range |
|---|---|---|---|
| Inflow (L x$10^3$) | 16.9 | 12.2 | [1.5, 96] |
| Outflow (L x $10^3$) | 5.4 | 0.14 | [0, 54] |
| Reduction (%) | 76 | 97.8 | [24, 100] |

Table A-3. Curve Number data and average for measured data.

| Event # | Date | AMC | Rainfall | Inflow Obs. | Inflow Match | S | CN | |
|---|---|---|---|---|---|---|---|---|
| | | | in | L | L | | | |
| 1 | 6/6/2013 | 1 | 0.45 | 1537 | 1537 | 1.41 | 87.7 | |
| 2 | 6/9/2013 | 1 | 1.08 | 4671 | 4671 | 3.17 | 75.9 | |
| 3 | 6/18/2013 | 1 | 0.74 | 2892 | 2892 | 2.23 | 81.7 | |
| 4 | 7/11/2013 | 1 | 0.72 | 3221 | 3221 | 2.09 | 82.7 | |
| 5 | 7/17/2013 | 1 | 1.11 | 4387 | 4387 | 3.34 | 75.0 | |
| 6 | 9/2/2013 | 1 | 0.33 | 11760 | 11760 | 0.27 | 97.3 | |
| 7 | 9/21/2013 | 1 | 1.93 | 95980 | 95980 | 0.94 | 91.4 | |
| 8 | 9/28/2013 | 1 | 0.35 | 20382 | 20382 | 0.12 | 98.8 | |
| 9 | 10/5/2013 | 1 | 0.39 | 21786 | 21786 | 0.15 | 98.6 | |
| 10 | 10/18/2013 | | 0.25 | 7566 | 7566 | 0.20 | 98.0 | |
| 12 | 3/16/2014 | 1 | 1 | 3709 | 3709 | 2.56 | 79.6 | |
| 23 | 10/2/2014 | 1 | 0.29 | 12157 | 12157 | 0.19 | 98.1 | |
| 24 | 10/11/2014 | 2 | 0.33 | 6995 | - | - | - | |
| 27 | 12/18/2014 | 1 | 0.4 | 15193 | 15193 | 0.30 | 97.0 | |

| CN Summary | |
|---|---|
| Avg | 89 |
| St. Dev | 9 |
| Range | [75:99] |

Table A-4. Events arranged in order of increasing storm size.

| Event Number | Date | Rainfall cm | Inflow L | Outflow L | Reduction % |
|---|---|---|---|---|---|
| **10** | 10/18/2013 | 0.254 | 1999 | 0 | 100.00 |
| **23** | 10/2/2014 | 0.7366 | 12159 | 8 | 99.94 |
| **6** | 9/2/2013 | 0.8382 | 11761 | 2498 | 78.76 |
| **24** | 10/11/2014 | 0.8382 | 6995 | 0 | 100.00 |
| **8** | 9/28/2013 | 0.889 | 20384 | 9312 | 54.32 |
| **9** | 10/5/2013 | 0.9906 | 21789 | 288 | 98.68 |
| **27** | 12/18/2014 | 1.016 | 15195 | 15 | 99.90 |
| **1** | 6/6/2013 | 1.143 | 1537 | 11 | 99.26 |
| **15** | 5/25/2014 | 1.397 | 5059 | 11220 | -121.78 |
| **22** | 8/6/2014 | 1.4224 | 5364 | 10550 | -96.69 |
| **18** | 6/23/2014 | 1.5494 | 6990 | 1435 | 79.48 |
| **13** | 4/7/2014 | 1.6256 | 82371 | 7075 | 91.41 |
| **4** | 7/11/2013 | 1.8288 | 3221 | 72 | 97.77 |
| **3** | 6/18/2013 | 1.8796 | 2892 | 61 | 97.91 |
| **17** | 6/9/2014 | 1.8796 | 11927 | 9032 | 24.27 |
| **19** | 7/3/2014 | 2.0828 | 15401 | 11315 | 26.53 |
| **12** | 3/16/2014 | 2.2098 | 3710 | 79 | 97.86 |
| **20** | 7/17/2014 | 2.2606 | 18672 | 10005 | 46.42 |
| **21** | 7/31/2014 | 2.5654 | 24716 | 18068 | 26.90 |
| **2** | 6/9/2013 | 2.7432 | 4671 | 204 | 95.62 |
| **5** | 7/17/2013 | 2.8194 | 4387 | 53 | 98.79 |
| **7** | 9/21/2013 | 4.9022 | 95990 | 54112 | 43.63 |

| **LEGEND** |
|---|
| Top 20% in terms of Rainfall Depth |
| Bottom 10% in terms of Rainfall Depth |
| Calculated using SCS Curve Number method |
| Negative Reduction caused by smaller estimated inflow |

Table A-5. Nitrate as nitrogen Reduction Data for 19 events.

| Event # | Date | Nitrate EMC in (mg/L) | Nitrate EMC out (mg/L) | Reduction % |
|---|---|---|---|---|
| 3 | 06/18/2013 | 2.15 | 1.16 | 46.05 |
| 4 | 07/11/2013 | 1.11 | 0.62 | 44.14 |
| 5 | 07/17/2013 | 1.2 | 0.78 | 35.00 |
| 10 | 10/18/2013 | 1.11 | 0 | 100.00 |
| 11 | 11/04/2013 | 0.19 | 0.25 | -31.58 |
| 12 | 03/16/2014 | 1.67 | 0.88 | 47.31 |
| 13 | 04/07/2014 | 0.48 | 0.53 | -10.42 |
| 17 | 06/09/2014 | 0.66 | 1.14 | -72.73 |
| 21 | 07/31/2014 | 0.51 | 0.43 | 15.69 |
| 22 | 08/06/2014 | 1.11 | 0.16 | 85.59 |
| 24 | 10/11/2014 | 1.11 | 0 | 100.00 |
| 25 | 10/13/2014 | 0.029 | 0.029 | 0.00 |
| 26 | 11/04/2014 | 0.37 | 0.44 | -18.92 |
| 28 | 12/23/2014 | 0.54 | 0.59 | -9.26 |
| 29 | 01/21/2015 | 1.39 | 0.68 | 51.08 |
| 30 | 01/31/2015 | 0.83 | 0.69 | 16.87 |
| 31 | 02/16/2015 | 1.6 | 0.88 | 45.00 |
| 32 | 02/22/2015 | 1.07 | 0.78 | 27.10 |
| 33 | 02/28/2015 | 4.02 | 2.72 | 32.34 |
| Average | | 1.11 | 0.67 | 26.49 |

| Legend |
|---|
| Calculated Values |

Table A-6. Saturated hydraulic conductivity for 30 soil samples in 10 locations in the bioretention cell.

| Sample # | Sample Name | Trial | Ksat (cm/hr) | Ksat Avg (cm/hr) |
|---|---|---|---|---|
| 1 | 403A | 1 | 16.21 | 13.95 |
| | | 2 | 15.28 | |
| | | 3 | 10.36 | |
| 2 | 308B | 1 | 252.06 | 234.44 |
| | | 2 | 237.49 | |
| | | 3 | 213.78 | |
| 3 | 302B | 1 | 114.74 | 137.08 |
| | | 2 | 163.75 | |
| | | 3 | 132.74 | |
| 4 | 104B | 1 | 118.05 | 86.81 |
| | | 2 | 73.88 | |
| | | 3 | 68.48 | |
| 5 | 408B | 1 | 36.81 | 34.51 |
| | | 2 | 33.28 | |
| | | 3 | 33.44 | |
| 6 | 308A | 1 | 40.88 | 42.44 |
| | | 2 | 44.38 | |
| | | 3 | 42.05 | |
| 7 | 307B | 1 | 78.43 | 83.61 |
| | | 2 | 85.87 | |
| | | 3 | 86.53 | |
| 8 | 208E | 1 | 289.45 | 225.88 |
| | | 2 | 248.07 | |
| | | 3 | 140.11 | |
| 9 | 404A | 1 | 106.87 | 88.41 |
| | | 2 | 82.92 | |
| | | 3 | 75.45 | |
| 10 | 406B | 1 | 132.66 | 118.42 |
| | | 2 | 116.60 | |
| | | 3 | 106.00 | |

Table A-7. Nitrate as nitrogen concentration and mean mass reduction calculation summary for 10 events.

| Event Number | Date | Nitrate In mg/L | Nitrate Out mg/L | Concentration Reduction, % | Inflow L | Outflow L | Vol. Red. % | Mass in mg | Mass out mg | Mean Mass Reduction, % |
|---|---|---|---|---|---|---|---|---|---|---|
| **3** | 6/18/2013 | 2.15 | 1.16 | 46.0 | 2892 | 60.6 | 97.9 | 6217.9 | 70.3 | 98.9 |
| **4** | 7/11/2013 | 1.11 | 0.62 | 44.1 | 3221.4 | 71.9 | 97.8 | 3575.7 | 44.6 | 98.8 |
| **5** | 7/17/2013 | 1.2 | 0.78 | 35.0 | 4387.3 | 53.0 | 98.8 | 5264.7 | 41.3 | 99.2 |
| **10** | 10/18/2013 | 1.11 | 0 | 100.0 | 1998.7 | 0 | 100 | 2218.5 | 0.0 | 100.0 |
| **12** | 3/16/2014 | 1.67 | 0.88 | 47.3 | 3709.7 | 79.5 | 97.9 | 6195.2 | 70.0 | 98.9 |
| **13** | 4/7/2014 | 0.48 | 0.53 | -10.4 | 82370.8 | 7074.9 | 91.4 | 39538.0 | 3749.7 | 90.5 |
| **17** | 6/9/2014 | 0.66 | 1.14 | -72.7 | 18672.1 | 9032 | 51.6 | 12323.6 | 10296.4 | 16.4 |
| **21** | 7/31/2014 | 0.51 | 0.43 | 15.7 | 24715.7 | 18067.7 | 26.9 | 12605.0 | 7769.1 | 38.4 |
| **22** | 8/6/2014 | 1.11 | 0.16 | 85.6 | 5363.8 | 10549.9 | -96.7 | 5953.9 | 1688.0 | 71.6 |
| **24** | 10/11/2014 | 1.11 | 0 | 100.0 | 6995.4 | 0 | 100 | 7764.9 | 0.0 | 100.0 |
| **Average** | | | | **39.1** | | | | | | **81.3** |

| **Legend** |
|---|
| Calculated Values |

Table A-8. Hydrus storm input for the three simulations.

| Storm | 9.2.13 | Storm | 9.21.13 | Storm | 9.28.13 |
|---|---|---|---|---|---|
| Time (hrs) | Precip. And Runoff (cm/hr) | Time (hrs) | Precip. And Runoff (cm/hr) | Time (hrs) | Precip. And Runoff (cm/hr) |
| 0.911 | 0.000 | 1.000 | 0.102 | 0.917 | 0.000 |
| 1.000 | 0.102 | 2.000 | 0.965 | 1.000 | 0.635 |
| 2.000 | 0.187 | 2.083 | 1.012 | 1.083 | 0.635 |
| 2.083 | 0.152 | 2.167 | 17.496 | 1.167 | 1.184 |
| 2.167 | 7.228 | 2.250 | 28.970 | 1.250 | 10.116 |
| 2.250 | 7.475 | 2.333 | 25.564 | 1.333 | 12.724 |
| 2.333 | 4.020 | 2.417 | 15.669 | 1.417 | 7.549 |
| 2.417 | 2.559 | 2.500 | 7.300 | 1.500 | 4.916 |
| 2.500 | 1.684 | 2.583 | 4.914 | 1.583 | 3.870 |
| 2.583 | 0.943 | 2.667 | 3.783 | 1.667 | 3.453 |
| 2.667 | 0.584 | 2.750 | 2.973 | 1.750 | 3.618 |
| 2.750 | 0.343 | 2.833 | 2.484 | 1.833 | 3.850 |
| 2.833 | 0.235 | 2.917 | 2.138 | 1.917 | 5.150 |
| 2.917 | 0.191 | 3.000 | 2.275 | 2.000 | 8.256 |
| 3.000 | 0.025 | 3.083 | 2.301 | 2.083 | 15.598 |
| 4.000 | 0.000 | 3.167 | 2.423 | 2.167 | 14.087 |
| 6.000 | 0.025 | 3.250 | 2.498 | 2.250 | 9.187 |
| 7.000 | 0.051 | 3.333 | 2.528 | 2.333 | 6.646 |
| 8.000 | 0.356 | 3.417 | 2.451 | 2.417 | 5.041 |
| 9.000 | 0.000 | 3.500 | 2.259 | 2.500 | 4.075 |
| 10.000 | 0.076 | 3.583 | 2.158 | 2.583 | 2.964 |
| 11.000 | 0.025 | 3.667 | 2.031 | 2.667 | 2.158 |
| 12.250 | 0.206 | 3.750 | 1.892 | 2.750 | 1.762 |
| 12.333 | 2.795 | 3.833 | 11.368 | 2.833 | 1.371 |
| 12.417 | 11.196 | 3.917 | 45.283 | 2.917 | 1.080 |
| 12.500 | 10.711 | 4.000 | 44.909 | 3.000 | 0.770 |
| 12.583 | 6.133 | 4.083 | 30.281 | 3.083 | 0.602 |
| 12.667 | 4.210 | 4.167 | 18.958 | 3.167 | 0.441 |
| 12.750 | 3.189 | 4.250 | 7.173 | 3.250 | 0.328 |
| 12.833 | 2.583 | 4.333 | 5.078 | 3.333 | 0.244 |
| 12.917 | 2.178 | 4.417 | 4.302 | 3.417 | 0.192 |
| 13.000 | 1.742 | 4.500 | 4.091 | 3.500 | 0.140 |

Table A-8 Continued.

| Storm | 9.2.13 | Storm | 9.21.13 | Storm | 9.28.13 |
|---|---|---|---|---|---|
| Time (hrs) | Precip. And Runoff (cm/hr) | Time (hrs) | Precip. And Runoff (cm/hr) | Time (hrs) | Precip. And Runoff (cm/hr) |
| 13.083 | 1.518 | 4.583 | 3.820 | 3.583 | 0.112 |
| 13.167 | 1.214 | 4.667 | 3.341 | 3.667 | 0.104 |
| 13.250 | 0.902 | 4.750 | 2.690 | 3.750 | 0.108 |
| 13.333 | 0.692 | 4.833 | 2.054 | 3.833 | 0.025 |
| 13.417 | 0.494 | 4.917 | 1.514 | 4.000 | 0.102 |
| 13.500 | 0.297 | 5.000 | 0.963 | 4.083 | 0.148 |
| 13.583 | 0.246 | 5.083 | 0.748 | 4.167 | 0.143 |
| 13.667 | 0.157 | 5.167 | 0.519 | 4.250 | 0.102 |
| 13.750 | 0.097 | 5.250 | 0.317 | 4.500 | 0.259 |
| 13.833 | 0.052 | 5.333 | 0.192 | 4.583 | 0.464 |
| 13.917 | 0.000 | 5.417 | 0.104 | 4.667 | 0.772 |
| 14.917 | 0.037 | 5.500 | 0.025 | 4.750 | 1.091 |
| 15.000 | 0.186 | 7.000 | 0.813 | 4.833 | 1.346 |
| 15.083 | 0.266 | 7.333 | 0.861 | 4.917 | 1.173 |
| 15.167 | 0.271 | 7.417 | 1.115 | 5.000 | 0.824 |
| 15.250 | 0.239 | 7.500 | 2.106 | 5.083 | 0.692 |
| 15.333 | 0.223 | 7.583 | 8.269 | 5.167 | 0.531 |
| 15.417 | 0.171 | 7.667 | 18.872 | 5.250 | 0.368 |
| 15.500 | 0.091 | 7.750 | 25.239 | 5.333 | 0.284 |
| 15.583 | 0.073 | 7.833 | 25.827 | 5.417 | 0.218 |
| 15.667 | 0.050 | 7.917 | 18.644 | 5.500 | 0.161 |
| 15.750 | 0.000 | 8.000 | 9.486 | 5.583 | 0.135 |
| 15.833 | 0.000 | 8.083 | 6.436 | 5.667 | 0.091 |
| 15.917 | 0.065 | 8.167 | 4.322 | 5.750 | 0.079 |
| 16.000 | 0.000 | 8.250 | 3.134 | 5.833 | 0.066 |
| 16.417 | 0.063 | 8.333 | 2.379 | 5.917 | 0.073 |
| 16.500 | 0.043 | 8.417 | 1.808 | 6.000 | 0.000 |
| 16.583 | 0.037 | 8.500 | 1.376 | 8.000 | 0.000 |
| 16.667 | 0.000 | 8.583 | 1.102 | 10.000 | 0.000 |
| 21.000 | 0.000 | 8.667 | 0.883 | | |

Table A-8 Continued.

| Storm | 9.2.13 | Storm | 9.21.13 | Storm | 9.28.13 |
|---|---|---|---|---|---|
| Time (hrs) | Precip. And Runoff (cm/hr) | Time (hrs) | Precip. And Runoff (cm/hr) | Time (hrs) | Precip. And Runoff (cm/hr) |
| | | 8.750 | 0.772 | | |
| | | 8.833 | 0.698 | | |
| | | 8.917 | 0.710 | | |
| | | 9.000 | 0.885 | | |
| | | 9.083 | 1.144 | | |
| | | 9.167 | 1.514 | | |
| | | 9.250 | 1.928 | | |
| | | 9.333 | 2.119 | | |
| | | 9.417 | 2.135 | | |
| | | 9.500 | 2.080 | | |
| | | 9.583 | 2.119 | | |
| | | 9.667 | 2.119 | | |
| | | 9.750 | 2.080 | | |
| | | 9.833 | 1.928 | | |
| | | 9.917 | 1.727 | | |
| | | 10.000 | 1.451 | | |
| | | 10.083 | 1.275 | | |
| | | 10.167 | 1.091 | | |
| | | 10.250 | 0.954 | | |
| | | 10.333 | 0.869 | | |
| | | 10.417 | 0.759 | | |
| | | 10.500 | 0.603 | | |
| | | 10.583 | 0.511 | | |
| | | 10.667 | 0.378 | | |
| | | 10.750 | 0.282 | | |
| | | 10.833 | 0.263 | | |
| | | 10.917 | 0.278 | | |
| | | 11.000 | 0.769 | | |
| | | 11.083 | 1.120 | | |
| | | 11.167 | 1.743 | | |
| | | 11.250 | 2.534 | | |
| | | 11.333 | 3.469 | | |
| | | 11.417 | 4.071 | | |
| | | 11.500 | 4.436 | | |

Table A-8 Continued.

| Storm | 9.2.13 | Storm | 9.21.13 | Storm | 9.28.13 |
|---|---|---|---|---|---|
| Time (hrs) | Precip. And Runoff (cm/hr) | Time (hrs) | Precip. And Runoff (cm/hr) | Time (hrs) | Precip. And Runoff (cm/hr) |
| | | 11.583 | 4.472 | | |
| | | 11.667 | 4.997 | | |
| | | 11.750 | 6.249 | | |
| | | 11.833 | 7.482 | | |
| | | 11.917 | 7.863 | | |
| | | 12.000 | 7.526 | | |
| | | 12.083 | 7.005 | | |
| | | 12.167 | 5.344 | | |
| | | 12.250 | 3.980 | | |
| | | 12.333 | 2.945 | | |
| | | 12.417 | 2.438 | | |
| | | 12.500 | 2.094 | | |
| | | 12.583 | 2.034 | | |
| | | 12.667 | 2.211 | | |
| | | 12.750 | 2.315 | | |
| | | 12.833 | 2.397 | | |
| | | 12.917 | 2.455 | | |
| | | 13.000 | 3.025 | | |
| | | 13.083 | 4.141 | | |
| | | 13.167 | 6.349 | | |
| | | 13.250 | 7.703 | | |
| | | 13.333 | 7.653 | | |
| | | 13.417 | 7.037 | | |
| | | 13.500 | 6.364 | | |
| | | 13.583 | 5.471 | | |
| | | 13.667 | 4.635 | | |
| | | 13.750 | 3.917 | | |
| | | 13.833 | 3.649 | | |
| | | 13.917 | 3.484 | | |
| | | 14.000 | 3.108 | | |
| | | 14.083 | 2.959 | | |
| | | 14.167 | 2.538 | | |

Table A-8 Continued.

| Storm | 9.2.13 | Storm | 9.21.13 | Storm | 9.28.13 |
|---|---|---|---|---|---|
| Time (hrs) | Precip. And Runoff (cm/hr) | Time (hrs) | Precip. And Runoff (cm/hr) | Time (hrs) | Precip. And Runoff (cm/hr) |
| | | 14.250 | 1.978 | | |
| | | 14.333 | 1.591 | | |
| | | 14.417 | 1.228 | | |
| | | 14.500 | 0.948 | | |
| | | 14.583 | 0.696 | | |
| | | 14.667 | 0.527 | | |
| | | 14.750 | 0.434 | | |
| | | 14.833 | 0.331 | | |
| | | 14.917 | 0.322 | | |
| | | 15.000 | 0.253 | | |
| | | 15.083 | 0.216 | | |
| | | 15.167 | 0.183 | | |
| | | 15.250 | 0.132 | | |
| | | 15.333 | 0.144 | | |
| | | 15.417 | 0.152 | | |
| | | 15.500 | 0.112 | | |
| | | 15.750 | 0.104 | | |
| | | 15.833 | 0.093 | | |
| | | 15.917 | 0.095 | | |
| | | 16.000 | 0.058 | | |
| | | 16.083 | 0.000 | | |
| | | 17.000 | 0.025 | | |
| | | 18.000 | 0.076 | | |
| | | 18.333 | 0.123 | | |
| | | 18.417 | 0.190 | | |
| | | 18.500 | 0.352 | | |

Table A-8 Continued.

| Storm | 9.2.13 | Storm | 9.21.13 | Storm | 9.28.13 |
|---|---|---|---|---|---|
| Time (hrs) | Precip. And Runoff (cm/hr) | Time (hrs) | Precip. And Runoff (cm/hr) | Time (hrs) | Precip. And Runoff (cm/hr) |
| | | 18.583 | 0.439 | | |
| | | 18.667 | 0.454 | | |
| | | 18.750 | 0.445 | | |
| | | 18.833 | 0.415 | | |
| | | 18.917 | 0.373 | | |
| | | 19.000 | 0.317 | | |
| | | 19.083 | 0.327 | | |
| | | 19.167 | 0.297 | | |
| | | 19.250 | 0.269 | | |
| | | 19.333 | 0.263 | | |
| | | 19.417 | 0.292 | | |
| | | 19.500 | 0.322 | | |
| | | 19.583 | 0.398 | | |
| | | 19.667 | 0.517 | | |
| | | 19.750 | 0.619 | | |
| | | 19.833 | 0.667 | | |
| | | 19.917 | 0.730 | | |
| | | 20.000 | 0.596 | | |
| | | 20.083 | 0.501 | | |
| | | 20.167 | 0.425 | | |
| | | 20.250 | 0.345 | | |
| | | 20.333 | 0.297 | | |
| | | 20.417 | 0.234 | | |
| | | 20.500 | 0.176 | | |
| | | 20.583 | 0.140 | | |
| | | 20.667 | 0.097 | | |
| | | 20.750 | 0.070 | | |
| | | 20.833 | 0.079 | | |
| | | 20.917 | 0.065 | | |
| | | 21.000 | 0.056 | | |
| | | 21.083 | 0.000 | | |
| | | 23.000 | 0.025 | | |
| | | 24.000 | 0.000 | | |
| | | 26.000 | 0.000 | | |

Table A-9. Measured data and simulated data (0%, 5%, 11% error) for the storm on September 21, 2013.

| Field Measurements | | Simulated | 0% Error | Simulated | 5% Error | Simulated | 11% Error |
|---|---|---|---|---|---|---|---|
| Time (hrs) | Cum. Depth Out (cm) | Time (hrs) | Cum. Depth Out (cm) | Time (hrs) | Cum. Depth Out (cm) | Time (hrs) | Cum. Depth Out (cm) |
| 0.00 | | 0.06 | 0.00 | 0.02 | 0.00 | 0.06 | 0.00 |
| 0.08 | 0.00 | 0.08 | 0.00 | 0.08 | 0.00 | 0.08 | 0.00 |
| 0.17 | 0.00 | 0.17 | 0.00 | 0.17 | 0.00 | 0.17 | 0.00 |
| 0.25 | 0.00 | 0.25 | 0.00 | 0.25 | 0.00 | 0.25 | 0.00 |
| 0.33 | 0.00 | 0.33 | 0.00 | 0.33 | 0.00 | 0.33 | 0.00 |
| 0.42 | 0.00 | 0.42 | 0.00 | 0.42 | 0.00 | 0.42 | 0.00 |
| 0.50 | 0.00 | 0.50 | 0.00 | 0.50 | 0.00 | 0.50 | 0.00 |
| 0.58 | 0.00 | 0.58 | 0.00 | 0.58 | 0.00 | 0.58 | 0.00 |
| 0.67 | 0.00 | 0.66 | 0.00 | 0.66 | 0.00 | 0.66 | 0.00 |
| 0.75 | 0.00 | 0.75 | 0.00 | 0.75 | 0.00 | 0.75 | 0.00 |
| 0.83 | 0.00 | 0.83 | 0.00 | 0.83 | 0.00 | 0.83 | 0.00 |
| 0.92 | 0.00 | 0.91 | 0.00 | 0.91 | 0.00 | 0.91 | 0.00 |
| 1.00 | 0.00 | 1.00 | 0.00 | 1.00 | 0.00 | 1.00 | 0.00 |
| 1.08 | 0.00 | 1.08 | 0.00 | 1.08 | 0.00 | 1.08 | 0.00 |
| 1.17 | 0.00 | 1.16 | 0.00 | 1.16 | 0.00 | 1.16 | 0.00 |
| 1.25 | 0.00 | 1.25 | 0.00 | 1.25 | 0.00 | 1.25 | 0.00 |
| 1.33 | 0.00 | 1.33 | 0.00 | 1.33 | 0.00 | 1.33 | 0.00 |
| 1.42 | 0.00 | 1.41 | 0.00 | 1.41 | 0.00 | 1.41 | 0.00 |
| 1.50 | 0.00 | 1.49 | 0.00 | 1.49 | 0.00 | 1.49 | 0.00 |
| 1.58 | 0.00 | 1.58 | 0.00 | 1.58 | 0.00 | 1.58 | 0.00 |
| 1.67 | 0.00 | 1.66 | 0.00 | 1.66 | 0.00 | 1.66 | 0.00 |
| 1.75 | 0.00 | 1.74 | 0.00 | 1.74 | 0.00 | 1.74 | 0.00 |
| 1.83 | 0.00 | 1.83 | 0.00 | 1.83 | 0.00 | 1.83 | 0.00 |
| 1.92 | 0.00 | 1.91 | 0.00 | 1.91 | 0.00 | 1.91 | 0.00 |
| 2.00 | 0.00 | 2.00 | 0.00 | 2.00 | 0.00 | 2.00 | 0.00 |
| 2.08 | 0.00 | 2.08 | 0.00 | 2.08 | 0.00 | 2.08 | 0.00 |
| 2.17 | 0.00 | 2.17 | 0.00 | 2.16 | 0.00 | 2.17 | 0.00 |
| 2.25 | 0.00 | 2.25 | 0.00 | 2.25 | 0.00 | 2.25 | 0.00 |

Table A-9 Continued.

| Time (hrs) | Cum. Depth Out (cm) | Time (hrs) | Cum. Depth Out (cm) | Time (hrs) | Cum. Depth Out (cm) | Time (hrs) | Cum. Depth Out (cm) |
|---|---|---|---|---|---|---|---|
| 2.33 | 0.00 | 2.33 | 0.00 | 2.33 | 0.00 | 2.33 | 0.00 |
| 2.42 | 0.00 | 2.42 | 0.00 | 2.42 | 0.00 | 2.42 | 0.00 |
| 2.50 | 0.00 | 2.50 | 0.00 | 2.50 | 0.00 | 2.50 | 0.00 |
| 2.58 | 0.00 | 2.58 | 0.00 | 2.58 | 0.00 | 2.58 | 0.00 |
| 2.67 | 0.00 | 2.67 | 0.00 | 2.67 | 0.00 | 2.67 | 0.00 |
| 2.75 | 0.00 | 2.75 | 0.00 | 2.75 | 0.00 | 2.75 | 0.00 |
| 2.83 | 0.00 | 2.83 | 0.00 | 2.83 | 0.00 | 2.83 | 0.00 |
| 2.92 | 0.00 | 2.92 | 0.00 | 2.92 | 0.00 | 2.92 | 0.00 |
| 3.00 | 0.00 | 3.00 | 0.00 | 3.00 | 0.00 | 3.00 | 0.00 |
| 3.08 | 0.00 | 3.08 | 0.00 | 3.08 | 0.00 | 3.08 | 0.00 |
| 3.17 | 0.00 | 3.17 | 0.00 | 3.17 | 0.00 | 3.17 | 0.00 |
| 3.25 | 0.00 | 3.25 | 0.00 | 3.25 | 0.00 | 3.25 | 0.00 |
| 3.33 | 0.00 | 3.33 | 0.00 | 3.33 | 0.00 | 3.33 | 0.00 |
| 3.42 | 0.00 | 3.42 | 0.00 | 3.42 | 0.00 | 3.42 | 0.00 |
| 3.50 | 0.00 | 3.50 | 0.00 | 3.50 | 0.00 | 3.50 | 0.00 |
| 3.58 | 0.00 | 3.58 | 0.00 | 3.58 | 0.00 | 3.58 | 0.00 |
| 3.67 | 0.00 | 3.67 | 0.00 | 3.67 | 0.00 | 3.67 | 0.00 |
| 3.75 | 0.00 | 3.75 | 0.00 | 3.75 | 0.00 | 3.75 | 0.00 |
| 3.83 | 0.00 | 3.83 | 0.00 | 3.83 | 0.00 | 3.83 | 0.00 |
| 3.92 | 0.02 | 3.92 | 0.00 | 3.92 | 0.00 | 3.92 | 0.00 |
| 4.00 | 0.14 | 4.00 | 0.00 | 4.00 | 0.00 | 4.00 | 0.00 |
| 4.08 | 0.96 | 4.08 | 0.00 | 4.08 | 0.00 | 4.08 | 0.00 |
| 4.17 | 1.84 | 4.17 | 0.00 | 4.17 | 0.00 | 4.17 | 0.00 |
| 4.25 | 2.77 | 4.25 | 0.00 | 4.25 | 0.00 | 4.25 | 0.00 |
| 4.33 | 3.65 | 4.33 | 0.00 | 4.33 | 0.00 | 4.33 | 0.00 |
| 4.42 | 4.49 | 4.42 | 0.00 | 4.42 | 0.00 | 4.42 | 0.00 |
| 4.50 | 4.66 | 4.50 | 0.00 | 4.50 | 0.00 | 4.50 | 0.00 |
| 4.58 | 5.45 | 4.58 | 0.00 | 4.58 | 0.00 | 4.58 | 0.00 |

Table A-9 Continued.

| Time (hrs) | Cum. Depth Out (cm) | Time (hrs) | Cum. Depth Out (cm) | Time (hrs) | Cum. Depth Out (cm) | Time (hrs) | Cum. Depth Out (cm) |
|---|---|---|---|---|---|---|---|
| 4.67 | 6.23 | 4.67 | 0.00 | 4.67 | 0.00 | 4.67 | 0.05 |
| 4.75 | 6.98 | 4.75 | 0.00 | 4.75 | 0.00 | 4.75 | 0.36 |
| 4.83 | 7.69 | 4.83 | 0.00 | 4.83 | 0.00 | 4.83 | 0.69 |
| 4.92 | 8.38 | 4.92 | 0.00 | 4.92 | 0.00 | 4.92 | 1.00 |
| 5.00 | 8.51 | 5.00 | 0.00 | 5.00 | 0.00 | 5.00 | 1.29 |
| 5.08 | 9.13 | 5.08 | 0.00 | 5.08 | 0.00 | 5.08 | 1.55 |
| 5.17 | 9.72 | 5.17 | 0.00 | 5.17 | 0.00 | 5.17 | 1.78 |
| 5.25 | 10.22 | 5.25 | 0.00 | 5.25 | 0.00 | 5.25 | 1.98 |
| 5.33 | 10.56 | 5.33 | 0.00 | 5.33 | 0.00 | 5.33 | 2.16 |
| 5.42 | 10.81 | 5.42 | 0.00 | 5.42 | 0.00 | 5.42 | 2.32 |
| 5.50 | 10.84 | 5.50 | 0.00 | 5.50 | 0.00 | 5.50 | 2.45 |
| 5.58 | 10.94 | 5.59 | 0.00 | 5.59 | 0.00 | 5.59 | 2.59 |
| 5.67 | 11.03 | 5.69 | 0.00 | 5.64 | 0.00 | 5.69 | 2.71 |
| 5.75 | 11.11 | 5.77 | 0.00 | 5.77 | 0.00 | 5.77 | 2.80 |
| 5.83 | 11.18 | 5.81 | 0.00 | 5.81 | 0.00 | 5.81 | 2.84 |
| 5.92 | 11.23 | 5.89 | 0.00 | 5.94 | 0.00 | 5.89 | 2.93 |
| 6.00 | 11.23 | 6.02 | 0.00 | 6.02 | 0.00 | 6.02 | 3.05 |
| 6.08 | 11.27 | 6.06 | 0.02 | 6.06 | 0.00 | 6.06 | 3.09 |
| 6.17 | 11.31 | 6.18 | 0.08 | 6.10 | 0.00 | 6.18 | 3.20 |
| 6.25 | 11.34 | 6.25 | 0.13 | 6.25 | 0.00 | 6.25 | 3.26 |
| 6.33 | 11.37 | 6.35 | 0.19 | 6.35 | 0.00 | 6.35 | 3.34 |
| 6.42 | 11.40 | 6.39 | 0.22 | 6.39 | 0.00 | 6.39 | 3.38 |
| 6.50 | 11.40 | 6.52 | 0.31 | 6.52 | 0.00 | 6.52 | 3.48 |
| 6.58 | 11.43 | 6.56 | 0.34 | 6.56 | 0.00 | 6.56 | 3.52 |
| 6.67 | 11.45 | 6.64 | 0.40 | 6.64 | 0.00 | 6.64 | 3.59 |
| 6.75 | 11.48 | 6.72 | 0.46 | 6.72 | 0.00 | 6.72 | 3.66 |
| 6.83 | 11.50 | 6.84 | 0.55 | 6.84 | 0.00 | 6.84 | 3.76 |
| 6.92 | 11.51 | 6.89 | 0.59 | 6.89 | 0.00 | 6.89 | 3.80 |

Table A-9 Continued.

| Time (hrs) | Cum. Depth Out (cm) | Time (hrs) | Cum. Depth Out (cm) | Time (hrs) | Cum. Depth Out (cm) | Time (hrs) | Cum. Depth Out (cm) |
|---|---|---|---|---|---|---|---|
| 7.00 | 11.52 | 7.00 | 0.67 | 7.00 | 0.00 | 7.00 | 3.89 |
| 7.08 | 11.53 | 7.10 | 0.75 | 7.06 | 0.00 | 7.10 | 3.97 |
| 7.17 | 11.55 | 7.14 | 0.78 | 7.14 | 0.00 | 7.14 | 4.00 |
| 7.25 | 11.56 | 7.26 | 0.88 | 7.26 | 0.01 | 7.26 | 4.10 |
| 7.33 | 11.58 | 7.33 | 0.93 | 7.33 | 0.04 | 7.33 | 4.16 |
| 7.42 | 11.59 | 7.42 | 1.00 | 7.42 | 0.08 | 7.42 | 4.23 |
| 7.50 | 11.60 | 7.50 | 1.07 | 7.50 | 0.13 | 7.50 | 4.30 |
| 7.58 | 11.68 | 7.58 | 1.14 | 7.58 | 0.19 | 7.58 | 4.37 |
| 7.67 | 11.89 | 7.67 | 1.22 | 7.67 | 0.26 | 7.67 | 4.46 |
| 7.75 | 12.25 | 7.75 | 1.48 | 7.75 | 0.49 | 7.75 | 4.72 |
| 7.83 | 12.80 | 7.83 | 2.72 | 7.83 | 1.69 | 7.83 | 5.96 |
| 7.92 | 13.43 | 7.92 | 4.58 | 7.92 | 3.54 | 7.92 | 7.82 |
| 8.00 | 13.56 | 8.00 | 6.07 | 8.00 | 5.03 | 8.00 | 9.31 |
| 8.08 | 14.20 | 8.08 | 7.18 | 8.08 | 6.15 | 8.08 | 10.43 |
| 8.17 | 14.81 | 8.17 | 8.05 | 8.17 | 7.02 | 8.17 | 11.30 |
| 8.25 | 15.44 | 8.25 | 8.73 | 8.25 | 7.70 | 8.25 | 11.98 |
| 8.33 | 16.06 | 8.33 | 9.28 | 8.33 | 8.25 | 8.33 | 12.53 |
| 8.42 | 16.63 | 8.42 | 9.75 | 8.42 | 8.71 | 8.42 | 12.99 |
| 8.50 | 16.73 | 8.50 | 10.13 | 8.50 | 9.09 | 8.50 | 13.38 |
| 8.58 | 17.14 | 8.58 | 10.46 | 8.58 | 9.42 | 8.58 | 13.70 |
| 8.67 | 17.43 | 8.67 | 10.74 | 8.67 | 9.71 | 8.67 | 13.99 |
| 8.75 | 17.62 | 8.75 | 10.98 | 8.75 | 9.95 | 8.75 | 14.23 |
| 8.83 | 17.75 | 8.83 | 11.20 | 8.83 | 10.16 | 8.83 | 14.44 |
| 8.92 | 17.85 | 8.92 | 11.38 | 8.92 | 10.35 | 8.92 | 14.63 |
| 9.00 | 17.86 | 9.00 | 11.55 | 9.00 | 10.51 | 9.00 | 14.80 |
| 9.08 | 17.94 | 9.08 | 11.70 | 9.08 | 10.67 | 9.08 | 14.95 |
| 9.17 | 18.03 | 9.17 | 11.84 | 9.17 | 10.80 | 9.17 | 15.09 |
| 9.25 | 18.11 | 9.25 | 11.97 | 9.25 | 10.93 | 9.25 | 15.21 |

Table A-9 Continued.

| Time (hrs) | Cum. Depth Out (cm) | Time (hrs) | Cum. Depth Out (cm) | Time (hrs) | Cum. Depth Out (cm) | Time (hrs) | Cum. Depth Out (cm) |
|---|---|---|---|---|---|---|---|
| 9.33 | 18.20 | 9.33 | 12.09 | 9.33 | 11.05 | 9.33 | 15.34 |
| 9.42 | 18.30 | 9.42 | 12.21 | 9.42 | 11.18 | 9.42 | 15.46 |
| 9.50 | 18.39 | 9.50 | 12.34 | 9.50 | 11.30 | 9.50 | 15.58 |
| 9.58 | 18.49 | 9.58 | 12.46 | 9.58 | 11.43 | 9.58 | 15.71 |
| 9.67 | 18.59 | 9.67 | 12.60 | 9.67 | 11.56 | 9.67 | 15.84 |
| 9.75 | 18.68 | 9.75 | 12.74 | 9.75 | 11.70 | 9.75 | 15.98 |
| 9.83 | 18.78 | 9.83 | 12.89 | 9.83 | 11.85 | 9.83 | 16.13 |
| 9.92 | 18.88 | 9.92 | 13.04 | 9.92 | 12.00 | 9.92 | 16.28 |
| 10.00 | 18.97 | 10.00 | 13.19 | 10.00 | 12.16 | 10.00 | 16.44 |
| 10.08 | 19.05 | 10.08 | 13.35 | 10.08 | 12.31 | 10.08 | 16.59 |
| 10.17 | 19.13 | 10.17 | 13.50 | 10.17 | 12.47 | 10.17 | 16.75 |
| 10.25 | 19.20 | 10.25 | 13.65 | 10.25 | 12.61 | 10.25 | 16.89 |
| 10.33 | 19.27 | 10.33 | 13.79 | 10.33 | 12.76 | 10.33 | 17.04 |
| 10.42 | 19.32 | 10.42 | 13.93 | 10.42 | 12.89 | 10.42 | 17.17 |
| 10.50 | 19.36 | 10.50 | 14.06 | 10.50 | 13.02 | 10.50 | 17.30 |
| 10.58 | 19.41 | 10.58 | 14.18 | 10.58 | 13.14 | 10.58 | 17.42 |
| 10.67 | 19.44 | 10.67 | 14.29 | 10.67 | 13.26 | 10.67 | 17.54 |
| 10.75 | 19.48 | 10.75 | 14.40 | 10.75 | 13.36 | 10.75 | 17.64 |
| 10.83 | 19.51 | 10.83 | 14.49 | 10.83 | 13.46 | 10.83 | 17.74 |
| 10.92 | 19.54 | 10.92 | 14.59 | 10.92 | 13.55 | 10.92 | 17.83 |
| 11.00 | 19.57 | 11.00 | 14.67 | 11.00 | 13.63 | 11.00 | 17.91 |
| 11.08 | 19.61 | 11.08 | 14.75 | 11.08 | 13.71 | 11.08 | 17.99 |
| 11.17 | 19.65 | 11.17 | 14.82 | 11.17 | 13.78 | 11.17 | 18.06 |
| 11.25 | 19.71 | 11.25 | 14.89 | 11.25 | 13.85 | 11.25 | 18.13 |
| 11.33 | 19.80 | 11.33 | 14.96 | 11.33 | 13.92 | 11.33 | 18.20 |
| 11.42 | 19.90 | 11.42 | 15.04 | 11.42 | 14.00 | 11.42 | 18.28 |
| 11.50 | 20.01 | 11.50 | 15.13 | 11.50 | 14.09 | 11.50 | 18.38 |
| 11.58 | 20.15 | 11.58 | 15.25 | 11.58 | 14.21 | 11.58 | 18.50 |

Table A-9 Continued.

| Time (hrs) | Cum. Depth Out (cm) | Time (hrs) | Cum. Depth Out (cm) | Time (hrs) | Cum. Depth Out (cm) | Time (hrs) | Cum. Depth Out (cm) |
|---|---|---|---|---|---|---|---|
| 11.67 | 20.30 | 11.67 | 15.41 | 11.67 | 14.37 | 11.67 | 18.66 |
| 11.75 | 20.47 | 11.75 | 15.61 | 11.75 | 14.58 | 11.75 | 18.86 |
| 11.83 | 20.66 | 11.83 | 15.88 | 11.83 | 14.84 | 11.83 | 19.12 |
| 11.92 | 20.87 | 11.92 | 16.22 | 11.92 | 15.18 | 11.92 | 19.47 |
| 12.00 | 21.12 | 12.00 | 16.65 | 12.00 | 15.61 | 12.00 | 19.89 |
| 12.08 | 21.39 | 12.08 | 17.15 | 12.08 | 16.12 | 12.08 | 20.40 |
| 12.17 | 21.65 | 12.17 | 17.70 | 12.17 | 16.66 | 12.17 | 20.94 |
| 12.25 | 21.92 | 12.25 | 18.23 | 12.25 | 17.19 | 12.25 | 21.48 |
| 12.33 | 22.21 | 12.33 | 18.72 | 12.33 | 17.69 | 12.33 | 21.97 |
| 12.42 | 22.44 | 12.42 | 19.17 | 12.42 | 18.13 | 12.42 | 22.42 |
| 12.50 | 22.63 | 12.50 | 19.56 | 12.50 | 18.52 | 12.50 | 22.81 |
| 12.58 | 22.78 | 12.58 | 19.91 | 12.58 | 18.87 | 12.58 | 23.15 |
| 12.67 | 22.91 | 12.67 | 20.22 | 12.67 | 19.18 | 12.67 | 23.46 |
| 12.75 | 23.02 | 12.75 | 20.50 | 12.75 | 19.46 | 12.75 | 23.74 |
| 12.83 | 23.14 | 12.83 | 20.75 | 12.83 | 19.72 | 12.83 | 24.00 |
| 12.92 | 23.25 | 12.92 | 20.99 | 12.92 | 19.96 | 12.92 | 24.24 |
| 13.00 | 23.36 | 13.00 | 21.22 | 13.00 | 20.19 | 13.00 | 24.47 |
| 13.08 | 23.47 | 13.08 | 21.44 | 13.08 | 20.41 | 13.08 | 24.69 |
| 13.17 | 23.62 | 13.17 | 21.68 | 13.17 | 20.64 | 13.17 | 24.92 |
| 13.25 | 23.79 | 13.25 | 21.93 | 13.25 | 20.89 | 13.25 | 25.17 |
| 13.33 | 24.00 | 13.33 | 22.24 | 13.33 | 21.21 | 13.33 | 25.49 |
| 13.42 | 24.25 | 13.42 | 22.65 | 13.42 | 21.61 | 13.42 | 25.90 |
| 13.50 | 24.52 | 13.50 | 23.13 | 13.50 | 22.09 | 13.50 | 26.37 |
| 13.58 | 24.78 | 13.58 | 23.64 | 13.58 | 22.61 | 13.58 | 26.89 |
| 13.67 | 25.06 | 13.67 | 24.17 | 13.67 | 23.13 | 13.67 | 27.41 |
| 13.75 | 25.31 | 13.75 | 24.66 | 13.75 | 23.62 | 13.75 | 27.90 |
| 13.83 | 25.55 | 13.83 | 25.11 | 13.83 | 24.07 | 13.83 | 28.36 |
| 13.92 | 25.75 | 13.92 | 25.53 | 13.92 | 24.50 | 13.92 | 28.78 |

Table A-9 Continued.

| Time (hrs) | Cum. Depth Out (cm) | Time (hrs) | Cum. Depth Out (cm) | Time (hrs) | Cum. Depth Out (cm) | Time (hrs) | Cum. Depth Out (cm) |
|---|---|---|---|---|---|---|---|
| 14.00 | 25.93 | 14.00 | 25.92 | 14.00 | 24.88 | 14.00 | 29.16 |
| 14.08 | 26.10 | 14.08 | 26.27 | 14.08 | 25.24 | 14.08 | 29.52 |
| 14.17 | 26.27 | 14.17 | 26.61 | 14.17 | 25.57 | 14.17 | 29.86 |
| 14.25 | 26.42 | 14.25 | 26.92 | 14.25 | 25.88 | 14.25 | 30.16 |
| 14.33 | 26.55 | 14.33 | 27.21 | 14.33 | 26.17 | 14.33 | 30.45 |
| 14.42 | 26.66 | 14.42 | 27.47 | 14.42 | 26.43 | 14.42 | 30.72 |
| 14.50 | 26.76 | 14.50 | 27.71 | 14.50 | 26.67 | 14.50 | 30.95 |
| 14.58 | 26.85 | 14.58 | 27.93 | 14.58 | 26.89 | 14.58 | 31.17 |
| 14.67 | 26.92 | 14.67 | 28.12 | 14.67 | 27.09 | 14.67 | 31.37 |
| 14.75 | 26.99 | 14.75 | 28.30 | 14.75 | 27.26 | 14.75 | 31.54 |
| 14.83 | 27.04 | 14.83 | 28.46 | 14.83 | 27.42 | 14.83 | 31.70 |
| 14.92 | 27.08 | 14.92 | 28.60 | 14.92 | 27.56 | 14.92 | 31.84 |
| 15.00 | 27.12 | 15.00 | 28.72 | 15.00 | 27.69 | 15.00 | 31.97 |
| 15.08 | 27.15 | 15.08 | 28.84 | 15.08 | 27.80 | 15.08 | 32.08 |
| 15.17 | 27.19 | 15.17 | 28.94 | 15.17 | 27.90 | 15.17 | 32.18 |
| 15.25 | 27.22 | 15.25 | 29.03 | 15.25 | 27.99 | 15.25 | 32.27 |
| 15.33 | 27.25 | 15.33 | 29.11 | 15.33 | 28.08 | 15.33 | 32.36 |
| 15.42 | 27.28 | 15.42 | 29.19 | 15.42 | 28.15 | 15.42 | 32.43 |
| 15.50 | 27.31 | 15.50 | 29.26 | 15.50 | 28.22 | 15.50 | 32.50 |
| 15.58 | 27.34 | 15.56 | 29.30 | 15.56 | 28.27 | 15.56 | 32.55 |
| 15.67 | 27.36 | 15.66 | 29.37 | 15.66 | 28.33 | 15.66 | 32.61 |
| 15.75 | 27.39 | 15.75 | 29.43 | 15.75 | 28.39 | 15.75 | 32.67 |
| 15.83 | 27.41 | 15.83 | 29.47 | 15.83 | 28.44 | 15.83 | 32.72 |
| 15.92 | 27.43 | 15.92 | 29.52 | 15.92 | 28.48 | 15.92 | 32.76 |
| 16.00 | 27.45 | 16.00 | 29.56 | 16.00 | 28.52 | 16.00 | 32.80 |
| 16.08 | 27.47 | 16.08 | 29.59 | 16.08 | 28.56 | 16.08 | 32.84 |
| 16.17 | 27.49 | 16.19 | 29.64 | 16.14 | 28.58 | 16.19 | 32.88 |
| 16.25 | 27.51 | 16.25 | 29.66 | 16.25 | 28.62 | 16.25 | 32.90 |

Table A-9 Continued.

| Time (hrs) | Cum. Depth Out (cm) | Time (hrs) | Cum. Depth Out (cm) | Time (hrs) | Cum. Depth Out (cm) | Time (hrs) | Cum. Depth Out (cm) |
|---|---|---|---|---|---|---|---|
| 16.33 | 27.53 | 16.31 | 29.68 | 16.31 | 28.64 | 16.31 | 32.93 |
| 16.42 | 27.55 | 16.43 | 29.72 | 16.39 | 28.67 | 16.43 | 32.97 |
| 16.50 | 27.56 | 16.52 | 29.74 | 16.52 | 28.71 | 16.52 | 32.99 |
| 16.58 | 27.58 | 16.56 | 29.76 | 16.56 | 28.72 | 16.56 | 33.00 |
| 16.67 | 27.59 | 16.60 | 29.77 | 16.60 | 28.73 | 16.60 | 33.01 |
| 16.75 | 27.60 | 16.68 | 29.79 | 16.72 | 28.76 | 16.68 | 33.03 |
| 16.83 | 27.62 | 16.81 | 29.82 | 16.85 | 28.79 | 16.81 | 33.06 |
| 16.92 | 27.63 | 16.90 | 29.84 | 16.90 | 28.80 | 16.90 | 33.08 |
| 17.00 | 27.64 | 17.00 | 29.85 | 17.00 | 28.82 | 17.00 | 33.10 |
| 17.08 | 27.65 | 17.10 | 29.87 | 17.06 | 28.83 | 17.10 | 33.12 |
| 17.17 | 27.66 | 17.18 | 29.88 | 17.18 | 28.85 | 17.18 | 33.13 |
| 17.25 | 27.67 | 17.23 | 29.89 | 17.26 | 28.86 | 17.23 | 33.13 |
| 17.33 | 27.68 | 17.35 | 29.91 | 17.31 | 28.86 | 17.35 | 33.15 |
| 17.42 | 27.69 | 17.39 | 29.91 | 17.43 | 28.88 | 17.39 | 33.16 |
| 17.50 | 27.70 | 17.50 | 29.93 | 17.50 | 28.89 | 17.50 | 33.17 |
| 17.58 | 27.71 | 17.60 | 29.94 | 17.60 | 28.90 | 17.60 | 33.18 |
| 17.67 | 27.72 | 17.68 | 29.95 | 17.68 | 28.91 | 17.68 | 33.19 |
| 17.75 | 27.73 | 17.76 | 29.96 | 17.76 | 28.92 | 17.76 | 33.20 |
| 17.83 | 27.74 | 17.79 | 29.96 | 17.81 | 28.93 | 17.79 | 33.20 |
| 17.92 | 27.75 | 17.81 | 29.96 | 17.89 | 28.93 | 17.81 | 33.21 |
| 18.00 | 27.75 | 18.00 | 29.98 | 18.00 | 28.95 | 18.00 | 33.23 |
| 18.08 | 27.76 | 18.09 | 29.99 | 18.09 | 28.96 | 18.09 | 33.24 |
| 18.17 | 27.77 | 18.15 | 30.00 | 18.15 | 28.96 | 18.15 | 33.24 |
| 18.25 | 27.78 | 18.26 | 30.01 | 18.26 | 28.97 | 18.26 | 33.25 |
| 18.33 | 27.79 | 18.33 | 30.01 | 18.33 | 28.98 | 18.33 | 33.26 |
| 18.42 | 27.79 | 18.42 | 30.02 | 18.42 | 28.98 | 18.42 | 33.27 |
| 18.50 | 27.80 | 18.50 | 30.03 | 18.50 | 28.99 | 18.50 | 33.27 |
| 18.58 | 27.81 | 18.58 | 30.04 | 18.58 | 29.00 | 18.58 | 33.28 |

Table A-9 Continued.

| Time (hrs) | Cum. Depth Out (cm) | Time (hrs) | Cum. Depth Out (cm) | Time (hrs) | Cum. Depth Out (cm) | Time (hrs) | Cum. Depth Out (cm) |
|---|---|---|---|---|---|---|---|
| 18.67 | 27.81 | 18.67 | 30.05 | 18.67 | 29.01 | 18.67 | 33.29 |
| 18.75 | 27.82 | 18.75 | 30.05 | 18.75 | 29.02 | 18.75 | 33.30 |
| 18.83 | 27.82 | 18.83 | 30.06 | 18.83 | 29.03 | 18.83 | 33.31 |
| 18.92 | 27.83 | 18.92 | 30.08 | 18.92 | 29.04 | 18.92 | 33.32 |
| 19.00 | 27.84 | 19.00 | 30.09 | 19.00 | 29.05 | 19.00 | 33.33 |
| 19.08 | 27.85 | 19.08 | 30.10 | 19.08 | 29.06 | 19.08 | 33.35 |
| 19.17 | 27.88 | 19.17 | 30.12 | 19.17 | 29.08 | 19.17 | 33.36 |
| 19.25 | 27.91 | 19.25 | 30.13 | 19.25 | 29.10 | 19.25 | 33.38 |
| 19.33 | 27.94 | 19.33 | 30.15 | 19.33 | 29.11 | 19.42 | 33.42 |
| 19.42 | 27.97 | 19.42 | 30.17 | 19.42 | 29.13 | 19.42 | 33.42 |
| 19.50 | 28.00 | 19.50 | 30.19 | 19.50 | 29.15 | 19.50 | 33.43 |
| 19.58 | 28.03 | 19.58 | 30.21 | 19.58 | 29.17 | 19.58 | 33.46 |
| 19.67 | 28.07 | 19.67 | 30.23 | 19.67 | 29.19 | 19.67 | 33.48 |
| 19.75 | 28.11 | 19.75 | 30.25 | 19.75 | 29.21 | 19.75 | 33.50 |
| 19.83 | 28.15 | 19.83 | 30.27 | 19.83 | 29.24 | 19.83 | 33.52 |
| 19.92 | 28.19 | 19.92 | 30.30 | 19.92 | 29.26 | 19.92 | 33.54 |
| 20.00 | 28.23 | 20.00 | 30.32 | 20.00 | 29.28 | 20.00 | 33.57 |
| 20.08 | 28.28 | 20.08 | 30.35 | 20.08 | 29.31 | 20.08 | 33.59 |
| 20.17 | 28.32 | 20.17 | 30.37 | 20.17 | 29.34 | 20.17 | 33.62 |
| 20.25 | 28.36 | 20.25 | 30.40 | 20.25 | 29.37 | 20.25 | 33.65 |
| 20.33 | 28.39 | 20.33 | 30.44 | 20.33 | 29.40 | 20.33 | 33.68 |
| 20.42 | 28.42 | 20.42 | 30.47 | 20.42 | 29.43 | 20.42 | 33.71 |
| 20.50 | 28.45 | 20.50 | 30.50 | 20.50 | 29.47 | 20.50 | 33.75 |
| 20.58 | 28.47 | 20.58 | 30.54 | 20.58 | 29.50 | 20.58 | 33.78 |
| 20.67 | 28.49 | 20.67 | 30.57 | 20.67 | 29.53 | 20.67 | 33.81 |
| 20.75 | 28.52 | 20.75 | 30.60 | 20.75 | 29.56 | 20.75 | 33.85 |
| 20.83 | 28.54 | 20.83 | 30.63 | 20.83 | 29.60 | 20.83 | 33.88 |
| 20.92 | 28.56 | 20.92 | 30.66 | 20.92 | 29.63 | 20.92 | 33.91 |

Table A-9 Continued.

| Time (hrs) | Cum. Depth Out (cm) | Time (hrs) | Cum. Depth Out (cm) | Time (hrs) | Cum. Depth Out (cm) | Time (hrs) | Cum. Depth Out (cm) |
|---|---|---|---|---|---|---|---|
| 21.00 | 28.57 | 21.00 | 30.69 | 21.00 | 29.65 | 21.00 | 33.94 |
| 21.08 | 28.59 | 21.08 | 30.72 | 21.08 | 29.68 | 21.08 | 33.96 |
| 21.17 | 28.60 | 21.17 | 30.74 | 21.17 | 29.71 | 21.17 | 33.99 |
| 21.25 | 28.62 | 21.25 | 30.77 | 21.25 | 29.73 | 21.25 | 34.01 |
| 21.33 | 28.63 | 21.33 | 30.79 | 21.33 | 29.75 | 21.33 | 34.03 |
| 21.42 | 28.65 | 21.41 | 30.81 | 21.41 | 29.77 | 21.41 | 34.06 |
| 21.50 | 28.66 | 21.50 | 30.83 | 21.50 | 29.79 | 21.50 | 34.07 |
| 21.58 | 28.67 | 21.58 | 30.85 | 21.58 | 29.81 | 21.58 | 34.09 |
| 21.67 | 28.68 | 21.62 | 30.86 | 21.66 | 29.83 | 21.66 | 34.11 |
| 21.75 | 28.69 | 21.75 | 30.88 | 21.75 | 29.84 | 21.75 | 34.13 |
| 21.83 | 28.71 | 21.83 | 30.90 | 21.83 | 29.86 | 21.83 | 34.14 |
| 21.92 | 28.72 | 21.91 | 30.91 | 21.91 | 29.87 | 21.91 | 34.15 |
| 22.00 | 28.73 | 22.04 | 30.93 | 22.04 | 29.89 | 22.04 | 34.17 |
| 22.08 | 28.74 | 22.08 | 30.93 | 22.08 | 29.90 | 22.08 | 34.18 |
| 22.17 | 28.75 | 22.16 | 30.94 | 22.16 | 29.91 | 22.16 | 34.19 |
| 22.25 | 28.75 | 22.24 | 30.95 | 22.24 | 29.92 | 22.24 | 34.20 |
| 22.33 | 28.77 | 22.33 | 30.96 | 22.33 | 29.93 | 22.33 | 34.21 |
| 22.42 | 28.77 | 22.41 | 30.97 | 22.41 | 29.94 | 22.41 | 34.22 |
| 22.50 | 28.78 | 22.50 | 30.98 | 22.50 | 29.95 | 22.50 | 34.23 |
| 22.58 | 28.79 | 22.58 | 30.99 | 22.58 | 29.95 | 22.58 | 34.23 |
| 22.67 | 28.80 | 22.66 | 31.00 | 22.74 | 29.97 | 22.66 | 34.24 |
| 22.75 | 28.81 | 22.74 | 31.00 | 22.83 | 29.97 | 22.74 | 34.25 |
| 22.83 | 28.82 | 22.83 | 31.01 | 22.87 | 29.98 | 22.83 | 34.26 |
| 22.92 | 28.83 | 22.91 | 31.02 | 22.91 | 29.98 | 22.91 | 34.26 |
| 23.00 | 28.83 | 23.00 | 31.02 | 23.00 | 29.99 | 23.00 | 34.27 |
| 23.08 | 28.84 | 23.07 | 31.03 | 23.10 | 29.99 | 23.07 | 34.27 |
| 23.17 | 28.85 | 23.16 | 31.03 | 23.16 | 30.00 | 23.16 | 34.28 |
| 23.25 | 28.86 | 23.24 | 31.04 | 23.24 | 30.00 | 23.24 | 34.28 |

Table A-9 Continued.

| Time (hrs) | Cum. Depth Out (cm) | Time (hrs) | Cum. Depth Out (cm) | Time (hrs) | Cum. Depth Out (cm) | Time (hrs) | Cum. Depth Out (cm) |
|---|---|---|---|---|---|---|---|
| 23.33 | 28.86 | 23.32 | 31.04 | 23.32 | 30.01 | 23.32 | 34.29 |
| 23.42 | 28.87 | 23.41 | 31.05 | 23.41 | 30.01 | 23.41 | 34.29 |
| 23.50 | 28.87 | 23.49 | 31.05 | 23.53 | 30.02 | 23.49 | 34.30 |
| 23.58 | 28.88 | 23.57 | 31.06 | 23.57 | 30.02 | 23.57 | 34.30 |
| 23.67 | 28.89 | 23.66 | 31.06 | 23.66 | 30.02 | 23.66 | 34.31 |
| 23.75 | 28.89 | 23.75 | 31.06 | 23.75 | 30.03 | 23.75 | 34.31 |
| 23.83 | 28.90 | 23.86 | 31.07 | 23.82 | 30.03 | 23.86 | 34.31 |
| 23.92 | 28.90 | 23.90 | 31.07 | 23.90 | 30.03 | 23.90 | 34.32 |
| 24.00 | 28.91 | 24.00 | 31.07 | 24.00 | 30.04 | 24.00 | 34.32 |
| 24.08 | 28.91 | 24.07 | 31.08 | 24.06 | 30.04 | 24.07 | 34.32 |
| 24.17 | 28.91 | 24.15 | 31.08 | 24.15 | 30.04 | 24.15 | 34.32 |
| 24.25 | 28.92 | 24.24 | 31.08 | 24.28 | 30.04 | 24.24 | 34.33 |
| 24.33 | 28.92 | 24.32 | 31.08 | 24.32 | 30.05 | 24.32 | 34.33 |
| 24.42 | 28.93 | 24.40 | 31.09 | 24.40 | 30.05 | 24.40 | 34.33 |
| 24.50 | 28.93 | 24.49 | 31.09 | 24.53 | 30.05 | 24.49 | 34.33 |
| 24.58 | 28.93 | 24.61 | 31.09 | 24.65 | 30.05 | 24.61 | 34.33 |
| 24.67 | 28.94 | 24.69 | 31.09 | 24.69 | 30.05 | 24.69 | 34.34 |
| 24.75 | 28.94 | 24.78 | 31.09 | 24.73 | 30.05 | 24.78 | 34.34 |
| 24.83 | 28.94 | 24.82 | 31.09 | 24.82 | 30.06 | 24.82 | 34.34 |
| 24.92 | 28.94 | 24.90 | 31.09 | 24.90 | 30.06 | 24.90 | 34.34 |
| 25.00 | 28.95 | 25.00 | 31.09 | 25.00 | 30.06 | 25.00 | 34.34 |
| 25.08 | 28.95 | 25.07 | 31.09 | 25.07 | 30.06 | 25.07 | 34.34 |
| 25.17 | 28.95 | 25.15 | 31.10 | 25.15 | 30.06 | 25.15 | 34.34 |
| 25.25 | 28.96 | 25.23 | 31.10 | 25.23 | 30.06 | 25.23 | 34.34 |
| 25.33 | 28.96 | 25.32 | 31.10 | 25.32 | 30.06 | 25.32 | 34.34 |
| 25.42 | 28.96 | 25.44 | 31.10 | 25.40 | 30.06 | 25.44 | 34.34 |
| 25.50 | 28.96 | 25.48 | 31.10 | 25.52 | 30.06 | 25.48 | 34.34 |
| 25.58 | 28.97 | 25.59 | 31.10 | 25.59 | 30.06 | 25.59 | 34.34 |

Table A-9 Continued.

| Time (hrs) | Cum. Depth Out (cm) | Time (hrs) | Cum. Depth Out (cm) | Time (hrs) | Cum. Depth Out (cm) | Time (hrs) | Cum. Depth Out (cm) |
|---|---|---|---|---|---|---|---|
| 25.67 | 28.97 | 25.69 | 31.10 | 25.65 | 30.06 | 25.69 | 34.35 |
| 25.75 | 28.97 | 25.73 | 31.10 | 25.73 | 30.06 | 25.73 | 34.35 |
| 25.83 | 28.97 | 25.81 | 31.10 | 25.81 | 30.07 | 25.81 | 34.35 |
| 25.92 | 28.98 | 25.94 | 31.10 | 25.94 | 30.07 | 25.94 | 34.35 |
| 26.00 | 28.98 | 26.02 | 31.10 | 26.02 | 30.07 | 26.02 | 34.35 |
| 26.08 | 28.98 | 26.06 | 31.10 | 26.06 | 30.07 | 26.06 | 34.35 |
| 26.17 | 28.98 | 26.15 | 31.11 | 26.15 | 30.07 | 26.15 | 34.35 |
| 26.25 | 28.98 | 26.25 | 31.11 | 26.25 | 30.07 | 26.25 | 34.35 |
| 26.33 | 28.99 | 26.39 | 31.11 | 26.31 | 30.07 | 26.39 | 34.35 |
| 26.42 | 28.99 | 26.44 | 31.11 | 26.39 | 30.07 | 26.44 | 34.35 |
| 26.50 | 28.99 | 26.52 | 31.11 | 26.48 | 30.07 | 26.52 | 34.35 |
| 26.58 | 28.99 | 26.56 | 31.11 | 26.60 | 30.07 | 26.56 | 34.35 |
| 26.67 | 29.00 | 26.68 | 31.11 | 26.68 | 30.07 | 26.68 | 34.36 |
| 26.75 | 29.00 | 26.73 | 31.11 | 26.77 | 30.07 | 26.73 | 34.36 |
| 26.83 | 29.00 | 26.84 | 31.11 | 26.81 | 30.07 | 26.84 | 34.36 |
| 26.92 | 29.01 | 26.93 | 31.11 | 26.93 | 30.08 | 26.93 | 34.36 |
| 27.00 | 29.01 | 27.02 | 31.11 | 27.02 | 30.08 | 27.02 | 34.36 |
| 27.08 | 29.01 | 27.10 | 31.11 | 27.10 | 30.08 | 27.10 | 34.36 |
| 27.17 | 29.02 | 27.14 | 31.11 | 27.14 | 30.08 | 27.14 | 34.36 |
| 27.25 | 29.02 | 27.27 | 31.12 | 27.22 | 30.08 | 27.27 | 34.36 |
| 27.33 | 29.02 | 27.31 | 31.12 | 27.35 | 30.08 | 27.31 | 34.36 |
| 27.42 | 29.03 | 27.39 | 31.12 | 27.43 | 30.08 | 27.39 | 34.36 |
| 27.50 | 29.03 | 27.50 | 31.12 | 27.50 | 30.08 | 27.50 | 34.36 |
| 27.58 | 29.03 | 27.56 | 31.12 | 27.56 | 30.08 | 27.56 | 34.36 |
| 27.67 | 29.04 | 27.68 | 31.12 | 27.68 | 30.08 | 27.68 | 34.37 |
| 27.75 | 29.04 | 27.76 | 31.12 | 27.72 | 30.08 | 27.76 | 34.37 |
| 27.83 | 29.05 | 27.81 | 31.12 | 27.81 | 30.08 | 27.81 | 34.37 |
| 27.92 | 29.05 | 27.93 | 31.12 | 27.93 | 30.09 | 27.93 | 34.37 |

Table A-9 Continued.

| Time (hrs) | Cum. Depth Out (cm) | Time (hrs) | Cum. Depth Out (cm) | Time (hrs) | Cum. Depth Out (cm) | Time (hrs) | Cum. Depth Out (cm) |
|---|---|---|---|---|---|---|---|
| 28.00 | 29.05 | 28.01 | 31.12 | 28.05 | 30.09 | 28.01 | 34.37 |
| 28.08 | 29.06 | 28.09 | 31.12 | 28.09 | 30.09 | 28.09 | 34.37 |
| 28.17 | 29.06 | 28.14 | 31.12 | 28.18 | 30.09 | 28.14 | 34.37 |
| 28.25 | 29.06 | 28.22 | 31.13 | 28.26 | 30.09 | 28.22 | 34.37 |
| 28.33 | 29.07 | 28.34 | 31.13 | 28.30 | 30.09 | 28.34 | 34.37 |
| 28.42 | 29.07 | 28.41 | 31.13 | 28.41 | 30.09 | 28.41 | 34.37 |
| 28.50 | 29.07 | 28.51 | 31.13 | 28.51 | 30.09 | 28.51 | 34.37 |
| 28.58 | 29.08 | 28.59 | 31.13 | 28.59 | 30.09 | 28.59 | 34.37 |
| 28.67 | 29.08 | 28.68 | 31.13 | 28.68 | 30.09 | 28.68 | 34.37 |
| 28.75 | 29.08 | 28.75 | 31.13 | 28.75 | 30.09 | 28.75 | 34.38 |
| 28.83 | 29.09 | 28.84 | 31.13 | 28.84 | 30.09 | 28.84 | 34.38 |
| 28.92 | 29.09 | 28.93 | 31.13 | 28.93 | 30.10 | 28.93 | 34.38 |
| 29.00 | 29.09 | 29.01 | 31.13 | 29.01 | 30.10 | 29.01 | 34.38 |
| 29.08 | 29.10 | 29.10 | 31.13 | 29.06 | 30.10 | 29.10 | 34.38 |
| 29.17 | 29.10 | 29.13 | 31.13 | 29.13 | 30.10 | 29.13 | 34.38 |
| 29.25 | 29.10 | 29.26 | 31.13 | 29.22 | 30.10 | 29.26 | 34.38 |
| 29.33 | 29.11 | 29.34 | 31.13 | 29.34 | 30.10 | 29.34 | 34.38 |
| 29.42 | 29.11 | 29.38 | 31.13 | 29.42 | 30.10 | 29.38 | 34.38 |
| 29.50 | 29.11 | 29.51 | 31.13 | 29.51 | 30.10 | 29.51 | 34.38 |
| 29.58 | 29.12 | 29.59 | 31.13 | 29.59 | 30.10 | 29.59 | 34.38 |
| 29.67 | 29.12 | 29.66 | 31.13 | 29.66 | 30.10 | 29.66 | 34.38 |
| 29.75 | 29.12 | 29.76 | 31.13 | 29.76 | 30.10 | 29.76 | 34.38 |
| 29.83 | 29.12 | 29.84 | 31.13 | 29.84 | 30.10 | 29.84 | 34.38 |
| 29.92 | 29.13 | 29.92 | 31.13 | 29.92 | 30.10 | 29.92 | 34.38 |
| 30.00 | 29.13 | 30.00 | 31.13 | 30.00 | 30.10 | 30.00 | 34.38 |